Statistical Distributions in the Thermal Model

Michael Hauer

January 2006

Thesis submitted in fulfilment of
the requirements for the degree of Master of Science
at the University of Cape Town

Abstract

An attempt is made to use the thermal model to determine statistical particle number fluctuations in the presence of exact conservation laws. A basis is provided, which will be useful to extend the range of applications of the thermal model, with both a large number of conserved charges as well as quantum statistics. The central limit theorem and its related expansions provide a flexible mathematical tool for calculation of statistical fluctuations, and allows for application of the canonical ensemble to high energy particle collision data. A first analysis of the NA49 CC data suggests that statistical multiplicity fluctuations can be understood within the statistical hadronization model.

Acknowledgements

First of all I would like to thank 'The Team', Rory Adams, Bruce Becker, Sarah Blyth, Jean Cleymans, Heather Gray, Mark Horner, Azwindinni Muronga, Nawahl Razak, Maciej Stankiewicz, Artur Szostak, Gareth De Vaux, Zeblon Vilakazi, Spencer Wheaton, and Shaun Wyngard, for a greatly enjoyable working environment.

I would like to thank my supervisor, Prof. Jean Cleymans, for his guidance and the influence he had on my work.

I am especially indebted to Spencer Wheaton for his never ending patience, critical comments and constant encouragement, without whom this thesis would not exist.

Thanks to Dr. Peter Steinberg for setting up my trip to Brookhaven.

I am grateful to the National Research Foundation (NRF) for financial assistance.

Contents

List of Figures

List of Tables

Chapter 1

Introduction

1.1 History and Considerations of the Thermal Model

The thermal model seeks to describe particle production and global thermal properties of strongly interacting matter. Since it's invention in the 1950s and 60s it was successfully applied to a wide range of physical scenarios from elementary particle collisions to neutron stars and still enjoys great popularity, but is generally thought to be on rather weak theoretical foundations. Although it is a phenomenological model, not a theory, it shares common aspects with quantum chromo dynamics, QCD, the correct theory of the strong interaction, which ultimately governs the hadronization process. This introduction will first discuss its basic considerations and recent additions, followed by an overview of its application to high energy physics. Its main ingredients are the hadronic mass spectrum, and its quantum number configuration, and freeze-out conditions.

The model was originally put forward by Koppe [1] and Fermi [2] around 1950, and then developed further by Hagedorn [3, 4] in 1965, in an attempt to describe hadron abundances in collider experiments and cosmic rays. The idea of a limiting temperature was used to explain the lack of heavier resonances and an almost unchanged mean transverse momentum of observed particles when energy and size of colliding systems was increased.

Their picture was, that of some sort of volume, a fireball or bag, would emit hadronic black body radiation at a temperature T_H or below, rather than a quark gluon plasma, QGP, which was predicted by QCD. The concept of a deconfined state of quarks and gluons, was yet to be formulated. This idea owns two strong concepts. The first one gives justification to the applictation of the thermal model to elementary particle collisions where only few particles

are produced, hence one can hardly talk about a gas of hadrons. But black body radiation can be described by thermodynamics even if only very few photons are emitted. The second one gave rise to the statistical bootstrap or self consistency condition, a corner stone of the thermal model. Hagedorn assumed further that fireballs consist of fireballs, which consist of fireballs and so on, and are no different to the observed hadrons and resonances themselves. Resonances (fireballs or bags) would thus decay successively in a self similar fashion into resonances until only 'stable' particles (or bags) would exist. The nature of the for the black body radiation required temperature bath, which obviously does not exist, is unclear and Hagedorn called it a fiction, but assumed a 'virtual temperature bath operated and controlled by the strong interaction.' The thermodynamic partition function can be written as

$$\mathcal{Z} = \exp\left[\int_0^\infty \rho\left(m\right) F\left(m,T\right) dm\right], \tag{1.1}$$

where the unknown function $\rho(m)dm$ gives the number of hadron states between m and $m+dm$, while the known function $F(m,T)$ gives the occupation probability of some particular energy state. On the other hand

$$\mathcal{Z} = \int_0^\infty \sigma\left(E\right) \exp\left[-\frac{E}{T}\right] dE, \tag{1.2}$$

where $\sigma(E)$ is the number of states between E and $E+dE$. The bootstrap requires both functions, $\rho(x)$ and $\sigma(x)$, to asymptotically approach each other and leads to an exponentially growing mass spectrum of resonances determined by a limiting temperature $T_H \approx 160MeV$.

$$\rho(m) \quad \underset{m\to\infty}{\longrightarrow} \frac{const}{m^{5/2}} \exp\left[m/T_H\right] \tag{1.3}$$

Furthermore can the defining equation for the density of mass states $\rho(m)$, be solved analytically, leaving us with only two parameters to determine the Hagedorn temperature T_H. A composition volume, related to the intrinsic range of the strong interaction and a mass parameter m_0. Hagedorn [3] proposed the pion mass m_π as the scaling parameter which yields $T_H \approx 150MeV$, while [5] in the limit $m_0 \to 0$ and taking the range of the strong interaction to be about $1fm$ gives $T_H \approx 200MeV$. These findings are remarkable given the fact that Hagedorn only had a good table of resonances up to a mass of some $0.8GeV$, yet his findings, or predictions, are verified by the today known resonance spectrum up to a mass of $1.8GeV$. In fact, following the assumption [6] that some high lying states are part of chiral multiplets and

including unobserved, but required, resonances, the exponential rise of the meson spectrum can be continued up to a mass of just below $2.5GeV$. Not only has Hagedorn predicted the hadronic resonance spectrum, but he also gave the first estimate of the 'boiling temperature' of hadronic matter, above which a hadronic partition function can not be defined and all thermodynamical quantities would diverge. Moreover required the data of transverse momentum spectra a temperature between $T \approx 120$ and $160MeV$. He concluded that he had found the highest possible temperature and that the domain on the other side of the phase transition of boiling hadronic matter will be 'forever inaccessible'.

1.2 High Energy Collisions

In modern collider experiments elementary particles or ions are accelerated to relativistic energies. In the case of ions they would approach each other as highly Lorentz contracted pancakes. On collision some of the available energy is deposited in a central region by participating nucleons or elementary particles. Colliding energy, particle type or ion size, and degree of stopping determines the energy density and size of the created system. After some initial formation time a colorless massive extended object of deconfined quarks and gluons, the QGP, may be formed, leaving matter under extreme conditions. Temperature, energy density, and pressure of this kind are believed to have existed in the very early universe ($\sim 10^{-6}\ sec$). Now hydrodynamical evolutions sets in and the system expands and subsequently cools down. Once the energy density drops below a critical value inelastic collision cease and hadron abundances are fixed at a temperature T_{chem} close to and below T_H. This is commonly referred to as chemical freeze-out. From there on only elastic processes drive the evolution until, on thermal freeze-out, finally all interactions cease and the system breaks up. Momentum spectra would thus show a lower temperature T_{ther} due to elastic scattering and, additionally, resonance decay.
Cooper and Frye [7] provided a Lorentz invariant formula which is now, in several approximations and rigorous forms widely used in high energy physics. Particles are assumed to be emitted, according to their share of the available phase space, from a 4 dimensional freeze-out surface defined by a critical value of energy density. One important peculiarity of boost invariant expansion models, e.g. Bjorken expansion [8], is that ratios of fully phase space integrated yields, and their higher moments, are equal to ratios of their respective rapidity distributions [9]. This is what the thermal model ultimately exploits and allows for its application to the mid rapidity (central) region and

for calculation of distributions therein. The thermal model assumes that this central region can be well described by one set of parameters (temperature and chemical potentials) and is in local statistical equilibrium at the point of break up. Hence jet production, due to hard scattering of quarks and gluons, or in this picture particle emission from a hot spot inside the fireball, is not contained in the thermal model. The statistical hadronization model can be considered a model for strong bag decay, while the particle production mechanism [10] itself is dominated by the available phase space. Hagedorn's fictitious temperature bath, which he thought to be controlled and operated by the strong interaction, could ultimately have its origin in the vacuum bag pressure. Several freely available codes like THERMUS [11], SHARE [12] implemented single freeze-out models (chemical and thermal at once), either as purely statistical models for phase space integrated particle multiplicities for static sources, or THERMINATOR [13], which incorporated the Cracow single freeze-out model [14] and blast wave model, and allows additionally for computation of spectra.

1.3 The Phase Diagram

The thermal model itself, a phenomenological model, does not provide reasonable values for its parameters, most importantly fireball temperature and chemical potentials. Hence conditions at freeze-out need to be inferred from either theory or fits to experimental data. The baryon chemical potential takes a special role in heavy ion collisions as it is essentially a measure of the excess of quarks over anti-quarks. A systematic evolution of freeze-out temperature and baryon chemical potential marks the transition line between ordinary hadronic matter and the QGP.
In thermal model calculation freeze-out conditions, like the average energy per particle [15, 16], normalized entropy density [17], or net-baryon density [18] replace the critical energy density criterion which is used in QCD calculations and hydrodynamics. Model fits to experimental data allowed to find a $\mu_B(T)$ [19] parametrization and to map the phase diagram in figure 1.1. The remaining chemical potentials (μ_S, μ_Q) are commonly fixed by requiring the central fireball to be strangeness neutral and to have the charge to baryon ratio of the incident beam particles. As the colliding energy is increased more and more energy becomes available for anti-particle production, and thus a further systematic evolution of the baryon chemical potential with beam energy $\sqrt{s}(\mu_B)$ [20] for ion ion collisions gives the thermal even predictive qualities and justification to its application. These values can once

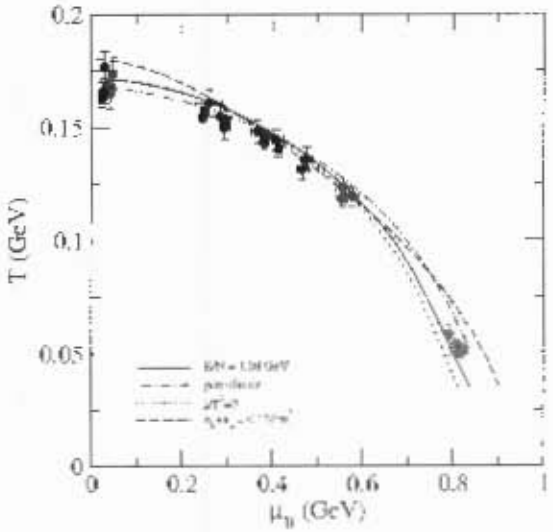

Figure 1.1: Comparison of freeze-out conditions in a thermal model phase diagram by J.Cleymans, H.Oeschler, K.Redlich, and S.Wheaton [19]

again be compared to lattice QCD results. For low baryon chemical potential [21] lattice QCD predicts a critical temperature of $T_c \approx 172MeV$ for a net-baryon free system, and further finds a drop in the critical temperature

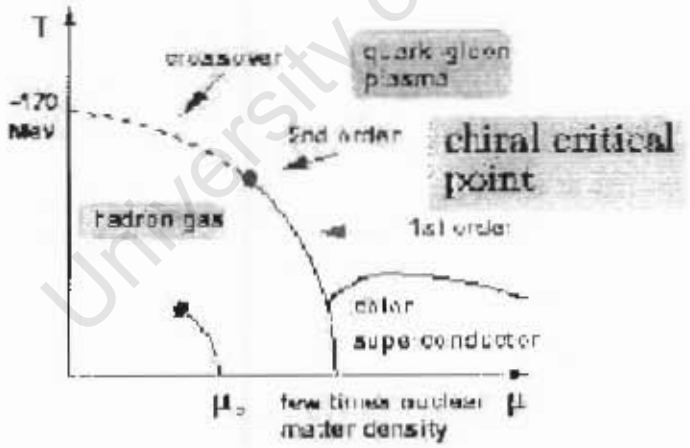

Figure 1.2: QCD phase diagram by F.Karsch [21]

for growing baryon density, see figure 1.2. For vanishing μ_B lattice calculations suggest a rapid crossover, rather than a phase transition from the QGP

to a hadron gas, at low μ_B and high T, and a 1st order phase transition at high μ_B and low T. Thus somewhere inbetween a chiral critical point and a second order phase transition should exist. In particular determines the order of phase transition the nature of statistical fluctuations. Excluded volume corrections, which account for eigen volume taken up by resonances, allow for incorporation of phase transitions [22] into the thermal model and have considerable effect on parameter set, yields and fluctuations, but are for technical reasons omitted in this thesis. While phase transitions will leave a signature in the fluctuations, they are not the only source of a non trivial deviation from a Poisson distribution. Exactly enforced conservation laws tend to suppress fluctuations [23, 24, 25] while quantum statistics [26] and non-equilibrium [9] tend to enhance. The thermal model is well suited for this kind of discussion and will allow to distinguish those effects. As phase transition are not contained in a standard thermal model, deviations from thermal model predictions are expected to be largest in the vicinity of such critical points, while being small for a cross over.

1.4 Motivation and Summary

There has been a score of publications exploring theoretical foundations and several attempts have been made to cast light on the question why should the thermal model work and where should it break. Various hadronization models [27, 28] have been put forward which could in the language of thermodynamics help to distinguish ideas about the nature of the particle production mechanism, or at the very least differentiate in general terms global properties of the system in the very late stages of the evolution. The nature of phase transition is a further question mark in high energy physics. The existence of a QGP, where the degrees of freedom are electrically neutral gluons and quarks, which carry fractional charges, might lead to a different statistical picture [29] than fluctuations of the number of charged hadrons with integer charges. It will be the focus of this work to explore some aspects of statistical properties of a simple free Hamiltonian with a large number of degrees of freedom. A number of phenomenological concepts and experimental results has allowed us to put strong constraints on the thermal parameters in use. The success of the thermal model lies definitely in the small number of parameters it uses to describe a complicated physical situation and the comparably simple mathematical framework needed to conduct calculations. The idea will be to test the thermal model even further and see where it fails to reproduce experimental data. The question of its meaning is undoubtfully linked to its ability to describe further aspects of heavy ion collisions and

will remain a subject of discussion. This approach thus favors the former of the two scenarios proposed in reference [5]:

- Each collision produces a thermal system and thus corresponds to an ensemble of many partitions: nuclear collision produce matter.
- Each collision is one partition, and only the ensemble over many collisions forms a thermal ensemble: nuclear collisions simulate matter

Chapter 2 is dedicated to a relativistic particle anti-particle gas. Various aspects of grand canonical and canonical ensembles are discussed, in both Boltzmann approximation and quantum statistics. Chapter 3 discusses a relativistic hadron gas in a canonical ensemble in Boltzmann approximation. Special emphasis is given on freeze-out conditions and particle decay. An application of the proposed formalism is given with the pre-analysis of NA49 Carbon Carbon data in chapter 4 and will be a test of the provided code (appendix G). Lastly will chapter 5 address some of the constraints of the software and show how one can use the central limit theorem and further volume dependent corrections to produce reasonable approximations to quantum statistical partition functions in basically any ensemble. A conclusion and further outlook close this thesis.

Chapter 2

Particle Anti-particle Gas

The aim of this chapter is to provide a systematic discussion of statistical distributions in the context of a hypothetical relativistic particle anti-particle gas (pion gas) in Boltzmann approximation which will serve as a basis for the following. Its simple mathematical structure allows for analytical solutions and instructive examples. Two statistical ensembles are considered, the grand canonical (GC), where both charge and energy fluctuations are allowed, and the charge canonical (QC), where electrical charge is conserved exactly while energy is only conserved on average. Due to the relativistic Hamiltonian with energy eigenvalues $E_j = \sqrt{p^2 + m_j^2} - \mu_j$, the free solutions of the Klein Gordon equation with a uniform potential, particle production and annihilation are possible and conserved quantities will be quantum numbers rather than particle numbers. For the purposes of this thesis chemical potentials referring to a particle's quantum numbers (charges) shall be denoted by the Greek letter μ_j, where the subscript j stands for the particle species, while for particle specific chemical potentials referring to the particle itself the letter ν_j is used. Particle specific chemical potentials are always set to zero and are only used for derivatives. It should be stressed that this distinction is only for the purpose of mathematical notation and not a physical distinction. Finite particle specific chemical potentials could be used to model some increased (decreased) cross section of some particle production channel of hadronic matter in a fireball. Throughout this thesis frequently appearing physical constants are set to unity, $\hbar = k_B = c = 1$, which allows for more convenient notation. A description of those natural units is given in appendix A.

2.1 Primordial Expectation Values

The particle gas will be described by a set of parameters, namely volume, temperature and a charge chemical potential and its constituent particles. As this is a hypothetical gas of Boltzmann particles, one does not have to employ the picture of a in high energy collisions produced hadronic gas, which is subject to evolution and some relevant freeze-out conditions. The gas is a static one, in terms of its parameters, while, depending on the choice of statistical ensemble, Abelian charges, quantum numbers, are either conserved on average or exactly. Only one kind of particle, and its anti-particle, is contained in the fireball, hence particle decay chains can be omitted and will be discussed in the following chapter.

2.1.1 Grand Canonical Ensemble

In the simplest case, the GC, neither charge nor energy are conserved and the density of states in momentum space is determined by the Boltzmann factor, the particle's degeneracy $g = 2J + 1$, i.e. 1 or pions, fireball volume V, and for a relativistic gas, e.g. allowing for particle production and annihilation, energy eigenvalues $E = \sqrt{p^2 + m^2}$.

$$\frac{dN}{d^3p} = \frac{gV}{(2\pi)^3} e^{-\frac{E}{T}+\frac{\mu}{T}} \tag{2.1}$$

The chemical potential μ can have different interpretations as simply a Lagrange multiplier or a physical meaning as an effective potential within which the particles are free to move. After integration over momentum space one obtains for the expectation value of a particle's multiplicity

$$\langle N \rangle = \int d^3p \frac{dN}{d^3p} = \frac{gV}{2\pi^2} e^{\frac{\mu}{T}} m^2 T K_2\left(\frac{m}{T}\right). \tag{2.2}$$

The grand canonical expectation value for the number of particles is thus equal to the single particle partition function $z = \langle N \rangle$. The number of states available to a gas made up of a number P of such particle species, is given by the system partition function

$$\mathcal{Z}^{GC} = \exp\left(\sum_{j=1}^{P} z_j\right) = Tr\left[\exp\left(\sum_{j=1}^{P} -\frac{\hat{H}_j}{T} + \frac{\mu_j \hat{N}_j}{T}\right)\right], \tag{2.3}$$

where $\hat{H}_j = \sqrt{p^2 + m_j^2}$ is the relativistic free particle Hamiltonian and $\hat{N}_j$ the particle number operator. A derivation of equation 2.2, the single particle

partition function, and equation 2.3, the system partition function, can be found in appendices C and B respectively. All physical quantities are directly related to the partition function via the Helmholtz potential $F = -\frac{1}{\beta}\ln\mathcal{Z}$ and the Maxwell relations of thermodynamics. The focus will be on the experimentally accessible observable multiplicity and its respective higher moments. It might be convenient to include the particle specific chemical potential ν_j into a vector notation $\vec{\mu}_j = (\mu_B, \mu_S, \mu_Q, \nu_j)$ and $\vec{Q}_j = (B_j, S_j, Q_j, 1)$ for a canonical resemble in which baryon number, strangeness and charge are conserved exactly. Depending on the sign of a particle's effective chemical potential $\mu_j = \vec{Q}_j \cdot \vec{\mu}$, either the particle or its anti-particle, which carries opposite quantum numbers, will be preferred in the system. Both definitions of the system partition function lead to

$$\langle N_j \rangle = \frac{1}{\mathcal{Z}^{GC}} \left(T \frac{\partial}{\partial \nu_j} \right) \mathcal{Z}^{GC} \Big|_{\nu_j = 0} = z_j. \tag{2.4}$$

Recurrent application of the operator $\left(T\frac{\partial}{\partial \nu_j}\right)$ will give higher moments of the corresponding expectation value.

$$\langle N_j^n \rangle = \frac{1}{\mathcal{Z}^{GC}} \left(T \frac{\partial}{\partial \nu_j} \right)^n \mathcal{Z}^{GC} \Big|_{\nu_j = 0} \tag{2.5}$$

Or, in the case of $n = 2$, the important second moment

$$\langle N_j^2 \rangle = \frac{1}{\mathcal{Z}^{GC}} \left(T \frac{\partial}{\partial \nu_j} \right)^2 \mathcal{Z}^{GC} \Big|_{\nu_j = 0} = z_j^2 + z_j. \tag{2.6}$$

For the variance of a random variable knowledge of the first two moments is sufficient

$$\Delta N^2 \equiv \kappa_2 = \langle N^2 \rangle - \langle N \rangle^2, \tag{2.7}$$

where κ_2 is the second cumulant of the particle's multiplicity distribution. Cumulants will be introduced in chapter 5 and have proven a useful tool when dealing with multiplicity distributions [30]. For a relativistic grand canonical Boltzmann gas $\kappa_n = \langle N \rangle$ for all positive integers n, in particular $\kappa_1 \equiv \langle N \rangle$, which is the condition for a Poissonian distribution. The scaled variance ω [23] has been suggested as a measure for the relative width of a multiplicity distribution in high energy physics and is used throughout this thesis. For a grand canonical hadronic gas in Boltzmann approximation the scaled variance ω is thus always equal to one.

$$\omega = \frac{\langle N^2 \rangle - \langle N \rangle^2}{\langle N \rangle} = \frac{\kappa_2}{\kappa_1} = 1 \tag{2.8}$$

2.1.2 Canonical Ensemble

Starting off from a grand canonical description one can get to a QC by imposing charge conservation by only counting states which correspond to a particular net-charge $\vec{Q}$ and discarding all others. So reads the system partition function with a set $\vec{Q}$ of d conserved Abelian charges after using the Fourier integral representation of the δ function and inserting a factor $\exp\left(i\vec{Q}_j\vec{\phi}_Q\right)$ in addition to the particle specific fugacity:

$$\begin{aligned}\mathcal{Z}^C_{\vec{Q}} &= Tr\left[\exp\left(\sum_{j=1}^{P} -\frac{\hat{H}_j}{T} + \frac{\mu_j \hat{N}_j}{T}\right)\right]\delta\left(\sum_{j=1}^{P} N_j\vec{Q}_j - \vec{Q}\right) \\ &= \int_{-\pi}^{\pi}\frac{d\vec{\phi}}{(2\pi)^d}e^{-i\vec{Q}\vec{\phi}_Q}\exp\left(\sum_{j=1}^{P} z_j e^{\frac{\nu_j}{T}}e^{i\vec{Q}_j\vec{\phi}_Q}\right)\Big|_{\nu_j=0}. \end{aligned} \tag{2.9}$$

Expectation values are done in the same way as before, but the system is additionally kept at a fixed total charge state $\vec{Q}$.

$$\begin{aligned}\langle N_j\rangle &= \frac{1}{\mathcal{Z}^C_{\vec{Q}}}\left(T\frac{\partial}{\partial\nu_j}\right)\int_{-\pi}^{\pi}\frac{d\vec{\phi}}{(2\pi)^d}e^{-i\vec{Q}\vec{\phi}_Q}\exp\left(\sum_{j=1}^{P} z_j e^{\frac{\nu_j}{T}}e^{i\vec{Q}_j\vec{\phi}_Q}\right)\Big|_{\nu_j=0} \\ &= \frac{1}{\mathcal{Z}^C_{\vec{Q}}}\int_{-\pi}^{\pi}\frac{d\vec{\phi}}{(2\pi)^d}e^{-i(\vec{Q}-\vec{Q}_j)\vec{\phi}_Q}\exp\left(\sum_{j=1}^{P} z_j e^{i\vec{Q}_j\vec{\phi}_Q}\right) z_j \\ &= \frac{\mathcal{Z}^C_{\vec{Q}-\vec{Q}_j}}{\mathcal{Z}^C_{\vec{Q}}}\, z_j \end{aligned} \tag{2.10}$$

The number of produced particles, unlike in the GC, where the total yield scales linearly with the volume, depends now via the ratio of partition functions on the volume leading to further canonical suppression when the number of produced particles is small. The second moment is required for fluctuations:

$$\begin{aligned}\langle N_j^2\rangle &= \frac{1}{\mathcal{Z}^C_{\vec{Q}}}\left(T\frac{\partial}{\partial\nu_j}\right)^2\int_{-\pi}^{\pi}\frac{d\vec{\phi}}{(2\pi)^d}e^{-i\vec{Q}\vec{\phi}_Q}\exp\left(\sum_{j=1}^{P} z_j e^{\frac{\nu_j}{T}}e^{i\vec{Q}_j\vec{\phi}_Q}\right)\Big|_{\nu_j=0} \\ &= \frac{\mathcal{Z}^C_{\vec{Q}-2\vec{Q}_j}}{\mathcal{Z}^C_{\vec{Q}}}z_j^2 + \frac{\mathcal{Z}^C_{\vec{Q}-\vec{Q}_j}}{\mathcal{Z}^C_{\vec{Q}}}z_j. \end{aligned} \tag{2.11}$$

As a simple example one can calculate the partition function $\mathcal{Z}^{C,\pi}_Q$ for a pure pion gas, which is used for all examples in this chapter, and therefore only

one conserved charge is necessary.

$$\begin{aligned} \mathcal{Z}_Q^{C,\pi} &= \int_{-\pi}^{\pi} \frac{d\phi_Q}{2\pi} e^{-iQ\phi_Q} \exp\left(z_+ e^{i\phi_Q} + z_- e^{-i\phi_Q}\right) \\ &= \int_{-\pi}^{\pi} \frac{d\phi_Q}{2\pi} \sum_{n=0}^{\infty} \frac{z_+^n}{n!} \sum_{k=0}^{\infty} \frac{z_-^k}{k!} e^{i(n-k-Q)\phi_Q} \end{aligned} \tag{2.12}$$

Where $z_+ = ze^{\frac{\nu_+}{T}}$ and $z_- = ze^{\frac{\nu_-}{T}}$ are the single particle partition functions for the positive π^+ and the negative π^- pion respectively. Setting the particle specific chemical potentials ν_+ and ν_- to zero, and using the condition $Q = n - k$ and the definition of the modified Bessel functions [55] yields

$$\mathcal{Z}_Q^{C,\pi} = \sum_{n=0}^{\infty} \frac{z^n}{n!} \frac{z^{n-Q}}{(n-Q)!} = I_Q(2z). \tag{2.13}$$

The first and second moments of the expectation value for the positive pion multiplicity thus are

$$\langle N_+ \rangle = \frac{1}{\mathcal{Z}_Q^{C,\pi}} \left(T \frac{\partial}{\partial \nu_+}\right) \mathcal{Z}_Q^{C,\pi}\Big|_{\nu_+=0} = \frac{I_{Q-1}(2z)}{I_Q(2z)} z \tag{2.14}$$

$$\langle N_+^2 \rangle = \frac{1}{\mathcal{Z}_Q^{C,\pi}} \left(T \frac{\partial}{\partial \nu_+}\right)^2 \mathcal{Z}_Q^{C,\pi}\Big|_{\nu_+=0} = \frac{I_{Q-2}(2z)}{I_Q(2z)} z^2 + \frac{I_{Q-1}(2z)}{I_Q(2z)} z. \tag{2.15}$$

And hence the scaled variance can be expressed as [23]:

$$\omega = \frac{\langle N^2 \rangle - \langle N \rangle^2}{\langle N \rangle} = 1 + z\left(\frac{I_{Q-2}(2z)}{I_{Q-1}(2z)} - \frac{I_{Q-1}(2z)}{I_Q(2z)}\right) \tag{2.16}$$

Even under the thermodynamic limit this will not become a Poissonian distribution, e.g. $\omega = 1$, but will tend to a value of $\omega = 0.5$ for a electrically neutral gas. But this does in fact not mean that the well established equivalence of statistical ensembles is violated [24], as under the thermodynamic limit probability distributions for the densities, rather than the absolute number distribution, are the same in a grand canonical and a canonical ensemble, δ functions. In figure 2.1 the asymptotic behavior of the scaled variance in a simple Boltzmann pion gas is shown. The solid line is for the positive pion, which is affected by charge conservation and for comparison, the neutral pion (dashed line) is included, which exhibits, unconstrained by charge conservation, the usual grand canonical Poissonian behavior.

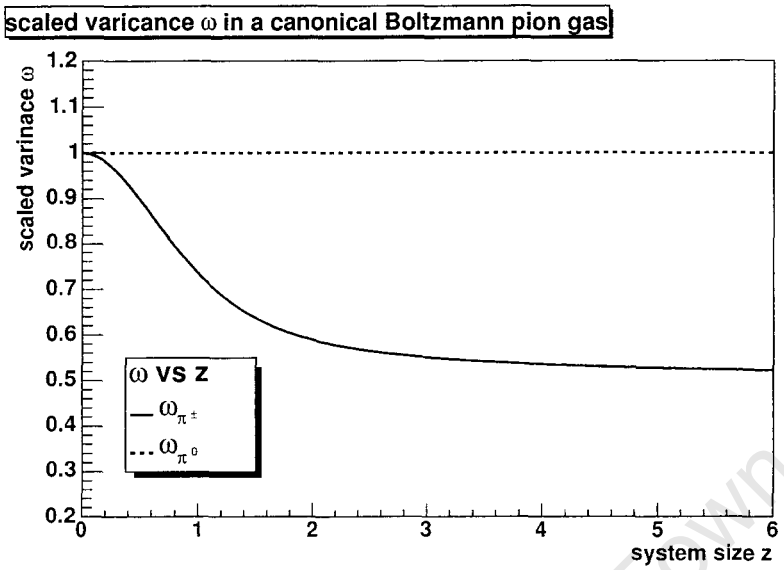

Figure 2.1: Scaled variance in a neutral canonical Boltzmann pion gas

2.2 Primordial Distributions

2.2.1 Charge Distribution

In order to calculate distributions from the thermal model, one needs to associate a probability with a certain constellation or charge configuration. Thus one interprets the partition function $\mathcal{Z}_Q^C$ as statistical weight factor. In a QC one counts the number of available states consistent with a particular charge state, while in a GC the sum over all possible charge configurations has to be taken. The normalization criterion requires that

$$\sum_{Q=-\infty}^{\infty} \mathcal{Z}_Q^C = \mathcal{Z}_{\langle Q \rangle}^{GC}, \tag{2.17}$$

where the subscript $\langle Q \rangle$ refers to the average charge in the GC with the same chemical potential used in both ensembles, such that $\langle Q \rangle$ is the most likely charge state. Therefore is the probability of finding a particular charge state realized, due to the presence of a charge bath, the number of states consistent with the selected charge configuration divided by all possible states.

$$P_{\langle Q \rangle}(Q) = \frac{\mathcal{Z}_Q^C}{\mathcal{Z}_{\langle Q \rangle}^{GC}} \tag{2.18}$$

In the case of a grand canonical Boltzmann pion gas the analytical solution is

$$\mathcal{Z}^{GC}_{\langle Q\rangle} = \exp\left(2z\cosh\left(\frac{\mu_Q}{T}\right)\right). \tag{2.19}$$

The expectation value for the average number of electrical charges is thus given by

$$\langle Q\rangle = \frac{1}{\mathcal{Z}^{GC}_{\langle Q\rangle}}\left(T\frac{\partial}{\partial\mu_Q}\right)\mathcal{Z}^{GC}_{\langle Q\rangle} = 2z\sinh\left(\frac{\mu_Q}{T}\right). \tag{2.20}$$

and the inverse of the expectation value of the net-charge therefore is the required chemical potential

$$\frac{\mu_Q}{T} = \sinh^{-1}\left(\frac{\langle Q\rangle}{2z}\right), \tag{2.21}$$

which is now used in the canonical partition function.

$$\begin{aligned}
\mathcal{Z}^{C}_{Q} &= \int_{-\pi}^{\pi}\frac{d\phi_Q}{2\pi}\,e^{-iQ\phi_Q}\exp\left(ze^{\frac{\mu_Q}{T}}e^{i\phi_Q} + ze^{-\frac{\mu_Q}{T}}e^{-i\phi_Q}\right)\\
&= \int_{-\pi}^{\pi}\frac{d\phi_Q}{2\pi}\sum_{n=0}^{\infty}\frac{z^n}{n!}\sum_{k=0}^{\infty}\frac{z^k}{k!}\,e^{i(n-k-Q)\phi_Q}\,e^{(n-k)\frac{\mu_Q}{T}}\\
&= \sum_{n=0}^{\infty}\frac{z^n}{n!}\frac{z^{n-Q}}{(n-Q)!}\,e^{Q\frac{\mu_Q}{T}} = I_Q(2z)\;e^{Q\frac{\mu_Q}{T}}.
\end{aligned} \tag{2.22}$$

Hence the probability of finding a net-charge Q in a GC is

$$P_{\langle Q\rangle}(Q) = I_Q(2z)\,\frac{e^{Q\frac{\mu_Q}{T}}}{\exp\left(2z\cosh\left(\frac{\mu_Q}{T}\right)\right)}. \tag{2.23}$$

In other words, were charge and energy fluctuation allowed, due to the presence of a charge and heat bath with temperature T and chemical potential μ_Q, the charge distribution in a sub-volume V is given by equation 2.23. The normalization condition $\sum_{Q=-\infty}^{\infty}P_{\langle Q\rangle}(Q) = 1$ can be checked using the relation

$$\sum_{k=-\infty}^{\infty} I_k(x)\,t^k = e^{\frac{1}{2}x\left(t+\frac{1}{t}\right)}. \tag{2.24}$$

Further using the identities

$$\exp\left(n\sinh^{-1}(x)\right) = \left(x+\sqrt{1+x^2}\right)^n \qquad \text{and} \tag{2.25}$$

$$\cosh\left(\sinh^{-1}(x)\right) = \sqrt{1+x^2} \tag{2.26}$$

the result of reference [24] is reproduced.

$$P_{\langle Q\rangle}(Q) = I_Q(2z)\,\frac{\left(\frac{\langle Q\rangle}{2z} + \sqrt{1+\left(\frac{\langle Q\rangle}{2z}\right)^2}\right)^Q}{\exp\left(2z\sqrt{1+\left(\frac{\langle Q\rangle}{2z}\right)^2}\right)} \tag{2.27}$$

The inclusion of chemical potentials into the partition function $\mathcal{Z}_Q^C$ effectively shifts its mean away from the origin $\langle Q\rangle = 0$, while leaving, probably surprisingly, average particle yields in Boltzmann approximation unaffected [31].

$$\langle N_+\rangle = \frac{1}{\mathcal{Z}_Q^C}\left(T\frac{\partial}{\partial\nu_+}\right)\int_{-\pi}^{\pi}\frac{d\phi_Q}{2\pi}e^{-iQ\phi_Q}\exp\left(z_+e^{\frac{\mu_Q}{T}}e^{i\phi_Q} + z_-e^{-\frac{\mu_Q}{T}}e^{-i\phi_Q}\right)\Big|_{\nu_+=0}, \tag{2.28}$$

where again z_+ and z_- are the single particle partition functions for the positve and negative pion with particle specific chemical potentials ν_+ and ν_-. Using the results given above this integral yields,

$$\begin{aligned}\langle N_+\rangle &= \frac{1}{\mathcal{Z}_Q^C}\,\mathcal{Z}_{Q-1}^C\,ze^{\frac{\mu_Q}{T}}\\ &= \frac{I_{Q-1}(2z)\,e^{(Q-1)\frac{\mu_Q}{T}}}{I_Q(2z)\,e^{Q\frac{\mu_Q}{T}}}\,ze^{\frac{\mu_Q}{T}}\\ &= \frac{I_{Q-1}(2z)}{I_Q(2z)}\,z,\end{aligned} \tag{2.29}$$

which is independent of μ_Q. The inclusion of chemical potentials is for two reasons. Firstly there is no contradiction in using them, even if average yields in Boltzmann approximation are unaffected, since charge distributions will be shifted. And secondly all distributions are sensitive to chemical potentials when quantum statistics is employed.

2.2.2 Grand Canonical Multiplicity Distributions

The general definition of probability, based on the assumption that all (micro) states are equally likely, allows to derive a probability distribution from the partition function.

$$P(N) = \frac{\text{all states which have N } \pi^+}{\text{all states}} \tag{2.30}$$

This is implemented by the Fourier representation of the δ function. The angle ϕ_+ will be specific to positive pions π^+ rather than to the particles electrical charge, particle number thus will be treated like a quantum number.

$$\mathcal{Z}^{GC} = \exp\left(ze^{\frac{\mu_Q}{T}}e^{i\phi_+} + ze^{-\frac{\mu_Q}{T}}\right)\Big|_{\phi_+=0} = \text{all states} \tag{2.31}$$

$$\int_{-\pi}^{\pi}\frac{d\phi_+}{2\pi}e^{-iN\phi_+}\mathcal{Z}^{GC} = \text{all states which have N } \pi^+ \tag{2.32}$$

Thus the ratio gives the probability

$$\begin{aligned} P(N) &= \frac{\int_{-\pi}^{\pi}\frac{d\phi_+}{2\pi}e^{-iN\phi_+}\mathcal{Z}^{GC}}{\mathcal{Z}^{GC}} \\ &= \frac{\int_{-\pi}^{\pi}\frac{d\phi_+}{2\pi}e^{-iN\phi_+}\exp\left(ze^{\frac{\mu_Q}{T}}e^{i\phi_+}\right)\exp\left(ze^{-\frac{\mu_Q}{T}}\right)}{\exp\left(ze^{\frac{\mu_Q}{T}}\right)\exp\left(ze^{-\frac{\mu_Q}{T}}\right)} \\ &= \exp\left(-ze^{\frac{\mu_Q}{T}}\right)\frac{\left(ze^{\frac{\mu_Q}{T}}\right)^N}{N!} \end{aligned} \tag{2.33}$$

Hence the GC produces naturally a Poisson distribution who's k-th moment can be obtained from the definition,

$$\langle N^k\rangle = \sum_{n=0}^{\infty}P(n)n^k, \tag{2.34}$$

and gives the same result as a successive application of the derivative operator.

2.2.3 Canonical Multiplicity Distributions

Conserving charges suppresses in particular the moments of higher order and will alter the shape of the distribution. Through the implementation of a second δ function, one for the particle number, one for the net-charge, one can simultaneously treat both numbers canonically. For the normalization one has to count only states that have a net-charge Q.

$$\begin{aligned} P_Q(N) &= \frac{\text{all states with N } \pi^+\text{and net-charge Q}}{\text{all states with net-charge Q}} \\ &= \frac{\int_{-\pi}^{\pi}\frac{d\phi_Q}{2\pi}\int_{-\pi}^{\pi}\frac{d\phi_+}{2\pi}e^{-iQ\phi_Q}e^{-iN\phi_+}\mathcal{Z}^{GC}}{\int_{-\pi}^{\pi}\frac{d\phi_Q}{2\pi}e^{-iQ\phi_Q}\mathcal{Z}^{GC}}, \end{aligned} \tag{2.35}$$

where the angle ϕ_Q refers to the electrical charge of the pion gas, while the angle ϕ_+ is related to the particle number of the, arbitrarily chosen, positive particle.

$$\mathcal{Z}^{GC} = \exp\left(ze^{\frac{\mu_Q}{T}}e^{i\phi_Q}e^{i\phi_+} + ze^{-\frac{\mu_Q}{T}}e^{-i\phi_Q}\right) \tag{2.36}$$

After having solved the integral using the constraining conditions from the δ functions, one obtains for the canonical multiplicity distribution

$$P_Q(N) = \frac{z^N}{N!}\frac{z^{N-Q}}{(N-Q)!}\left(I_Q\left(2z\right)\right)^{-1}. \tag{2.37}$$

Despite the fact that a chemical potential has been included, the result is independent of the same. In the special case $Q = 0$ one gets the result in reference [23] for a neutral Boltzmann pion gas. The expectation value (and higher moments) can be obtained directly form the definition after a short calculation

$$\langle N\rangle = \sum_{k=0}^{\infty} P_Q(k)\, k = \frac{I_{Q-1}\left(2z\right)}{I_Q\left(2z\right)}z. \tag{2.38}$$

2.2.4 Joint Probability Distribution

As a further instructive and useful example one can consider the joint probability of finding a particular charge and multiplicity state realized in a GC.

$$\begin{aligned} P(Q,N) &= \frac{\text{all states with net-charge Q and N } \pi^+}{\text{all states}} \\ &= \frac{\int_{-\pi}^{\pi}\frac{d\phi_Q}{2\pi}\int_{-\pi}^{\pi}\frac{d\phi_+}{2\pi}e^{-iQ\phi_Q}e^{-iN\phi_+}\mathcal{Z}^{GC}}{\mathcal{Z}^{GC}}, \end{aligned} \tag{2.39}$$

while on the other hand, after having multiplied both denominator and numerator with the charge canonical partition function $\mathcal{Z}_Q^C$

$$P(Q,N) = \frac{\int_{-\pi}^{\pi}\frac{d\phi_Q}{2\pi}\int_{-\pi}^{\pi}\frac{d\phi_+}{2\pi}e^{-iQ\phi_Q}e^{-iN\phi_+}\mathcal{Z}^{GC}}{\int_{-\pi}^{\pi}\frac{d\phi_Q}{2\pi}e^{-iQ\phi_Q}\mathcal{Z}^{GC}}\,\frac{\int_{-\pi}^{\pi}\frac{d\phi_Q}{2\pi}e^{-iQ\phi_Q}\mathcal{Z}^{GC}}{\mathcal{Z}^{GC}}, \tag{2.40}$$

the joint probability $P(Q,N)$ factorizes into the canonical multiplicity (conditional) distribution and a grand canonical (marginal) charge distribution.

$$P(Q,N) = P_Q(N)P(Q) \tag{2.41}$$

And can be therefore spelled out as

$$P(Q,N) = \frac{z^N}{N!}\frac{z^{N-Q}}{(N-Q)!}\frac{e^{Q\frac{\mu_Q}{T}}}{\exp\left(2z\cosh\left(\frac{\mu_Q}{T}\right)\right)}. \tag{2.42}$$

The figure 2.2 shows the joint probability of finding a on average neutral

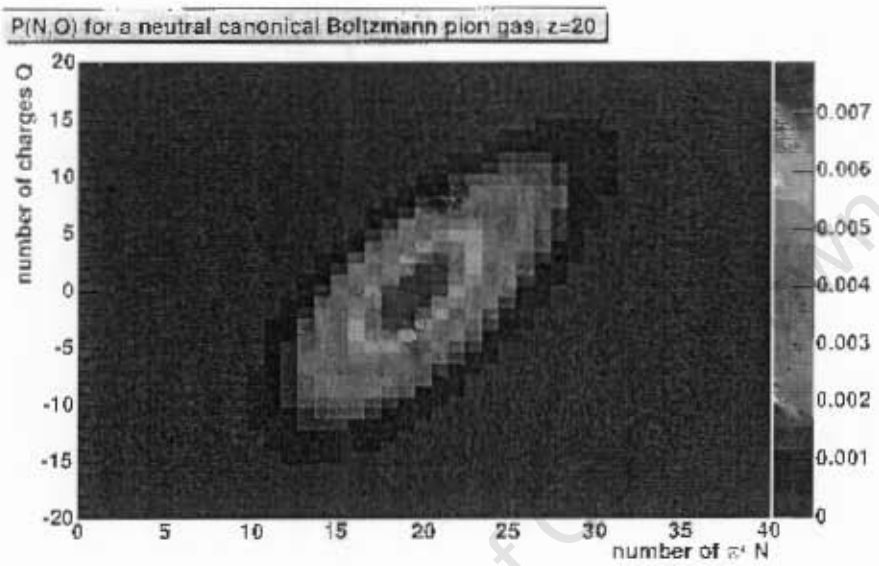

Figure 2.2: Joint probability of having N π^+ while the charge is Q

grand canonical Boltzmann pion gas in a particular charge and multiplicity state. The average system size was chosen to be $z = 20$. A non zero chemical potential would shift the distribution towards a higher or lower multiplicity of the positive pion and away from charge neutrality, while leaving the canonical multiplicity (conditional) distributions unaffected.

2.3 Particle Ratios

For the discussion of particle ratios it will be important to differentiate between

$$\frac{\langle N_j \rangle}{\langle N_k \rangle} = \frac{\sum_{n=0}^{\infty} P_j(n)\, n}{\sum_{m=0}^{\infty} P_k(m)\, m}, \tag{2.43}$$

which is the ratio of average yields of species j and k, e.g. the first moment of the respective distributions, and the event-by-event measure used in this thesis, which is ultimately dependent on correlations due to exact conservation laws contained in the conditional distribution $P_{j,k}(N_j, N_k)$.

$$\langle \frac{N_j}{N_k} \rangle = \sum_{n=0}^{\infty} \sum_{m=1}^{\infty} P_{j,k}(n,m) \frac{n}{m} = \langle R \rangle \tag{2.44}$$

At least for large systems the expectation values for the event-by-event ratios are similar in both ensembles, $\langle R \rangle_{GC} \approx \langle R \rangle_{QC}$, but their relative width can be quite different, which could be a very good test for which statistical ensemble to use. As an example we first consider the ratio of positively charged pions to the sum of charged and uncharged pions in two statistical ensembles and than compare this to the ratio neutral to the sum of all pions.
Throughout this thesis the measure

$$RMS_{\langle R \rangle} = \sqrt{\langle R^2 \rangle - \langle R \rangle^2} \tag{2.45}$$

is used to describe the width of the ratio distribution.

2.3.1 Grand Canonical Ratios

For the purpose of this calculation we define the single particle partition functions for the charged pions π^+ and π^- with chemical potentials given by equation 2.20

$$z_{\pm} = gV \int \frac{d^3p}{(2\pi)^3} e^{-\frac{E_{\pm}}{T} \pm \frac{\mu_Q}{T}} = \tilde{z} e^{\pm \frac{\mu_Q}{T}}, \tag{2.46}$$

and include the neutral pion π^0 as well

$$z_0 = gV \int \frac{d^3p}{(2\pi)^3} e^{-\frac{E_0}{T}}. \tag{2.47}$$

The energy eigenvalues $E = \sqrt{p^2 + m^2}$ are different due to the different masses of the charged pions and the neutral pion. In order to treat the number of π^+ as well as the sum of all pions, $\pi^+ + \pi^- + \pi^0$, canonically,

e.g. deriving multiplicity distributions, the total partition function has to be written as

$$\mathcal{Z} = \exp\left(z_+ e^{i\phi_+} e^{i\phi_N} + z_- e^{i\phi_N} + z_0 e^{i\phi_N}\right), \tag{2.48}$$

where the angle ϕ_+ refers only to the π^+ while all particles (π^+, π^- and π^0) have an angle ϕ_N. The definition for the probability reads

$$P_{\langle Q\rangle}(N_+, N) = \frac{\text{all states with } N_+ \ \pi^+ \text{ and } N \ \pi^x}{\text{all states}}.$$

The subscript $\langle Q\rangle$ denotes the use of a chemical potential and refers to the most likely charge state of the system. In terms of the system partition function one has to solve the integral

$$\begin{aligned} P_{\langle Q\rangle}(N_+, N) &= \frac{\int_{-\pi}^{\pi}\frac{d\phi_+}{2\pi}\int_{-\pi}^{\pi}\frac{d\phi_N}{2\pi} e^{-iN_+\phi_+} e^{-iN\phi_N}\mathcal{Z}}{\mathcal{Z}} \\ &= e^{-(z_+ + z_- + z_0)}\frac{z_+^{N_+}}{N_+!}\sum_{m=0}^{N-N_+}\frac{z_-^m}{m!}\frac{z_0^{N-N_+-m}}{(N-N_+-m)!}. \end{aligned} \tag{2.49}$$

2.3.2 Canonical Ratios

Comparison of the grand canonical result requires that we choose $Q = \langle Q\rangle$ for the charge state of the QC. The single particle partition functions z_+, z_- and z_0 are defined as before and the total partition function becomes, after inserting a further angle ϕ_Q for charge conservation

$$\mathcal{Z} = \exp\left(z_+ e^{i\phi_+} e^{i\phi_N} e^{i\phi_Q} + z_- e^{i\phi_N} e^{-i\phi_Q} + z_0 e^{i\phi_N}\right) \tag{2.50}$$

and hence we have to solve a triple integral and divide by the number of all states consistent with a net-charge Q, the canonical partition function $\mathcal{Z}_Q^C$.

$$\begin{aligned} P_Q(N_+, N) &= \frac{\text{all states with net-charge } Q, \ N_+ \ \pi^+, \text{ and } N \ \pi^x}{\text{all states with net-charge Q}} \\ &= \frac{\int_{-\pi}^{\pi}\frac{d\phi_+}{2\pi}\int_{-\pi}^{\pi}\frac{d\phi_N}{2\pi}\int_{-\pi}^{\pi}\frac{d\phi_Q}{2\pi} e^{-iN_+\phi_+} e^{-iN\phi_N} e^{-iQ\phi_Q}\mathcal{Z}}{\int_{-\pi}^{\pi}\frac{d\phi_Q}{2\pi} e^{-iQ\phi_Q}\mathcal{Z}} \\ &= \left(e^{z_0} I_Q(2\tilde{z})\right)^{-1}\frac{\tilde{z}^{N_+}}{N_+!}\frac{\tilde{z}^{N_+-Q}}{(N_+-Q)!}\frac{z_0^{N-2N_+-Q}}{(N-2N_+-Q)!} \end{aligned} \tag{2.51}$$

Figure 2.3 shows the above ratios in a electrically neutral system. The rather similar values for the mean of the curves can be understood with the fact

$\langle R\rangle = \langle \frac{N_+}{N} \rangle$	$\langle Q\rangle = 0$	$Q = 0$	$\langle Q\rangle = 20$	$Q = 20$
$\langle N_+\rangle$	33.7147	33.4638	45.1665	44.9362
$\langle N\rangle$	101.506	101.004	104.409	103.949
$\langle R\rangle$	0.332146	0.331303	0.432591	0.433269
$RMS_{\langle R\rangle}$	0.0469821	0.0236724	0.0487226	0.0250319

Table 2.1: Event-by-event particle ratio $\langle \frac{N_+}{N} \rangle$ in a Boltzmann pion gas with $r = 6fm$, $T = 0.15GeV$, $\mu_{Q=0} = 0$ and $\mu_{Q=20} = 0.0439GeV$ respectively

that the system is rather large and a grand canonical treatment of yields, hence its mean value, but not the distribution, is sufficient. The height of the curve depends on the number of bins chosen. Fractions of small integers, and only integer particle numbers are allowed, lead to discrete probability distributions for particle ratios. Nevertheless, both curves are equally well fitted by Gaussians with almost same mean, but different width, see table 2.1. The second histogram 2.4 shows the distribution of for a system with a surplus of 20 positive charges what leads to a shift of the mean. Hence for this particular ratio, grand canonical and canonical ensemble lead to different distributions.

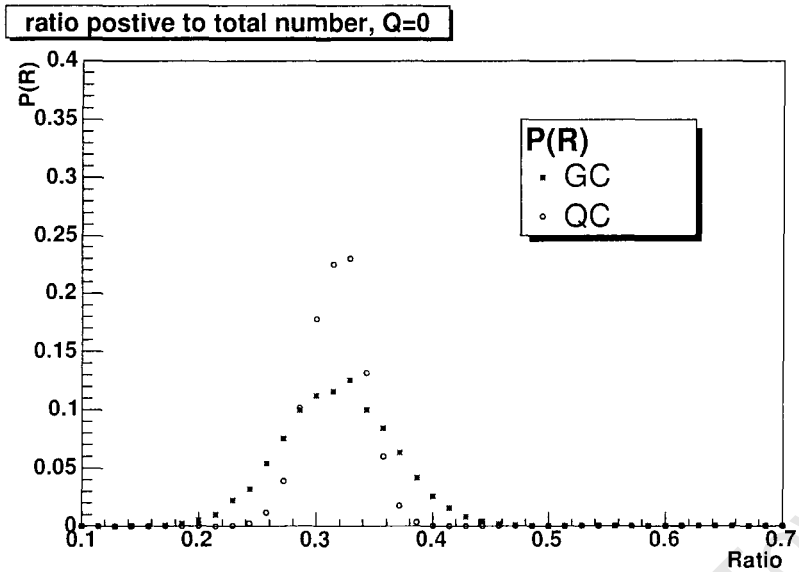

Figure 2.3: The ratio of the number of positive pions to the sum of all pions in a grand canonical and a canonical ensemble, with a zero net-charge

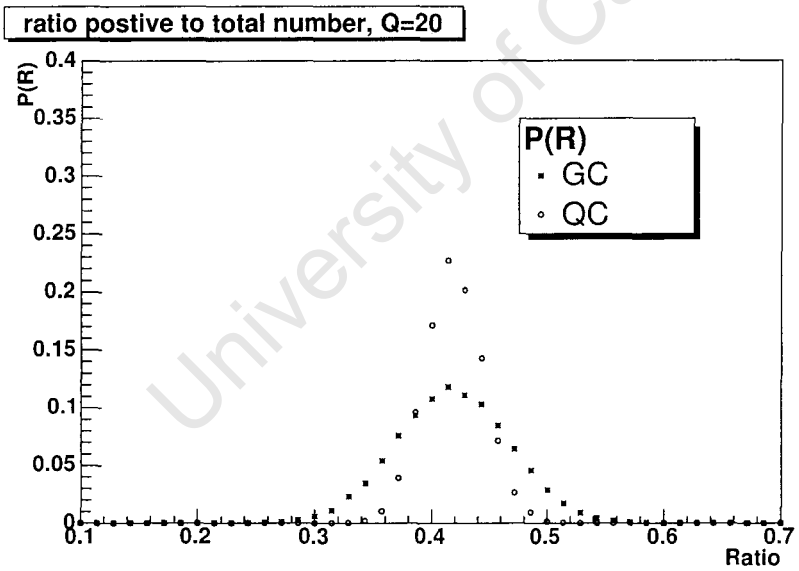

Figure 2.4: The ratio of the number of positive pions to the sum of all pions in a grand canonical and a canonical ensemble, with a net-charge of 20

2.3.3 Example II

As a further example we consider the ratio of the number of neutral pions to the sum of neutral and charged particles in both ensembles. The calculations are similar to the ones before and only the results are given. Grand canonically the individual multiplicity distributions are Poissonian

$$P_{\langle Q\rangle}(N_0, N) = e^{-(z_+ + z_- + z_0)} \frac{z_0^{N_0}}{N_0!} \sum_{m=0}^{N-N_0} \frac{z_+^m}{m!} \frac{z_-^{N-N_0-m}}{(N-N_0-m)!}. \tag{2.52}$$

While, when charge conservation is enforced, one cannot have any combination of N, N_0, and Q due the conditions $Q = N_+ - N_-$ and $N = N_+ + N_- + N_0$.

$$P_Q(N_0, N) = \left(e^{z_0}\, I_Q\left(2\tilde{z}\right)\right)^{-1} \frac{z_0^{N_0}}{N_0!} \frac{\tilde{z}^{\frac{N-N_0+Q}{2}}}{\left(\frac{N-N_0+Q}{2}\right)!} \frac{\tilde{z}^{\frac{N-N_0-Q}{2}}}{\left(\frac{N-N_0-Q}{2}\right)!} \tag{2.53}$$

Neither shape nor width of the distributions in figures 2.5 and 2.6 seem to be really affected by the choice of ensemble and seem to be rather robust when the number of charges in the system is changed. The same parameter set as above was used and the results are summarized in table 2.2.

$\langle R\rangle = \langle \frac{N_0}{N} \rangle$	$\langle Q\rangle = 0$	$Q = 0$	$\langle Q\rangle = 20$	$Q = 20$
$\langle N_0\rangle$	34.0763	34.0763	34.0763	34.0763
$\langle N\rangle$	101.506	101.004	104.409	103.949
$\langle R\rangle$	0.335709	0.337394	0.326373	0.327653
$RMS_{\langle R\rangle}$	0.0471072	0.0473462	0.0461115	0.0456418

Table 2.2: Event-by-event particle ratio $\langle \frac{N_0}{N} \rangle$ in a Boltzmann pion gas with $r = 6fm$, $T = 0.15GeV$, $\mu_{Q=0} = 0$ and $\mu_{Q=20} = 0.0439GeV$ respectively

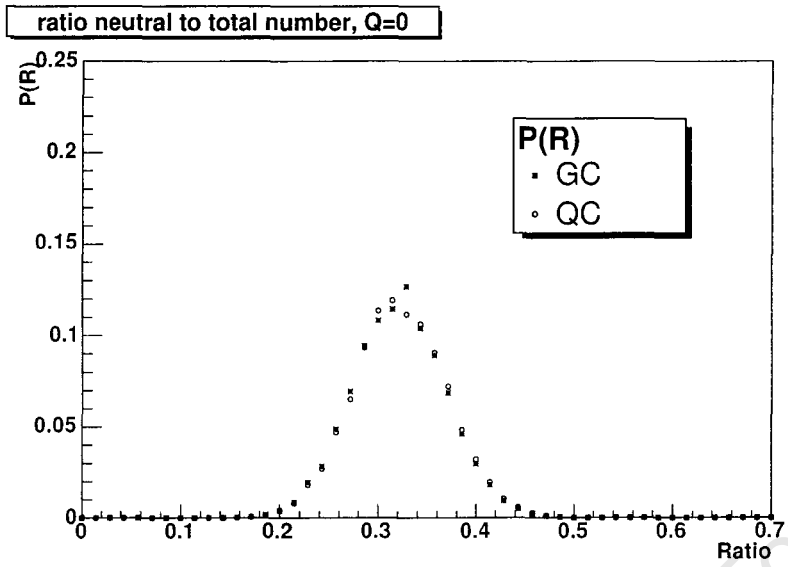

Figure 2.5: The ratio of the number of neutral pions to the sum of all pions in a grand canonical and a canonical ensemble, with a zero net-charge

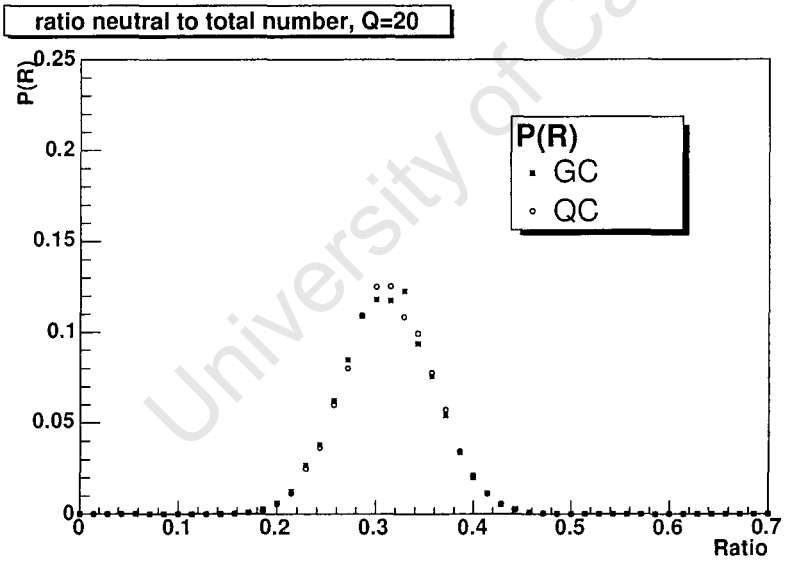

Figure 2.6: The ratio of the number of neutral pions to the sum of all pions in a grand canonical and a canonical ensemble, with a net-charge of 20

2.4 Systems in Thermal Contact

One could further assume two, or more, smaller systems embedded into a larger, canonical or grand canonical, one and ask what the respective distributions would be. For this let us assume two systems Ω' and $\tilde{\Omega}$ which are grand canonical in nature, but are subject to joint exact conservation of their net-charge, hence charges and heat are allowed to move between Ω' and $\tilde{\Omega}$, while the combined system Ω, a canonical one, is the sum of the two and is placed in a heat bath. Therefore $V = V' + \tilde{V}$ and $Q = Q' + \tilde{Q}$, where V denotes the volume and Q the charge state of the respective systems. If Ω' and $\tilde{\Omega}$ are both grand canonical systems, then the probability of finding them in a particular charge state is given by equation 2.23.

$$P_{\tilde{V}}\left(\tilde{Q}\right) = I_{\tilde{Q}}\left(2z_0\tilde{V}\right)\frac{e^{\tilde{Q}\frac{\mu_Q}{T}}}{\exp\left(2z_0\tilde{V}\cosh\left(\frac{\mu_Q}{T}\right)\right)}$$

Where we have assumed that both sub-systems share a common temperature T and a common chemical potential μ_Q and used $z = Vz_0$. For the system Ω, if it was further in contact with a even larger heat and charge bath, the probability of finding it in a chosen charge state would be

$$P_V(Q) = \sum_{\tilde{Q}=-\infty}^{\infty} P_{\tilde{V}}(\tilde{Q})P_{V-\tilde{V}}(Q-\tilde{Q}). \tag{2.54}$$

And Ω would be grand canonical and as well described by equation 2.23, while when Ω is kept at a fixed charge Q, this would be the statistical weight factor for the QC. For a Boltzmann pion gas this is a discrete convolution of the two sub-distributions, or essentially the sum over all possible charge split-ups between the two domains. Hence the effective charge distribution $\bar{P}_{\tilde{V}}(\tilde{Q})$ for the sub-system $\tilde{\Omega}$ is

$$\bar{P}_{\tilde{V}}(\tilde{Q}) = \frac{P_{\tilde{V}}(\tilde{Q})P_{V-\tilde{V}}(Q-\tilde{Q})}{P_V(Q)} = \frac{I_{\tilde{Q}}(\tilde{V})I_{Q-\tilde{Q}}(V-\tilde{V})}{I_Q(V)}, \tag{2.55}$$

where the normalization $\exp\left(2z_0V\cosh\left(\frac{\mu_Q}{T}\right)\right)$ and $\exp\left(Q\frac{\mu_Q}{T}\right)$ canceled out. The normalization condition $\sum_{\tilde{Q}=-\infty}^{\infty}\bar{P}_{\tilde{V}}(\tilde{Q}) = 1$ follows from

$$I_Q(V) = \sum_{\tilde{Q}=-\infty}^{\infty} I_{\tilde{Q}}(\tilde{V})I_{Q-\tilde{Q}}(V-\tilde{V}). \tag{2.56}$$

Hence, even though Ω' and $\tilde{\Omega}$ are in grand canonical contact, their respective charge distributions, owing to their finiteness, will not be. The GC is thus

in this picture the correct description for a small system embedded into a bigger one. In the large volume limit the mean values $\langle N \rangle$ converge rather quickly due to the asymptotics of the Bessel functions, yet their correlations will not. Therefore only in the thermodynamic limit $V, Q \to \infty$, $\frac{Q}{V} = \rho = const$, and when the volume of the system $\tilde{\Omega}$ is much larger than that of Ω' ($\frac{V}{V'} \ll 1$), while having the same chemical potential and therefore charge density $\tilde{\rho} = \rho'$, will the distributions of $\tilde{\Omega}$ be grand canonical or uncorrelated with Ω'. For RHIC experiments this condition could be sufficiently met as the mostly analyzed mid rapidity slice contains about 1/8 of the total multiplicity, allowing for a grand canonical description of those fluctuations [32].

2.5 Limited Geometrical Acceptance

Taking only one system, while assuming only information about a subsystem, i.e. due to a non-perfect detector, is similar to the concept of two systems in ideal thermal contact. Rather than a geometrical acceptance, a rapidity subset is chosen which allows to describe the longitudinal, e.g. along the beam axis, distribution of particles. This is not a kinematic correlation, for which the micro canonical ensemble would be the correct choice. Nevertheless show already the grand canonical and canonical ensembles remarkable differences. As it was pointed out in reference [23] if one adds some uncertainty to the multiplicity distribution, like a probability of detecting a particle, due to detector efficiency and geometric coverage of the interaction volume, one will, in the limit of a very bad detector with vanishing detection probability, recover a Poisson distribution. This section will thus discuss the multiplicity distributions for rapidity intervals (or windows) Δy.

2.5.1 Grand Canonical Multiplicity Distribution

In a GC, where by definition no correlations are imposed one does not expect a deviation from a Poisson distribution. Effectively can the observed subsystem be considered as embedded in a heat and charge bath. Generally one could define any such distribution by

$$P = \frac{\text{all states that meet some criterion}}{\text{all states}}. \tag{2.57}$$

For the following section this criterion will be a particle's rapidity y. The rapidity distribution 2.58 of produced particles is derived in appendix D.

$$\frac{dN}{dy} = \frac{gVT^3}{(2\pi)^2} e^{\frac{\mu}{T}} e^{-\frac{m\cosh(y)}{T}} \left(\frac{m^2}{T^2} - \frac{2m}{T\cosh(y)} + \frac{2}{\cosh(y)^2} \right) \tag{2.58}$$

Hence the partition function $\mathcal{Z}^{GC} = \exp(z_p + z_m)$ can be written as the sum of particles which fall into a chosen window Δy and the ones which do not $(\mathbf{R} \setminus \Delta y)$,

$$\mathcal{Z}^{GC} = \exp\left(\int_{\Delta y} \frac{dN_p}{dy} dy + \int_{\mathbf{R}\setminus\Delta y} \frac{dN_p}{dy} dy + \int_{-\infty}^{\infty} \frac{dN_m}{dy} dy \right). \tag{2.59}$$

For the following it will be convenient the use a shorthand notation for the integrals

$$\begin{aligned} \int_{\Delta y} \frac{dN_p}{dy} dy &= z_{p,\Delta y} \\ \int_{\mathbf{R}\setminus\Delta y} \frac{dN_p}{dy} dy &= z_{p,\overline{\Delta y}} \\ \int_{-\infty}^{\infty} \frac{dN_m}{dy} dy &= z_m, \end{aligned}$$

where again arbitrarily the positive pion (N_p) was chosen over the negative pion (N_m) for the calculation. The probability to find some number $N_{\Delta y}$ of π^+ in the rapidity window Δy is therefore

$$P(N_{\Delta y}) = \frac{\int_{-\pi}^{\pi} \frac{d\phi}{2\pi} e^{-iN_{\Delta y}\phi} \exp\left(z_{p,\Delta y} e^{i\phi} + z_{p,\overline{\Delta y}} + z_m \right)}{\exp\left(z_{p,\Delta y} + z_{p,\overline{\Delta y}} + z_m \right)}, \tag{2.60}$$

and one recovers a Poisson distribution, regardless of the rapidity subset chosen.

$$P(N_{\Delta y}) = \exp(-z_{p,\Delta y}) \frac{z_{p,\Delta y}^{N_{\Delta y}}}{N_{\Delta y}!} \tag{2.61}$$

2.5.2 Charge Distribution

Following the same arguments as above will the charge distribution of a embedded grand canonical sub-system be again grand canonical in nature,

and hence equation 2.23 can be applied. In case the total system is kept at a fixed net-charge, but one has only information about the sub-system which falls into the rapidity window Δy, this wont hold anymore and hence one expects correlations due to the finite charge in the system, as any excess in one rapidity interval will have to be balanced by the remaining system. The normalization will be the canonical partition function 2.22. And therefore

$$\mathcal{Z} = \exp\left(z_{p,\Delta y}e^{i\phi_{Q\Delta y}}e^{i\phi_Q} + z_{p,\overline{\Delta y}}e^{i\phi_Q} + z_{m,\Delta y}e^{-i\phi_{Q\Delta y}}e^{-i\phi_Q} + z_{m,\overline{\Delta y}}e^{-i\phi_Q}\right) \tag{2.62}$$

$$P_Q\left(Q_{\Delta y}\right) = \frac{\int_{-\pi}^{\pi}\frac{d\phi_Q}{2\pi}\int_{-\pi}^{\pi}\frac{d\phi_{Q\Delta y}}{2\pi}e^{-iQ\phi_Q}e^{-iQ_{\Delta y}\phi_{Q\Delta y}}\mathcal{Z}}{\int_{-\pi}^{\pi}\frac{d\phi_Q}{2\pi}e^{-iQ\phi_Q}\mathcal{Z}}. \tag{2.63}$$

As before cancel chemical potentials in a Boltzmann QC out, and one can drop the indexes p and m, thus particle and anti-particle have identical single particle partition functions $z_{p,\Delta y} = z_{m,\Delta y} = z_{\Delta y}$ and $z_{p,\overline{\Delta y}} = z_{m,\overline{\Delta y}} = z_{\overline{\Delta y}}$.

$$P_Q\left(Q_{\Delta y}\right) = \frac{I_{Q_{\Delta y}}\left(2z_{\Delta y}\right)I_{Q-Q_{\Delta y}}\left(2z_{\overline{\Delta y}}\right)}{I_Q\left(2\left(z_{\Delta y}+z_{\overline{\Delta y}}\right)\right)} \tag{2.64}$$

In the limit of a vanishing rapidity interval $\overline{\Delta y}$ contributions of the second Bessel function will be zero, except when $Q_{\Delta y} = Q$ and one gets 1.

2.5.3 Canonical Multiplicity Distribution

For canonical multiplicity distribution the total system is again kept at a fixed net-charge Q, while we consider a rapidity window Δy and count the number of positive and negative pions which fall into it.

$$P^Q_{\Delta y}\left(N_p, N_m\right) = \frac{z^{N_p}_{\Delta y}}{N_p!}\frac{z^{N_m}_{\Delta y}}{N_m!}\frac{I_{Q-N_p+N_m}\left(2z_{\overline{\Delta y}}\right)}{I_Q\left(2z_{\Delta y}+2z_{\overline{\Delta y}}\right)} \tag{2.65}$$

The probability distribution for only positive particles is therefore obtained via summation over a states N_m with a given N_p

$$P^Q_{\Delta y}\left(N_p\right) = \frac{z^{N_p}_{\Delta y}}{N_p!}\sum_{N_m=0}^{\infty}\frac{z^{N_m}_{\Delta y}}{N_m!}\frac{I_{Q-N_p+N_m}\left(2z_{\overline{\Delta y}}\right)}{I_Q\left(2z_{\Delta y}+2z_{\overline{\Delta y}}\right)}. \tag{2.66}$$

The further moments of this distribution can be now obtained from

$$\langle N^k_p\rangle = \sum_{n_p=0}^{\infty}P^Q_{\Delta y}\left(n_p\right)n^k_p. \tag{2.67}$$

As only the fraction λ of the observed phase space, rather than a particular rapidity window, matters one can define

$$z_{\Delta y} = \lambda z \qquad \text{and} \qquad z_{\overline{\Delta y}} = (1-\lambda)\, z. \tag{2.68}$$

Under the limit $\lambda \longrightarrow 1$ equation 2.37 is obtained. Figures 2.7 and 2.8 show the scaled variance ω for a large system with $z = 6$ and a small system $z = 2$ with charge contents $Q = 0\ , \pm 2$ as a function of the fraction λ of observed particles. A scaled variance of less than 0.5 quite possible when the number of particles, which are the charges carriers, is of the same magnitude as the total system $\langle N_p + N_m \rangle$, and a very narrow distribution is the result. Remarkably the function $\omega(\lambda)$ falls on straight lines. For quantum statistical or micro canonical ensembles this should not hold anymore, as in the case of the former equation 2.58 for the rapidity distribution $\frac{dN}{dy}$ is not valid, while in the case of the latter, due to energy and momentum conservation, the choice of subset would matter.
Nevertheless considering the limiting case where only a random subset of particles of the system is chosen for detection, e.g. particles are observed indepentently this can be parameterized as [23]:

$$\omega^{acc} = 1 - \lambda + \lambda\, \omega^{4\pi}, \tag{2.69}$$

where ω^{acc} refers to scaled variance of the subset of detected particles, while $\omega^{4\pi}$ is its value if all particles were observed. In reality this assumption is certainly not valid. Bose and Fermi statistics, exactly enforced energy and momentum conservation, particle decay, and collective motion correlates particles in momentum space. These effect would certainly by important in a rigouros comparison with heavy ion collision data.

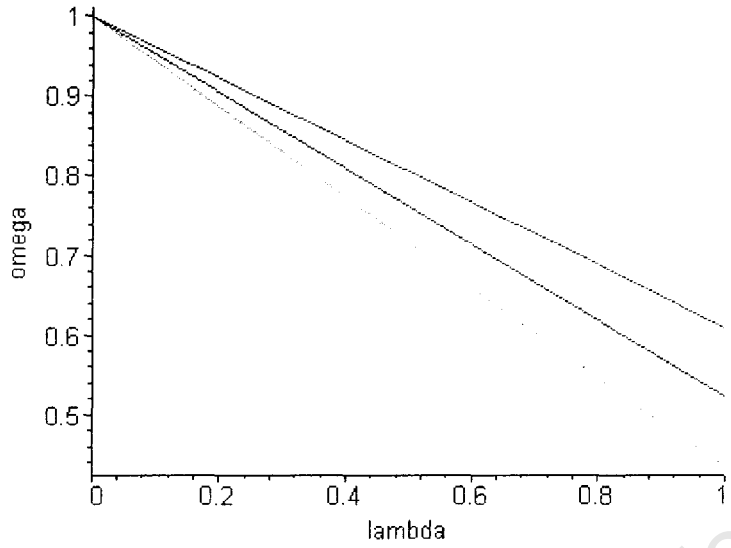

Figure 2.7: Scaled variance ω as a function of the observed fraction of positive pions in a canonical ensemble in Boltzmann approximation for $z = 6$ and a net-charge of $Q = -2$ (red line), $Q = 0$ (blue line), and $Q = 2$ (green line)

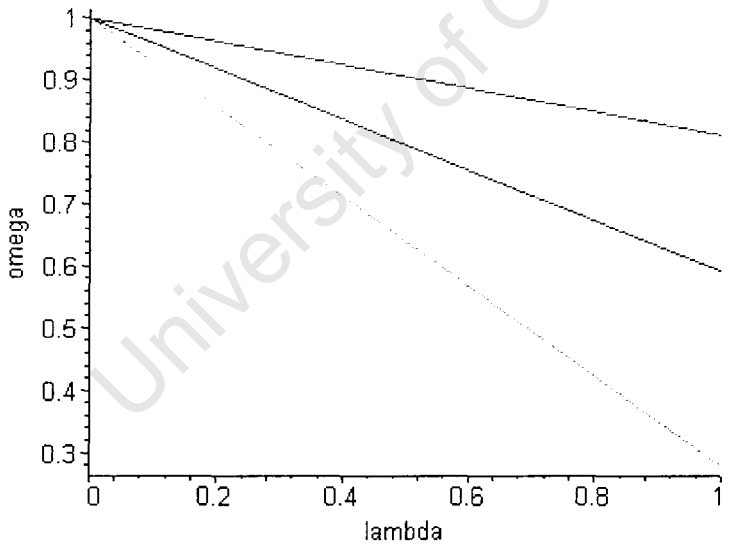

Figure 2.8: Scaled variance ω as a function of the observed fraction of positive pions in a canonical ensemble in Boltzmann approximation for $z = 2$ and a net-charge of $Q = -2$ (red line), $Q = 0$ (blue line), and $Q = 2$ (green line)

2.6 Quantum Statistics

It is known that even in the GC and under the thermodynamic limit fermions and bosons are not Poisson distributed and hence their distributions naturally deviate from the Boltzmann case. Further imposing conservation laws narrows distributions, while in a correct quantum statistical treatment in the presence of a chemical potential again enhances fluctuations in the case of bosons and further suppresses them for fermions [31]. This is a fundamental difference to the Boltzmann approximation, where chemical potentials in the GC only shifted the mean while they dropped out altogether in the QC and left multiplicity distributions thus unaffected. This section attempts to approximate the quantum statistical partition function as well as particle multiplicity distributions for finite systems through Taylor expansion of the characteristic function. Further will the final state distributions in chapter 3 be done using the same method, while a more detailed discussion of the meaning of the characteristic function is in chapter 5.
The single particle partition function for a positive particle reads

$$z_p = gV \int \frac{d^3p}{(2\pi)^3} \ln\left(1 \pm e^{-\frac{E}{T}} e^{\frac{\mu_Q}{T}} e^{\frac{\nu_p}{T}}\right)^{\pm 1}, \tag{2.70}$$

where the upper sign $(+)$ denotes to fermions and the lower sign $(-)$ to bosons. Using the identity for $\mid x \mid < 1$, what constrains the chemical potential and temperature range at a given mass,

$$\pm \ln(1 \pm x) = \sum_{n=1}^{\infty} (\mp 1)^{n+1} \frac{x^n}{n}, \tag{2.71}$$

one can re-write equation 2.70 into a sum of integrals of type 2.2

$$z_p = \sum_{n=1}^{\infty} (\mp 1)^{n+1} \frac{e^{n\frac{\mu_Q}{T}} e^{n\frac{\nu_p}{T}}}{n^4} \left[\frac{gV}{2\pi^2} n^2 m^2 T K_2\left(\frac{nm}{T}\right)\right]. \tag{2.72}$$

The upper sign (now $-$) still denotes to fermions and the lower one (now $+$) to bosons, while taking only the first term ($n = 1$) is the Boltzmann approximation. Using the shorthand notation $\langle N_n \rangle = \frac{gV}{2\pi^2} m^2 n^2 T K_2\left(\frac{mn}{T}\right)$, thus yields a sum over particles with n times the mass and quantum numbers of the original one

$$z_p = \sum_{n=1}^{\infty} (\mp 1)^{n+1} \langle N_n \rangle n^{-4} e^{n\frac{\mu_Q}{T}} e^{n\frac{\nu_p}{T}}. \tag{2.73}$$

And write for the negative particle with opposite sign for the charge, and particle specific chemical potential ν_m

$$z_m = \sum_{n=1}^{\infty} (\mp 1)^{n+1} \langle N_n \rangle n^{-4} e^{-n\frac{\mu_Q}{T}} e^{n\frac{\nu_m}{T}}. \tag{2.74}$$

The grand canonical partition function thus reads

$$\mathcal{Z}^{GC,Q} = \exp(z_p + z_m), \tag{2.75}$$

while the substitutions $\frac{\mu_Q}{T} \to \frac{\mu_Q}{T} + i\phi_Q$ and $\frac{\nu_{p,m}}{T} \to i\phi_{p,m}$ will be necessary for a canonical treatment for the respective quantum numbers.

2.6.1 Charge Distribution

Charge distributions generally depend on the chemical potentials as they determine the charge expectation value $\langle Q \rangle = \kappa_1$, and therefore the difference between the multiplicities of positive and negative particles. Hence should, as particle number distributions are different for the different statistics, the charge distributions for fermions, bosons and Boltzmann particles not be the same. Again the definition of the probability of finding a net-charge Q in a volume which is placed in a heat and charge bath as the ratio of canonical to grand canonical partition function

$$P(Q) = \frac{\int_{-\pi}^{\pi} \frac{d\phi_Q}{2\pi} e^{-iQ\phi_Q} \mathcal{Z}^{GC,Q}}{\mathcal{Z}^{GC,Q}}.$$

A analytical solution is unfortunately not known. Therefore the exponential of the integrand will be expanded in a complex Taylor series, who's expansion terms are the cumulants κ_q of order q.

$$\begin{aligned}
\kappa_q &= \left(-i\frac{\partial}{\partial\phi_Q}\right)^q \ln \mathcal{Z}^{GC,Q} \\
&= 2\sum_{n=1}^{\infty} (\mp 1)^{n+1} \langle N_n \rangle n^{q-4} \cosh\left(n\frac{\mu_Q}{T}\right) \quad q \text{ even} \qquad (2.76) \\
&= 2\sum_{n=1}^{\infty} (\mp 1)^{n+1} \langle N_n \rangle n^{q-4} \sinh\left(n\frac{\mu_Q}{T}\right) \quad q \text{ odd} \qquad (2.77)
\end{aligned}$$

The characteristic function $\Phi(\phi_Q)$ of this distribution $P(Q)$ can be expressed in terms of those cumulants.

$$\Phi(\phi_Q) = \exp\left(\sum_{q=1}^{\infty} \frac{\kappa_q}{q!} (i\phi_Q)^q\right)$$

$$= \exp\left(-\frac{\kappa_2}{2!}\phi_Q^2 + \frac{\kappa_4}{4!}\phi_Q^4 - \frac{\kappa_6}{6!}\phi_Q^6 + \ldots\right) \times \cos\left(\frac{\kappa_1}{1!}\phi_Q - \frac{\kappa_3}{3!}\phi_Q^3 + \frac{\kappa_5}{5!}\phi_Q^5 - \ldots\right) \quad (2.78)$$

Where the $0-th$ term of the Taylor expansion $\exp(\kappa_0) = \mathcal{Z}^{GC,Q}$ is the normalization. Thus the probability of finding some charge state realized is the Fourier integral with index Q over the characteristic function $\Phi(\phi_Q)$

$$P(Q) = \int_{-\pi}^{\pi} \frac{d\phi_Q}{2\pi} e^{-iQ\phi_Q}\Phi(\phi_Q). \quad (2.79)$$

The radius of convergence ρ of this expansion is given by the ratio of two successive elements and taking the limit of order goes to infinity.

$$\rho = \lim_{q\to\infty} \sqrt{|\frac{\kappa_q}{q!}\frac{(q+1)!}{\kappa_{q+1}}|} \quad (2.80)$$

Some special cases are given in appendix E. The radius needs to be compared to the decaying part of the generating function, which is given by the first few even cumulants, to ensure a reasonable approximation. In Boltzmann approximation only $n = 1$ is used:

$$\kappa_q = 2\langle N\rangle \cosh\left(\frac{\mu_Q}{T}\right) \quad q \text{ even}$$
$$\kappa_q = 2\langle N\rangle \sinh\left(\frac{\mu_Q}{T}\right) \quad q \text{ odd}$$

Therefore is the radius of convergence $\rho = \infty$. Even if only the first few expansion terms are used one finds good agreement with $P(Q)$ equation 2.23. Generally will the approximation not do a good job for low relative temperatures $(\frac{m}{T})$ and strong relative chemical potentials $(\frac{\mu_Q}{m})$. But never the less give the first two cumulants information about mean and width of the distribution, even if the whole distribution cannot be approximated. Figures 2.9, 2.10, and 2.11 show the charge distribution for a particle anti-particle gas with Fermi-Dirac statistics (red line), Bose-Einstein statistics (green line), and in Boltzmann approximation (blue line) for $\mu = 0$, $\mu = \frac{1}{2}m$, and $\mu = \frac{3}{4}m$ respectively. Further parameters are: $r = 3.0fm$, $T = 0.160GeV$, $m = 0.139$, while for all cases $g = 2$ was used to allow for better comparison. The first 10 cumulants were used. For the bosons only in the $\mu = \frac{3}{4}m$ case was the approximated function not 0 for angles larger the ρ, thus the oscillations on the tail of the Bose distribution in figure 2.11 indicates the break down of the approximation. Unfortunately could a similarly simple expression for

the radius of convergence for Fermi statistics not be derived yet, but despite the fact that their integrand is generally wider, the ratio of two successive cumulants seems to be larger than the same ratio for bosons, yet slightly more varying, and the approximation seems to be more stable.

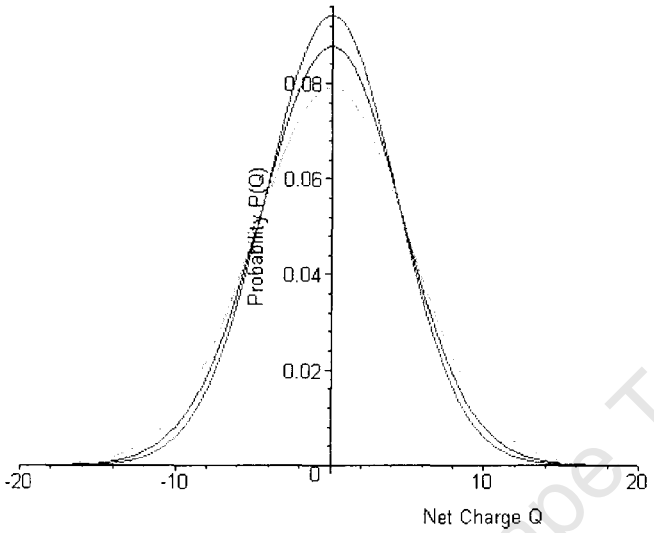

Figure 2.9: Charge distribution for a grand canonical particle anti-particle gas, $R = 3fm$, $T = 0.160GeV$, $m = 0.139GeV$, $\mu = 0$, Fermi-Dirac statistics (red), Bose-Einstein statistics (green), and Boltzmann approximation (blue)

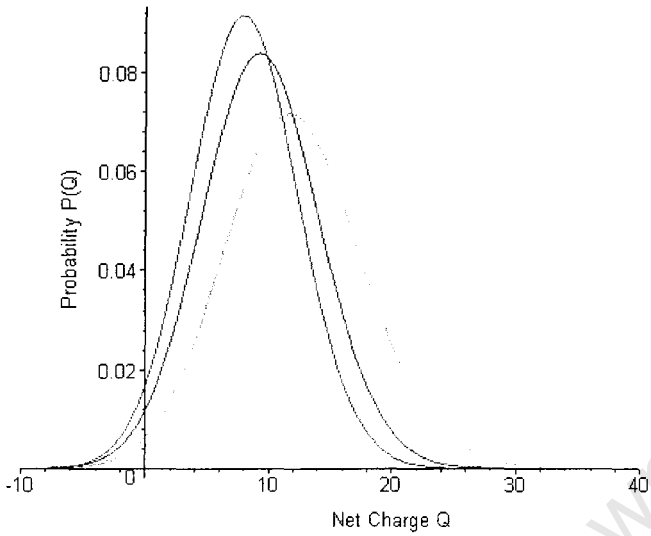

Figure 2.10: Charge distribution for a grand canonical particle anti-particle gas, $R = 3fm$, $T = 0.160GeV$, $m = 0.139GeV$, $\mu = \frac{1}{2}m$, Fermi-Dirac statistics (red), Bose-Einstein statistics (green), and Boltzmann approximation (blue)

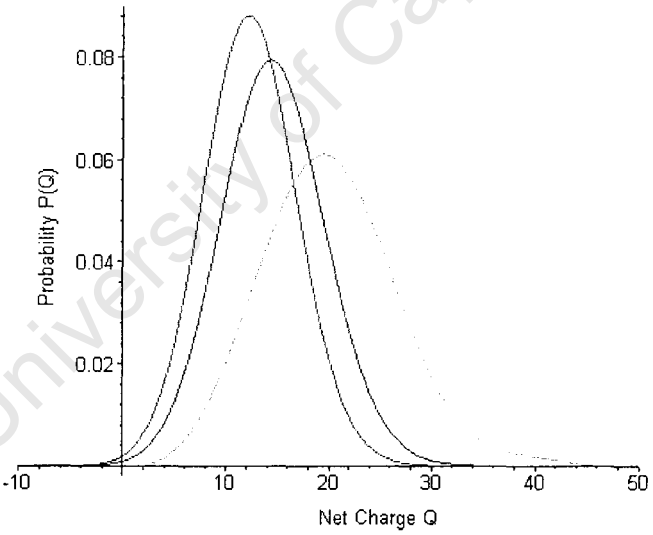

Figure 2.11: Charge distribution for a grand canonical particle anti-particle gas, $R = 3fm$, $T = 0.160GeV$, $m = 0.139GeV$, $\mu = \frac{3}{4}m$, Fermi-Dirac statistics (red), Bose-Einstein statistics (green), and Boltzmann approximation (blue)

2.6.2 Grand Canonical Particle Distributions

For the grand canonical particle distributions one has to take the derivatives with respect to the particle specific angles ϕ_p or ϕ_m to obtain the expansion terms or cumulants. Each differentiation brings one factor of n down, while the rest remains unchanged.

$$\kappa_l = \left(-i\frac{\partial}{\partial\phi_p}\right)^l \ln \mathcal{Z}^{GC,Q} = \sum_{n=1}^{\infty} (\mp 1)^{n+1} \langle N_n \rangle \, n^{l-4} \exp\left(n \, \frac{\mu_Q}{T}\right) \qquad (2.81)$$

As the mass contributions in the summation are decreasing with the index, $\langle N_{n+1} \rangle < \langle N_n \rangle$, one finds multiplicities, $\langle N \rangle = \kappa_1$, for Fermi-Dirac suppressed with respect to Boltzmann and Bose-Einstein.

$$\kappa_1^{FD} \quad < \quad \kappa_1^{Boltz} \quad < \quad \kappa_1^{BE}$$

For Boltzmann approximation only $n = 1$ is taken, hence for all integers l

$$\kappa_l = \langle N \rangle \exp\left(\frac{\mu_Q}{T}\right),$$

and one finds a Poisson distribution in the GC ensemble, and even when only a few cumulants are used, good agreement with $P(N)$ in equation 2.33. While for the width of the distributions $\omega = \frac{\langle N^2 \rangle - \langle N \rangle^2}{\langle N \rangle} = \frac{\kappa_2}{\kappa_1}$ at least for low chemical potentials

$$\omega^{FD} \quad < \quad 1 \quad < \quad \omega^{BE}$$

Figures 2.9, 2.10, and 2.11 show the multiplicity distribution of the positive particle with Fermi-Dirac statistics (red line), Bose-Einstein statistics (green line), and in Boltzmann approximation (blue line) for $\mu = 0$, $\mu = \frac{1}{2}m$, and $\mu = \frac{3}{4}m$ respectively. The same parameter set as for the charge distribution was used, and the same arguments for the convergence of the expansions hold.

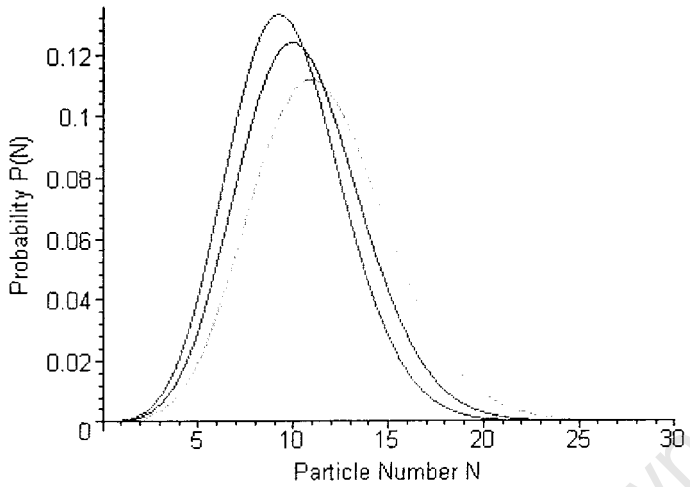

Figure 2.12: Particle number distribution for a grand canonical particle anti-particle gas, $R = 3fm$, $T = 0.160GeV$, $m = 0.139GeV$, $\mu = 0$, Fermi-Dirac statistics (red), Bose-Einstein statistics (green), and Boltzmann approximation (blue)

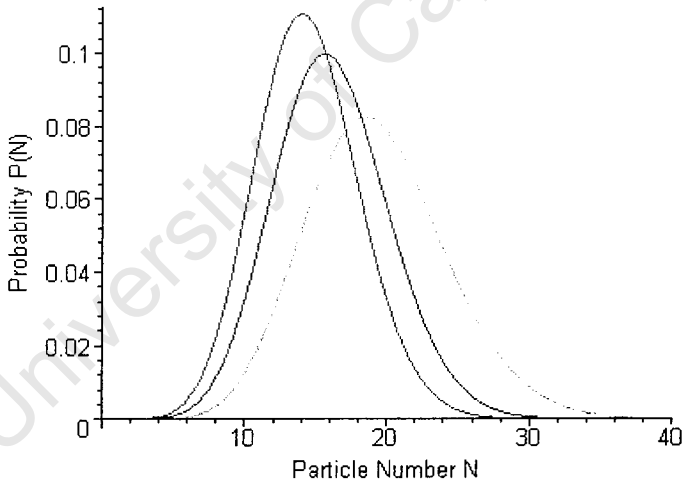

Figure 2.13: Particle number distribution for a grand canonical particle anti-particle gas, $R = 3fm$, $T = 0.160GeV$, $m = 0.139GeV$, $\mu = \frac{1}{2}m$, Fermi-Dirac statistics (red), Bose-Einstein statistics (green), and Boltzmann approximation (blue)

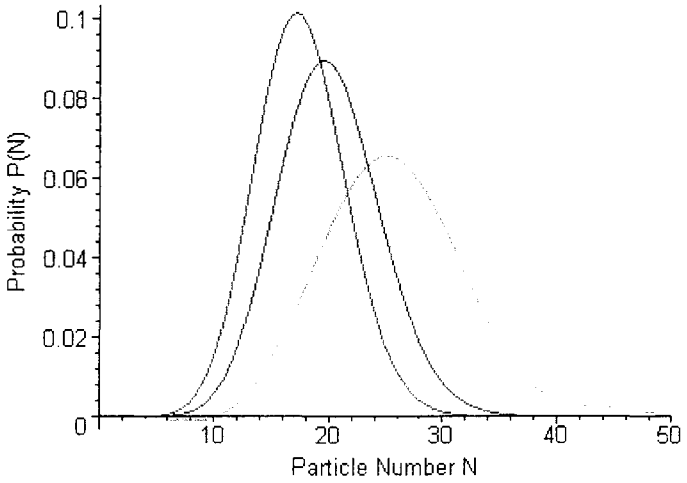

Figure 2.14: Particle number distribution for a grand canonical particle anti-particle gas, $R = 3fm$, $T = 0.160GeV$, $m = 0.139GeV$, $\mu = \frac{3}{4}m$, Fermi-Dirac statistics (red), Bose-Einstein statistics (green), and Boltzmann approximation (blue)

2.6.3 Canonical Multiplicity Distributions

The off-diagonal cumulants are a measure for the degree of correlation between two observables. In this case this will be net-charge and the multiplicity of the positive particle. Cumulants for Fermi-Dirac and Bose-Einstein statistics grow with their order and the correlation terms, which used to be zero in the grand canonical Boltzmann approximation and small in the canonical Boltzmann approximation, will follow suit. The expansion coefficients of order q for the charge and n for the positive particle are:

$$\kappa_{q,k} = \left(-i\frac{\partial}{\partial\phi_Q}\right)^q \left(-i\frac{\partial}{\partial\phi_p}\right)^k \ln \mathcal{Z}^{GC} \tag{2.82}$$

And as the structure is simple, one has only three cases to deal with. An even order in the charge and $0-th$ order in the particle number (2.76), an odd order in the charge and $0-th$ order in the particle number (2.77), and finally any non-zero order in the particle number (2.81). The integral to solve is the same as 2.39, just the more complicated integrand

$$P(Q,N) = \int_{-\pi}^{\pi} \frac{d\phi_Q}{2\pi} \int_{-\pi}^{\pi} \frac{d\phi_p}{2\pi} e^{-iQ\phi_Q} e^{-iN\phi_p} \Phi(\phi_Q, \phi_p).$$

The characteristic function reads in terms of the Taylor series

$$\Phi(\phi_Q, \phi_p) = \exp\left(\sum_{n=1}^{\infty} \frac{i^n}{n!} \sum_{l=0}^{n} \binom{n}{l} \kappa_{n-l,l}\ \phi_Q^{n-l}\ \phi_p^l\right), \tag{2.83}$$

which can now be be re-written in a product of an oscillating part and a decaying part

$$\begin{aligned} \Phi(\phi_Q, \phi_p) &= \exp\left(\sum_{a=1}^{\infty} (-1)^a \sum_{l=0}^{2a} \frac{1}{(2a)!} \binom{2a}{l} \kappa_{2a-l,l}\ \phi_Q^{2a-l}\ \phi_p^l\right) \\ &\times \cos\left(\sum_{a=0}^{\infty} (-1)^{a+1} \sum_{l=0}^{2a+1} \frac{1}{(2a+1)!} \binom{2a+1}{l} \kappa_{2a+1-l,l}\ \phi_Q^{2a+1-l}\ \phi_p^l\right). \end{aligned} \tag{2.84}$$

Boltzmann approximation is in good agreement with exact $P(Q, N)$ given by equation 2.42, even when only a low number of cumulants is used, while the approximation in the QC $P_Q(N)$ (equation 2.37) is even better when the same order of the expansion is employed. For a quantum statistical treatment the characteristic function can diverge for larger values of the variables of integration due to the strong correlation terms and the large coefficients they have. But it seems to be sufficient to truncate the mass sum at an index just below half of the order of the Taylor expansion to prevent this from happening. The basic properties, mean and variance are least affected by this. The plot 2.15 shows multiplicity distributions for Fermi-Dirac and Bose-Einstein statistics and Boltzmann approximation 2.37 for the parameter set $T = 0.170GeV$, $r = 4.0fm$, $m = 0.139GeV$, and $\mu = 0$. Degeneracy is in all three cases $g = 2$ to allow for better comparison. A mass order of 11 and cumulant order of 30 was used. The integration was done with Gauss-Laguerre method. Results are stable when more or slightly less mass terms and cumulants are take into account. For plot 2.16 a chemical

	ω_{Fermi}	ω_{Boltz}	ω_{Bose}
$\mu \approx -\frac{1}{4}m$	0.556	0.603	0.692
$\mu = 0$	0.469	0.509	0.568
$\mu \approx +\frac{1}{4}m$	0.384	0.405	0.441

Table 2.3: Scaled variance summary table

potential of $\mu_{pos} = 0.241m = 0.0335GeV$ was used. Apart for the obviously different mean values for the multiplicities are the expectation values for the net-charge $\langle Q \rangle_{Fermi} = 10.30$, $\langle Q \rangle_{Boltz} = 12$, and $\langle Q \rangle_{Bose} = 15.17$ respectively. Lastly in figure 2.17 a negative chemical potential of $\mu_{neg} = -0.241m$ is used

and still the distribution of positive particles is shown. This is equivalent to the distribution of negative particles at positive potential. The expectation values for the net-charge are thus the same as before, just with a negative sign.

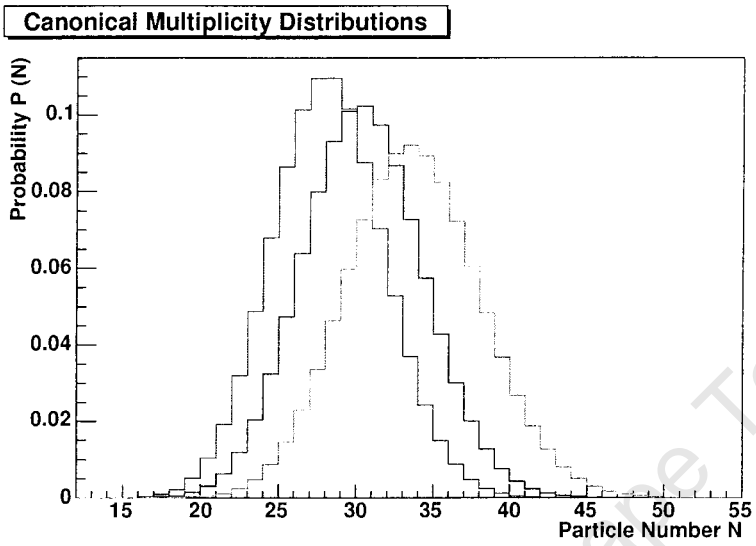

Figure 2.15: Particle number distribution for a canonical particle anti-particle gas, $R = 4fm$, $T = 0.170GeV$, $m = 0.139GeV$, $\mu = 0$, Fermi-Dirac statistics (red), Bose-Einstein statistics (green), and Boltzmann approximation (blue)

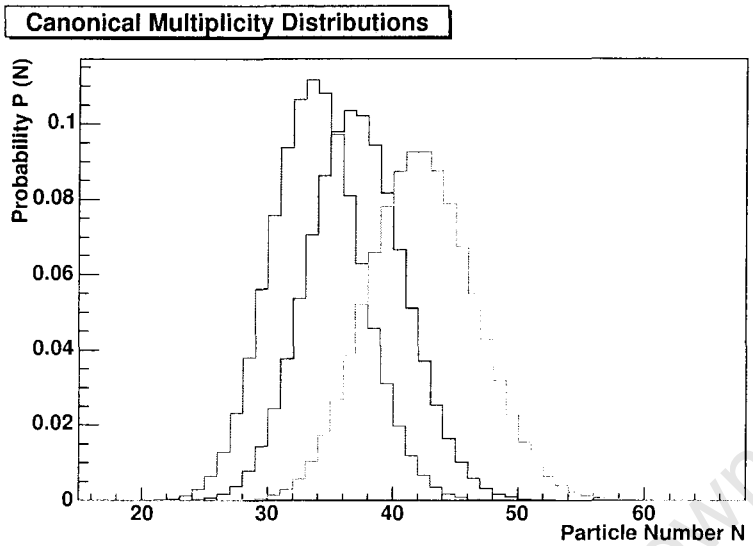

Figure 2.16: Particle number distribution for a canonical particle anti-particle gas, $R = 4fm$, $T = 0.170GeV$, $m = 0.139GeV$, $\mu \approx \frac{1}{4}m$, Fermi-Dirac statistics (red), Bose-Einstein statistics (green), and Boltzmann approximation (blue)

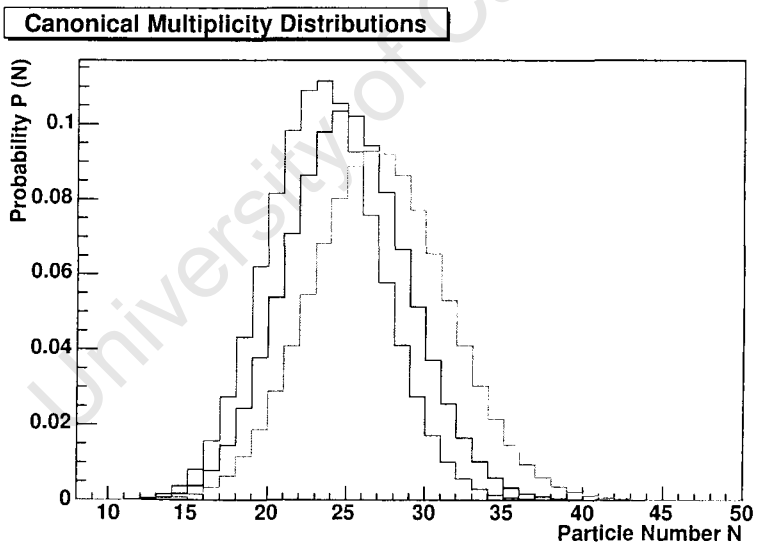

Figure 2.17: Particle number distribution for a canonical particle anti-particle gas, $R = 4fm$, $T = 0.170GeV$, $m = 0.139GeV$, $\mu \approx -\frac{1}{4}m$, Fermi-Dirac statistics (red), Bose-Einstein statistics (green), and Boltzmann approximation (blue)

2.7 Conclusion

Different kinds of correlations and fluctuations have been discussed in the context of a hypothetical particle anti-particle gas in two statistical ensembles, in both Boltzmann approximation and quantum statistics. In general are values for the scaled variance not as restricted as the use of Boltzmann approximation in a GC might suggest. Further drops the scaled variance for QC rather fast with system size in Boltzmann approximation, reaching some limiting value already for volumes and temperatures relevant to high energy collisions. Correlations, for which the respective off-diagonal moment or cumulant tensor elements are a suitable measure, were found to be small compared to the expectation values in Boltzmann approximation, which does not hold for quantum statical systems. A detailed discussion is presented in chapter 5. Therefore are generally particle ratios in large systems rather insensitive to the choice of statistical ensemble, when compared to yields, while on the other hand, some particular ratios can be sensitive, which would be an excellent test for the canonical formalism. The method of Fourier analysis has furthermore proven very successful and allows for a systematic discussion of various sub-distributions. For instance has a limited detector acceptance considerable effect on the scaled variance and a linear dependence on the fraction of detected particles was found. In the following chapter these results will be generalized to a Boltzmann canonical ensemble for a long hadronic resonance table as well as further conserved charges and serves to prepare the pre-analysis in chapter 4. Lastly could quantum statistical ensembles as well as final state distributions in chapter 3 be approximated by Taylor expansion, even for finite systems.

Chapter 3

Hadronic Resonance Gas

3.1 Introduction and Motivation

Although the thermal model is extremely successful in describing experimental data over a wide range of collision energies and colliding systems [33] it falls short of an explanation for the experimental results of the NA49 collaboration for charged particle fluctuations. The results of recent papers dealing with statistical equilibrium distributions of extensive observables in canonical and micro canonical ensembles are remarkable in the sense that they predict distributions significantly narrower than for the popular grand canonical ensemble [25, 26], while experiment finds distributions wider than this [34], raising questions on which would be the correct ensemble to apply to a particular colliding system, as well as the applicability of the thermal model to fluctuations found in high energy collisions itself. When concerned with yields, the canonical chemical potentials converge rather fast with the fireball radius to the grand canonical ones, allowing for description with the grand canonical ensemble (GC) and only at lower energies becomes a canonical treatment of conserved charges, in particular strangeness, necessary [35, 36]. The same does not hold for relative fluctuations as statistical distributions are, even under the thermodynamic limit, ensemble specific. On the experimental side purely technical constraints like geometric coverage of the interaction volume, particle acceptance and identification, momentum resolution as well as the difficulty to detect neutral particles make event-by-event data harder to obtain than event averages. Details of experimental set-ups determine not only the type of information available, but also the observed fraction of the interaction volume and detected particles therein, making the choice of thermodynamic ensemble even more important. So might a GC, based on the assumption that the observed region is in grand canonical con-

tact with the remainder of the system, be for instance applicable to the data of the STAR and PHENIX collaborations [32], where detailed information only about a mid rapidity slice is commonly used for thermal model fits and hence only a fraction ($\sim 1/8$) of the interaction volume is taken into account. For large acceptance detectors, like PHOBOS and NA49, should distributions further carry signatures of the exact conservation laws imposed by finiteness of the system. In general are fluctuations further not only more sensitive to the choice of ensemble but also to the statistics applied. So lead, in particular when quantum statistics are assumed, phase space suppression (enhancement) factors $\gamma \neq 1$, e.g. non equilibrium, to enhanced ($\gamma > 1$) or suppressed ($\gamma < 1$) statistical fluctuations, with strong correlations between the freeze-out temperature and the phase space occupancy [9]. A simultaneous fit of both yields or ratios and their fluctuations thus will put strong constraints on thermal parameters and might be able to verify, or falsify, hadronisation models [32, 37]. A canonical approach for particle distributions is therefore much desirable as it will be a further test for the statistical hadronisation model [10]. Due to the structure of the integration routine used in the THERMUS package for canonical ensembles only Boltzmann statistics are possible at the moment, and only one phase space suppression factor γ_S is employed. Unless stated otherwise the ensemble employed in this chapter is the baryon strangeness and charge canonical ensemble (BSQC) in Boltzmann approximation.

The main difference to chapter 2 is that in a hadron gas one needs additionally to the long list of hadrons take particle decay into account and further become phenomenological freeze-out conditions important as one cannot use the $\sqrt{s}$ (μ_B) [20] and $\mu_B(T)$ [19] parameterizations derived for the GC and strangeness canonical (SC) ensembles to classify events.

The focus of this chapter is on the technical aspects of how to conduct calculations and to prepare the pre-analysis in chapter 4 of the charged particle fluctuations for the Carbon Carbon at $158AGeV$. In chapter 5 it will be shown how one can make reasonable approximations to the partition function and the distributions for a quantum statistical canonical or even a micro canonical ensemble.

3.2 Canonical Partition Function

The canonical partition function is obtained by solving a integral over $\mathcal{Z}^{GC}$, with the first and foremost problem being of a numerical nature as every conserved charge, namely baryon number, strangeness and charge yields an additional Fourier integral, with high absolute values of charges resulting in a heavily oscillating integrand.

$$\begin{aligned}\mathcal{Z}^{B,S,Q} &= \int_{-\pi}^{\pi}\frac{d\phi_B}{2\pi}\int_{-\pi}^{\pi}\frac{d\phi_S}{2\pi}\int_{-\pi}^{\pi}\frac{d\phi_Q}{2\pi}e^{-iB\phi_B}e^{-iS\phi_S}e^{-iQ\phi_Q} \\ &\quad\times\exp\left(\sum_{j=1}^{P}z_j e^{iB_j\phi_B}e^{iS_j\phi_S}e^{iQ_j\phi_Q}\right) \qquad (3.1)\end{aligned}$$

Where B is the baryon number of the system, S the strangeness content, usually zero, and Q the electrical charge. The sum over the single particle partition functions z_j of type 2.2, e.g. Boltzmann approximation, includes all strange and light particles and resonances up to $2.6GeV$ as stated in the 2002 Particle Data Book [38]. Within the canonical formalism all chemical potential are usually set to zero, hence particle and anti-particle partition functions are identical $|z_j| = |z_{\bar{j}}|$, and angles (ϕ_B, ϕ_S, ϕ_Q) are introduced. Taking advantage of the fact that hadrons only come in quantum numbers $B = \pm 1, 0$ one can eliminate the integration over the baryon angle [39], leaving us with two.

$$\begin{aligned}\mathcal{Z}^{B,S,Q} &= \mathcal{Z}^0\int_{-\pi}^{\pi}\frac{d\phi_S}{2\pi}\int_{-\pi}^{\pi}\frac{d\phi_Q}{2\pi}\cos\left(S\phi_S+Q\phi_Q-B\arg\omega\left(\phi_S,\phi_Q\right)\right) \\ &\quad\times\exp\left(2\sum_{M}z_j\cos\left(S_j\phi_S+Q_j\phi_j\right)\right)I_B\left(2|\omega\left(\phi_S,\phi_Q\right)|\right) \qquad (3.2)\end{aligned}$$

Where the sums are now only taken over a mesons (M) and baryons (B) but not their respective anti-particles. The partition function $\mathcal{Z}^0$ contains all particles with $B_j = S_j = Q_j = 0$ which hence have no anti-particle, while baryons are represented by the complex variable

$$\omega = \sum_{B} z_j e^{i\left(S_j\phi_S+Q_j\phi_Q\right)}. \qquad (3.3)$$

3.3 Primordial Distributions

Basically all expectation values and distributions will be calculated from derivatives of the system partition function. The mathematical aspect of

these calculations is therefore, apart from a long list of hadrons and a increased number of conserved charges no different form those of chapter 2. In high energy collisions, according to Hagedorn's hypothesis, particles are produced according to their share of the total phase space determined by the Boltzmann factor $\exp(-\beta E)$. For small or cold systems will the available phase space be additionally dominated by exact conservation laws which have to be obeyed by particle and anti-particle production and hence a volume dependence is added. This concept has been successfully applied to heavy ion collisions in an attempt to explain the apparent strangeness enhancement when compared to proton proton collisions. Due to the smaller volume, and hence the small number of strange particles produced for collisions of small ions or at intermediate energies the SC should be applied [35, 36], while the data of proton proton collisions favors a complete canonical treatment [40]. Yet if the fireball is sufficiently large and hot the canonical volume dependence ceases and canonical and grand canonical ensembles will predict identical particle densities. Further has the evolution of strangeness phase space under-saturation γ_S with $\sqrt{s}$ and N_{part} been intensely studied in the past [41] and will have to be distinguished from those canonical effects.

3.3.1 Yields

The average yield of a particle carrying the label k can be obtained from the first derivative with respect to its particle specific chemical potential ν_k at the origin. The derivative does not change the structure of the integral, one only picks up an additional factor $\exp\left(i\vec{Q}_j\vec{\phi}\right)$ which changes the partition function index from $\vec{Q}$ to $\vec{Q}-\vec{Q}_j$. The ratio of the partition functions is therefore the canonical chemical factor (potential) replacing the grand canonical factor $\exp\left(\frac{\vec{Q}_j\vec{\mu}}{T}\right)$.

$$\langle N_j\rangle = \frac{1}{\mathcal{Z}^{\vec{Q}}}\left(T\frac{\partial}{\partial\nu_j}\right)\mathcal{Z}^{\vec{Q}}\Big|_{\nu_j=0} \tag{3.4}$$

$$\langle N_j\rangle = \frac{\mathcal{Z}^{\vec{Q}-\vec{Q}_j}}{\mathcal{Z}^{\vec{Q}}}\, z_j \tag{3.5}$$

Higher order moments are simply obtained from a successive application of the derivative operator $\left(T\frac{\partial}{\partial\nu_j}\right)$.

$$\langle N_j^n\rangle = \frac{1}{\mathcal{Z}^{\vec{Q}}}\left(T\frac{\partial}{\partial\nu_j}\right)^n\mathcal{Z}^{\vec{Q}}\Big|_{\nu_j=0} \tag{3.6}$$

Despite the rather fast convergence of $\frac{\mathcal{Z}^{\vec{Q}-\vec{Q}_j}}{\mathcal{Z}^{\vec{Q}}} \underset{VT^3 \text{large}}{\longrightarrow} e^{\frac{\vec{Q}_j\vec{\mu}}{T}}$ the higher chemical factors $\frac{\mathcal{Z}^{\vec{Q}-n\vec{Q}_j}}{\mathcal{Z}^{\vec{Q}}} < e^{n\frac{\vec{Q}_j\vec{\mu}}{T}}$ will always converge to values lower than those expected from a grand canonical treatment and hence have asymptotics of fluctuations in a statistical ensemble conserving baryon number B, strangeness S and electrical charge Q exactly been found to differ from the grand canonical prediction [42], indicating a inherit deviation from the grand canonical treatment which produces naturally a Poisson distribution.

3.3.2 Distributions

The canonical distributions are thus narrower than the grand canonical ones. Treating the particle number of species j as a conserved quantity and hence the interpretation of those correction factors as statistical weight factors allows to derive the distribution. This is done by inserting a further Fourier integral for the 'conserved' quantity particle number N_j with an associated angle ϕ_j.

$$P(N_j) = \frac{\int_{-\pi}^{\pi} \frac{d\phi_j}{2\pi} \int_{-\pi}^{\pi} \frac{d\phi_{\vec{Q}}}{(2\pi)^3} e^{-i\vec{Q}\phi_{\vec{Q}}} e^{-iN_j\phi_j} \mathcal{Z}^{GC}}{\int_{-\pi}^{\pi} \frac{d\phi_{\vec{Q}}}{(2\pi)^3} e^{-i\vec{Q}\phi_{\vec{Q}}} \mathcal{Z}^{GC}}$$

$$P(N_j) = \frac{\int_{-\pi}^{\pi} \frac{d\phi_j}{2\pi} \int_{-\pi}^{\pi} \frac{d\phi_{\vec{Q}}}{(2\pi)^3} e^{-i\vec{Q}\phi_{\vec{Q}}} e^{-iN_j\phi_j} \exp\left(\sum_{\substack{k=1 \\ k\neq j}}^{P} z_k e^{i\vec{Q}_k\phi_{\vec{Q}}}\right) \left(\sum_{n=0}^{\infty} \frac{z_j^n}{n!} e^{in\phi_j} e^{in\vec{Q}_j\phi_{\vec{Q}}}\right)}{\int_{-\pi}^{\pi} \frac{d\phi_{\vec{Q}}}{(2\pi)^3} e^{-i\vec{Q}\phi_{\vec{Q}}} \mathcal{Z}^{GC}} \tag{3.7}$$

By using the condition $n = N_j$ the integral over the angle ϕ_j can be solved. This yields for the probability

$$P(N_j) = \frac{z_j^{N_j}}{N_j!} \frac{\mathcal{Z}^{\vec{Q}-N_j\vec{Q}_j}_{\text{particle } j \text{ excl}}}{\mathcal{Z}^{\vec{Q}}_{\text{all particles}}}, \tag{3.8}$$

removing the single particle partition function z_j from the system partition function $\mathcal{Z}^{\vec{Q}-N_j\vec{Q}_j}$ in the numerator and leaves us with a ratio of partition functions of type 3.1 which can be easily integrated. The index $N_j\vec{Q}_j$ accounts for the quantum charges taken up by the N_j particles of species j which has quantum number $\vec{Q}_j = (B_j, S_j, Q_j)$. Grand canonically the usual result is obtained by applying the same formalism to the grand canonical partition function $\mathcal{Z}^{GC}$ producing a Poisson distribution with mean z_j, where a

chemical potential is to be included.

$$P(N_j) = \frac{z_j^{N_j}}{N_j!} \frac{\mathcal{Z}^{GC}_{\text{particle j excl}}}{\mathcal{Z}^{GC}_{\text{all particles}}} = \frac{z_j^{N_j}}{N_j!} \frac{\exp\left(\sum_{\substack{k=1 \\ k\neq j}}^{P} z_k\right)}{\exp\left(\sum_{k=1}^{P} z_k\right)} \tag{3.9}$$

$$P(N_j) = \frac{z_j^{N_j}}{N_j!} e^{-z_j} \tag{3.10}$$

Figure 3.1 shows an example distribution of primordial π^+ in a BSQC for the

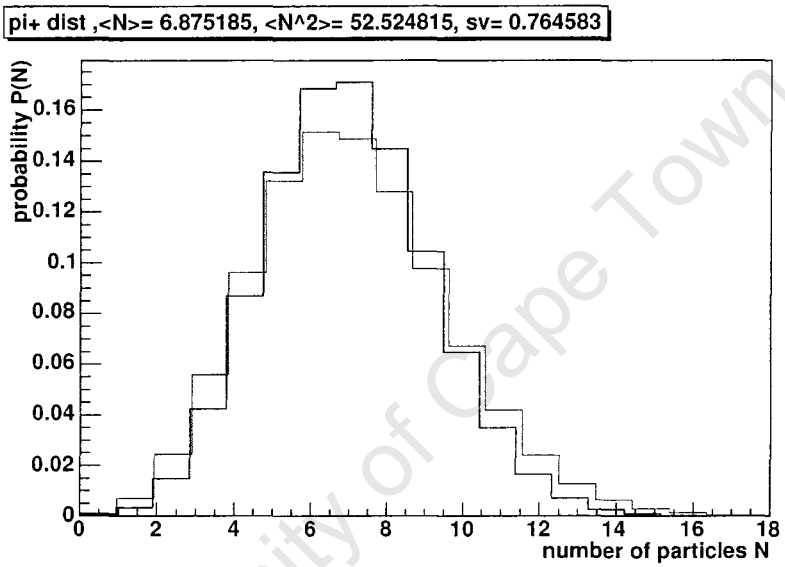

Figure 3.1: Primordial π^+ multiplicity distribution for a hadronic resonance gas in a BSQC, $\vec{Q} = (4, 0, 2)$, $T = 0.16377GeV$, $r = 3.225$, $\gamma_S = 0.6$, and $\frac{\langle E \rangle}{\langle N \rangle} = 1.0GeV$

parameter set obtained form the discussion in chapter 4. For comparison a Poisson distribution with same mean, red curve, is included. The narrowing in the distribution is the consequence of the correlation of the number of positive pions, or rather their charges, with the rest of the system which suppresses higher order moments and cumulants.

3.3.3 Ratios

As a measure for the correlation for two distributions, e.g. the correlations between K^+ and π^+ particles due to conserved electrical charge, one can use the $(1,1)$ element of the cumulant tensor $\kappa^{1,1}_{\pi^+,K^+} = \langle N_{\pi^+}\rangle\langle N_{K^+}\rangle - \langle N_{\pi^+}\cdot N_{K^+}\rangle$ which is 0 for uncorrelated observables. So are for instance the K^+ and π^+ distributions due the absence of a conserved charge linking them in a grand canonical or a strangeness canonical ensemble uncorrelated and hence the respective cumulant tensor element is zero. As with yields there is a event average measure (equation 2.43), free of such correlation terms, which is the commonly employed in thermal model calculations

$$\frac{\langle K^+\rangle}{\langle \pi^+\rangle} = \frac{\sum_{n=0}^{\infty} P_{K^+}(n)\, n}{\sum_{m=0}^{\infty} P_{\pi^+}(m)\, m},$$

and a event-by-event measure (equation 2.44)

$$\langle \frac{K^+}{\pi^+}\rangle = \sum_{n=0}^{\infty}\sum_{m=1}^{\infty} P_{K^+,\pi^+}(n,m)\,\frac{n}{k}.$$

To compute a conditional probability distribution $P(N_j, N_l)$ one inserts two further Fourier integrals and the corresponding angles ϕ_j and ϕ_l along with the usual normalization $\mathcal{Z}^{\vec{Q}}$.

$$\begin{aligned} P(N_j,N_l) &= \frac{\int_{-\pi}^{\pi}\frac{d\phi_j}{2\pi}\int_{-\pi}^{\pi}\frac{d\phi_l}{2\pi}\int_{-\pi}^{\pi}\frac{d\phi_{\vec{Q}}}{(2\pi)^3} e^{-i\vec{Q}\phi_{\vec{Q}}} e^{iN_j\phi_j} e^{iN_l\phi_l}\mathcal{Z}^{GC}}{\int_{-\pi}^{\pi}\frac{d\phi_{\vec{Q}}}{(2\pi)^3} e^{-i\vec{Q}\phi_{\vec{Q}}}\mathcal{Z}^{GC}} \\ P(N_j,N_l) &= \frac{z_j^{N_j}}{N_j!}\,\frac{z_l^{N_l}}{N_l!}\,\frac{\mathcal{Z}^{\vec{Q}-N_j\vec{Q}_j-N_l\vec{Q}_l}_{\text{particles } j \text{ and } l \text{ excl}}}{\mathcal{Z}^{\vec{Q}}_{\text{all particles}}} \end{aligned} \tag{3.11}$$

The result is analog to the distribution $P(N_j)$, the two single particle partition functions z_j and z_l, belonging to the particles j and l are to be removed from the integral in the numerator and the index is changed to $\vec{Q} - N_j\vec{Q}_j - N_l\vec{Q}_l$ to account for the quantum content taken up by the two particle species. Grand canonically the two particle distribution factorize into two Poissonian one particle distributions

$$P(N_j,N_l) = \frac{z_j^{N_j}}{N_j!}e^{-z_k}\cdot\frac{z_l^{N_l}}{N_l!}e^{-z_l}. \tag{3.12}$$

The event-by-event ratio can be obtain from the distribution $P(N_j, N_l)$ by defining the variable

$$R = \frac{N_l}{N_j} \tag{3.13}$$

while for the measure for the width of the ratio distribution again 2.45 is used. Due to the discrete nature of particle numbers the resulting shape of the distribution $P(R)$ will, in particular for small systems, depend on the choice of the increment ΔR. The values in table 3.1 are compiled from the distributions in figure 3.2 and contain GC and SC for comparison. Again the

$\langle R\rangle = \langle\frac{K^+}{\pi^+}\rangle$	BSQC	SC	GC
$\langle\pi^+\rangle$	6.87517	6.99386	6.99622
$\langle K^+\rangle$	1.41189	1.41747	1.47648
$\langle R\rangle$	0.236102	0.236604	0.244891
$RMS_{\langle R\rangle}$	0.219625	0.224856	0.235371
$\frac{\langle K^+\rangle}{\langle\pi^+\rangle}$	0.20536	0.202673	0.21104

Table 3.1: Primordial event-by-event particle ratio $\langle\frac{\pi^+}{K^+}\rangle$ for a hadronic resonance gas in a BSQC, $\vec{Q} = (4, 0, 2)$, $T = 0.16377GeV$, $r = 3.225fm$, $\gamma_S = 0.6$, and $\frac{\langle E\rangle}{\langle N\rangle} = 1.0GeV$

parameter set from the Carbon Carbon system is used for the primordial distributions. The GC and SC distributions were obtained by requiring the fireball to have the same baryon, strangeness and charge densities, temperature, radius and strangeness suppression factor. The chemical potentials are for SC: $\mu_B = 0.0715GeV$, $\mu_Q = -5.32\ 10^{-5}GeV$ and for GC: $\mu_B = 0.0709GeV$, $\mu_S = 0.0153GeV$, $\mu_Q = -5.46\ 10^{-5}GeV$. Therefore are average energy per particle, normalized entropy density and net baryon density similar but not the same as in the BSQC. The corresponding distributions $P(R)$ for the GC and SC are remarkably similar to the BSQC ratio distribution and are only mildly wider. A qualitative explanation for this is that correlation terms $\kappa^{1,1}_{\pi^+,K^+}$ in the BSQC are in Boltzmann approximation still small when compared to cumulants of same order $\kappa^2_{\pi^+}$ and $\kappa^2_{K^+}$. For a quantum statistical treatment this condition might not hold anymore (see chapter 5), and one expects a stronger dependence of event-by-event ratios on the choice of ensemble.

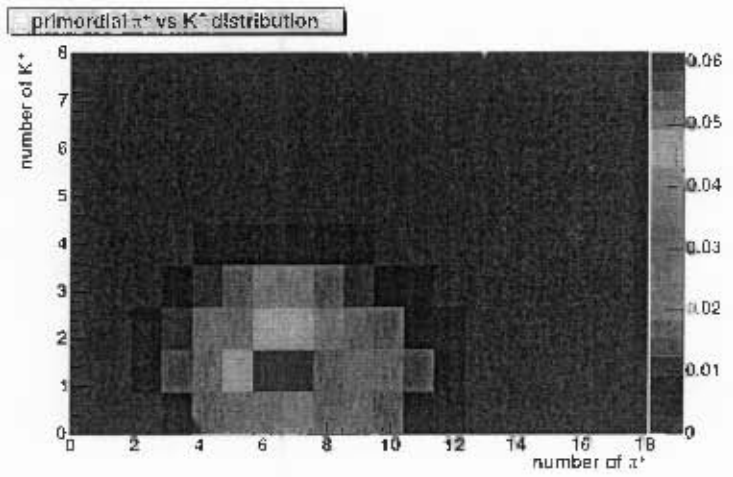

Figure 3.2: Primordial π^+ vs. K^+ multiplicity distribution for a hadronic resonance gas in a BSQC, $\vec{Q} - (4,0,2)$, $T - 0.16377GeV$, $r - 3.225fm$, $\gamma_S - 0.6$, and $\frac{\langle E \rangle}{\langle N \rangle} - 1.0GeV$

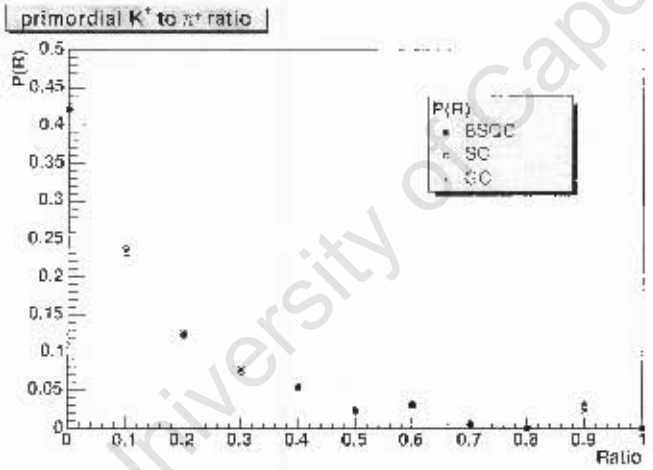

Figure 3.3: Primordial K^+ to π^- ratio distribution for a hadronic resonance gas in a BSQC, $\vec{Q} = (4,0,2)$, $T - 0.16377GeV$, $r - 3.225fm$, $\gamma_S = 0.6$, and $\frac{\langle E \rangle}{\langle N \rangle} = 1.0GeV$

3.4 Final State Distributions

Ultimately one would like to derive feed down, or particle decay, corrected or final state distributions, which is somewhat tricker to achieve. So could for

instance any given number of pions come from any combination of primordial pions and decay pions. In the case of the decay pions one would have to consider all different decay channels and their respective distributions. But it is rather easy to get the expectation values of final state yields, or more precisely the first few final state moments of the distribution. Once one has the moments, one can calculate the cumulants (a list of the most important relations in given in Appendix I), and approximate the cumulant generating function which can then be conveniently integrated. One should mention that one of the main uncertainties in thermal model implementations are ambiguities with decay chain in respective codes. Especially heavy resonances have not well established decay chains which affect yields of decay products [19]. This will have some even stronger influence on particle fluctuations. In this context strange particles are assumed to be stable as their live time is generaly large when compared to time of flight to the detector. Hence weak decay channels are usually omitted.
The assumptions made in this chapter are certainly only a first approximation. Particle decay itself is a random process and at the present stage it is not clear whether is can be included in a analytical fashion. Moreover there is one important simplification which reflects the limitations of the code employed. Multi-step decays, i.e. resonance decaying into resonances are omitted for the time being.

3.4.1 One Particle Distributions

This will be done in this section for both grand canonical and canonical one particle distributions in Boltzmann approximation, while the two particle (or conditional) distributions are in the next one. The expectation value for the multiplicity in a stable final state particle with label i is the sum over all primordial parent particle multiplicities N_j, taking their branching ratios $\Gamma_{j\to i}$ into account, and the particle's primordial expectation value itself.

$$\langle N_i \rangle = \langle \sum_{j=1}^{P} \tilde{N}_j \rangle = \sum_{j=1}^{P} \langle \tilde{N}_j \rangle \tag{3.14}$$

where the $\langle \tilde{N}_j \rangle$ are feed down corrected grand canonical or canonical Boltzmann approximation yields.

$$\langle \tilde{N}_j \rangle = \underbrace{\frac{g_j V}{2\pi^2} m_j^2 T K_2\left(\frac{m_j}{T}\right)}_{z_j} \cdot \Gamma_{j\to i} \cdot \begin{matrix} \tilde{Z}^{\vec{Q}-\vec{Q}_j} & \text{C} \\ e^{\frac{\mu_j}{T}} & \text{GC} \end{matrix} \tag{3.15}$$

,where we have introduced the shorthand notation $\tilde{\mathcal{Z}}^{\vec{Q}-\vec{Q}_j} = \mathcal{Z}^{\vec{Q}-\vec{Q}_j}/\mathcal{Z}^{\vec{Q}}$. When $e^{\frac{\mu_j}{T}}$ for a grand canonical treatment is used, neither two-particle nor any charge correlations are present. Only the effective interaction term $\mu_j = \mu_B B_j + \mu_S S_j + \mu_Q Q_j$ is used to shift the distributions to a chosen mean.

$$\begin{aligned}\langle N_i^2 \rangle &= \langle \left(\sum_{j=1}^{P} \tilde{N}_j \right)^2 \rangle \\ &= \langle \sum_{j=1}^{P} \tilde{N}_j^2 + \sum_{j=1}^{P} \sum_{\substack{k=1 \\ k \neq j}}^{P} \tilde{N}_j \cdot \tilde{N}_k \rangle \\ &= \sum_{j=1}^{P} \langle \tilde{N}_j^2 \rangle + \sum_{j=1}^{P} \sum_{\substack{k=1 \\ k \neq j}}^{P} \langle \tilde{N}_j \cdot \tilde{N}_k \rangle \end{aligned} \tag{3.16}$$

Grand canonically the higher moments can be calculated using the following recipe. The second moment of a parent particle contribution is

$$\langle \tilde{N}_j^2 \rangle = \left(z_j e^{\frac{\mu_j}{T}} \Gamma_{j \to i} \right)^2 + \left(z_j e^{\frac{\mu_j}{T}} \Gamma_{j \to i} \right), \tag{3.17}$$

while the correlation between the particles of species j and those of species k is given by

$$\langle \tilde{N}_j \cdot \tilde{N}_k \rangle = \left(z_j e^{\frac{\mu_j}{T}} \Gamma_{j \to i} \right) \cdot \left(z_k e^{\frac{\mu_k}{T}} \Gamma_{k \to i} \right). \tag{3.18}$$

The branching ratio of a stable particle to itself is 1. Considering a simple example of a gas consisting of two types of particles. A unstable particle B which decays into the other type of particle A, which is chosen to be stable, with a given branching ratio Γ. Both particles could have individual chemical potentials, $\mu_A \neq \mu_B$, due to different charges the carry.

$$\begin{aligned}\langle N_A \rangle_{\text{final}} &= \langle N_A \rangle + \langle \tilde{N}_B \rangle = z_A e^{\frac{\mu_A}{T}} + z_B \Gamma e^{\frac{\mu_B}{T}} \\ \langle N_A^2 \rangle_{\text{final}} &= \langle N_A^2 \rangle + \langle \tilde{N}_B^2 \rangle + 2 \langle N_A \cdot \tilde{N}_B \rangle \\ &= z_A^2 e^{\frac{2\mu_A}{T}} + z_A e^{\frac{\mu_A}{T}} + z_B^2 \Gamma^2 e^{\frac{2\mu_B}{T}} + z_B \Gamma e^{\frac{\mu_B}{T}} + 2 z_A e^{\frac{\mu_A}{T}} z_B \Gamma e^{\frac{\mu_B}{T}}\end{aligned}$$

As expected, the ratio of second to first cumulant is one, producing a Poissonian when one considers higher order corrections.

$$\kappa_A^2 \equiv \langle N_A^2 \rangle_{\text{final}} - \langle N_A \rangle_{\text{final}}^2 = z_A e^{\frac{\mu_A}{T}} + z_2 \Gamma e^{\frac{\mu_2}{T}} = \langle N_A \rangle_{\text{final}} = \kappa_A^1$$

In a canonical ensemble correlations are present and will significantly alter the moments and hence the distributions and the canonical correction factors

need to be employed, which do not follow the simple behavior form the GC, as $\mathcal{Z}^{\vec{Q}-2\vec{Q}_j} \neq \left(\mathcal{Z}^{\vec{Q}-\vec{Q}_j}\right)^2$. The second moment and the correlator are

$$\langle \tilde{N}_j^2 \rangle = (z_j \Gamma_{j\to i})^2 \, \tilde{\mathcal{Z}}^{\vec{Q}-2\vec{Q}_j} + (z_j \Gamma_{j\to i}) \, \tilde{\mathcal{Z}}^{\vec{Q}-\vec{Q}_j}, \tag{3.19}$$

and

$$\langle \tilde{N}_j \cdot \tilde{N}_k \rangle = (z_j \Gamma_{j\to i}) \, (z_k \Gamma_{k\to i}) \, \tilde{\mathcal{Z}}^{\vec{Q}-\vec{Q}_j-\vec{Q}_k}. \tag{3.20}$$

3.4.2 Two Particle Distributions

Finally the two particle distributions which are needed for the final state particle ratios. For the final state second moment one needs to consider all possible contributions of particles which could decay into one of the stable particles i and l.

$$\begin{aligned} \langle N_i \cdot N_l \rangle &= \langle \sum_{j=1}^{P} \tilde{N}_{j,i} \cdot \sum_{k=1}^{P} \tilde{N}_{k,l} \rangle \\ &= \sum_{j=1}^{P} \sum_{k=1}^{P} \langle \tilde{N}_{j,i} \cdot \tilde{N}_{k,l} \rangle \end{aligned} \tag{3.21}$$

where, as before

$$\langle \tilde{N}_{j,i} \rangle = \underbrace{\frac{g_j V}{2\pi^2} m_j^2 T K_2\left(\frac{m_j}{T}\right)}_{z_j} \cdot \Gamma_{j\to i} \cdot \underbrace{\tilde{\mathcal{Z}}^{\vec{Q}-\vec{Q}_j}}_{\text{C}} \cdot \underbrace{e^{\frac{\mu_j}{T}}}_{\text{GC}}$$

The first and second moment are to be done using the recipe from the previous section. Correlations from decay channels of the type $X \to K^+ + \pi^+$ will be omitted, as they are a) more complicated and b) not the dominant contribution, while when charge conservation laws linking two final state particles or their parent particles are absent, this would be the only source of non trivial correlation [32]. As an example for the higher moments we will discuss the third moments in appendix H. The results compiled in table 3.2 are calculated from the distribution in figure 3.4 and their grand canonical and strangeness canonical counterparts. The same parameter set as this of table 3.1 was used, while feed down was handled using the method described. Figure 3.5 shows the final state $R = \frac{K^+}{\pi^+}$ event-by-event ratio distribution for the three considered ensembles. Again the curves are remarkably similar, while the final state distributions are somewhat narrower than the primordial ones. The lower the value of R is due to the stronger decay contribution the π^+ receives when compared to the positive kaon.

$\langle R \rangle = \langle \frac{K^-}{\pi^+} \rangle$	BSQC	SC	GC
$\langle \pi^- \rangle$	21.6047	21.9527	22.0353
$\langle K^+ \rangle$	2.81581	2.82868	2.93129
$\langle R \rangle$	0.13617	0.135512	0.139881
$RMS_{\langle R \rangle}$	0.0808674	0.0819115	0.0911065
$\frac{\langle K^- \rangle}{\langle \pi^+ \rangle}$	0.130333	0.128853	0.133027

Table 3.2: Final state event-by-event particle ratio $\langle \frac{\pi^+}{K^+} \rangle$ for a hadronic resonance gas in a BSQC, $\vec{Q} = (4, 0, 2)$, $T = 0.16377GeV$, $r = 3.225fm$, $\gamma_S = 0.6$, and $\frac{\langle E \rangle}{\langle N \rangle} = 1.0GeV$

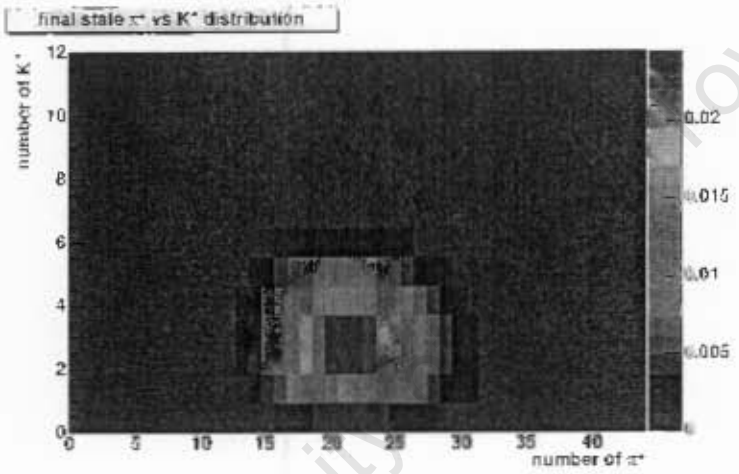

Figure 3.4: Final state π^+ vs. K^- multiplicity distribution for a hadronic resonance gas in a BSQC, $\vec{Q} = (4, 0, 2)$, $T = 0.16377GeV$, $r = 3.225fm$, $\gamma_S = 0.6$, and $\frac{\langle E \rangle}{\langle N \rangle} = 1.0GeV$

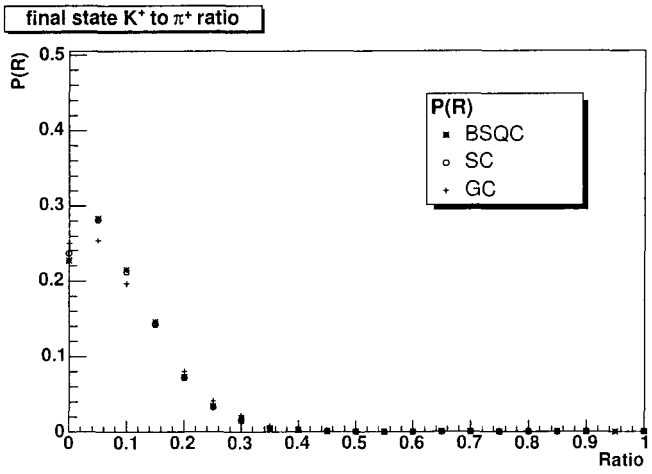

Figure 3.5: Final state K^+ to π^+ ratio distribution for a hadronic resonance gas in a BSQC, $\vec{Q} = (4, 0, 2)$, $T = 0.16377GeV$, $r = 3.255fm$, $\gamma_S = 0.6$, and $\frac{\langle E \rangle}{\langle N \rangle} = 1.0GeV$

3.5 Charged Particle Distributions

One might be interested in a particular subset, for instance only charged particles or only positively charged particles, and their respective fluctuations, which are measures employed for instance by the PHOBOS [43] and NA49 [34] collaborations. Essentially one could give any of the particles which meet some criteria a angle similar to what was done for the one particle distributions and the rapidity window subset in chapter 2. Unfortunately this becomes impractical for long hadronic tables. So again the moments are employed to approximate the distributions. Primordial this is very simple, one has to follow the recipe from the section above and sum over all chosen particles. For the final state distributions the list of selected particles has to be extended to all the resonances which can decay into a particle which then meets the criterion while taking their effective branching rations into account. In a grand canonical ensemble all ω values are equal to 1, while they only deviate slightly from unity in a strangeness canonical ensemble, as most charged particles are not carrying the quantum number strangeness, what makes them to a good approximation grand canonical (uncorrelated). The tables 3.3 and 3.4 show values for the final state scaled variance ω for the Carbon Carbon system in a BSQC and a SC respectively. In a ensemble which is conserving electrical charge one has to obtain a conditional distribution for positive and negative particles and only take events with a chosen

ω_{BSQ}	positive	negative	all charged
primordial	0.718095	0.736229	1.01382
final	0.652497	0.737072	1.02239

Table 3.3: Scaled variance ω^{BSQ} for $\vec{Q} = (4, 0, 2)$, $T = 0.16377GeV$, $R = 3.225fm$, $\gamma_s = 0.6$, and $\frac{\langle E \rangle}{\langle N \rangle} = 1.0GeV$ in a BSQC

ω_S	positive	negative	all charged
primordial	0.982941	0.980114	1.00194
final	0.985165	0.986065	1.00668

Table 3.4: Scaled variance ω^S for $S = 0$, $T = 0.16377GeV$, $R = 3.225fm$, $\mu_B = 0.0715GeV$, $\mu_Q = -5.32\ 10^{-5}GeV$ $\gamma_s = 0.6$ in a SC

$N_{chr} = N_{pos} + N_{neg}$, while $Q = N_{pos} - N_{neg}$, into account, what is ultimately responsible for the discrete distributions of charged particles.

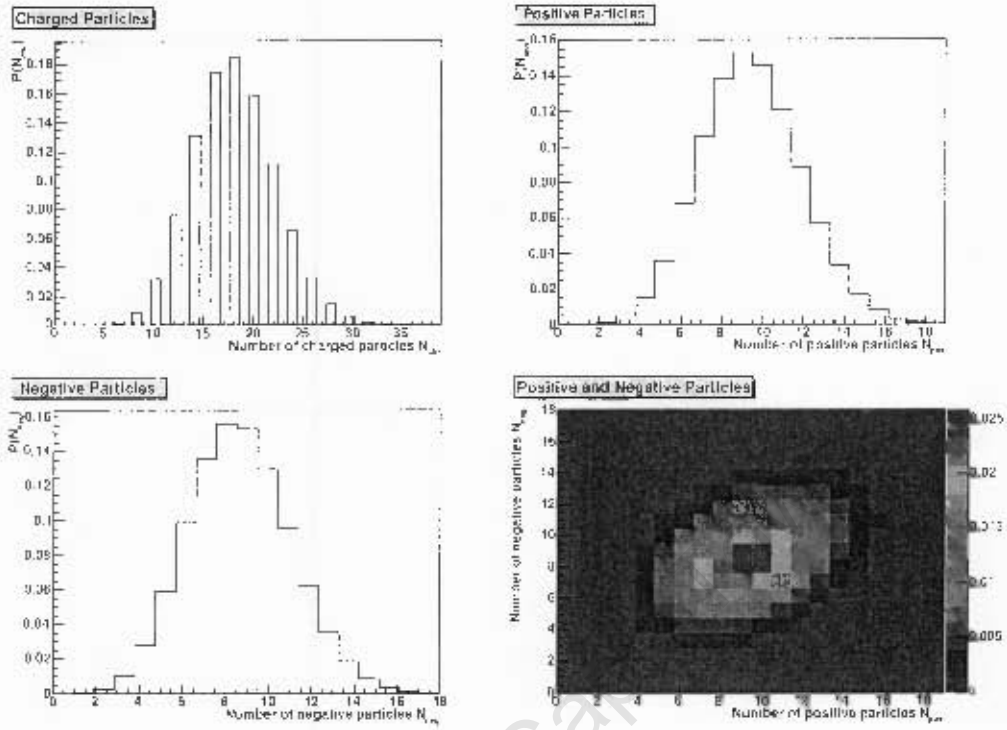

Figure 3.6: Primordial charged particle distributions, $\vec{Q} = (4, 0, 2)$. $R = 3.225 fm$, $T = 0.16377 GeV$, $\gamma_s = 0.6$, and $\frac{\langle E \rangle}{\langle N \rangle} = 1.0 GeV$ in a BSQC, clockwise from top left: all charged particles, positive particles, negative particles, positive and negative particles

3.6 Canonical Chemical Correction Factors

Canonical chemical correction factors evolve with baryon number in a similar fashion as chemical potentials in the GC for which a curve in the (T, μ_B) plane marks the phase boundary between a deconfined state and ordinary hadronic matter. Except that in a canonical ensemble the yields would be suppressed for small TV^3 with respect to the GC at 'same' chemical potential, therefore would canonical chemical correction factors be higher, when one requires both ensembles to have identical charge densities. This is strictly speaking only true when one has only one conserved charge to deal with. Interplay between quantum numbers, of which a particular particle can carry a few, makes the situation more complicated. So were the baryon chemical potentials found for the CC pre-analysis by demanding the same densities ρ_B, ρ_S, and ρ_Q at same temperature, volume, and strangeness suppression γ_S for the parameter

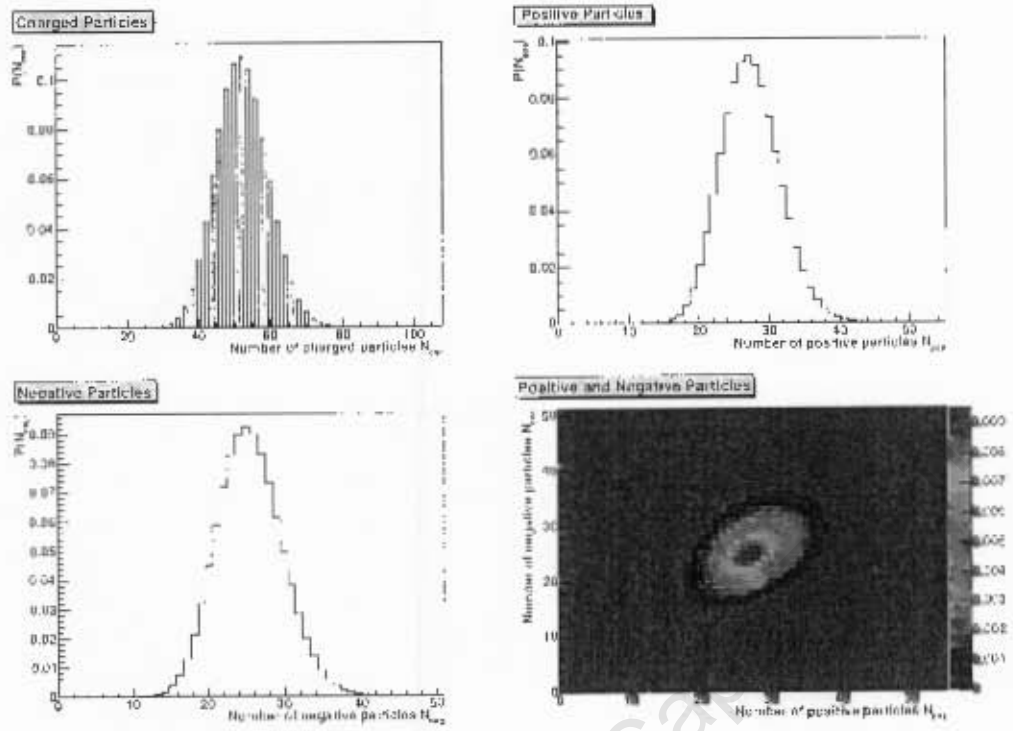

Figure 3.7: Final charged particle distributions $\vec{Q} = (4, 0, 2)$, $R = 3.225fm$, $T = 0.16377GeV$, $\gamma_s = 0.6$, and $\frac{\langle E \rangle}{\langle N \rangle} = 1.0GeV$ in a BSQC, clockwise from top left: all charged particles, positive particles, negative particles, positive and negative particles

set $\vec{Q} = (4, 0, 2)$, $T = 0.163776GeV$, $R = 3.225fm$, $\gamma_s = 0.6$ in the three ensembles:

	GC	SC	$BSQC$
μ_B	$70.87\ MeV$	$71.49\ MeV$	$66.13\ MeV$

Figure 3.8 shows the evolution of canonical chemical correction factors for the particles n, p, Λ, π^-, $\bar{K}^0$, K^0, and K^- for increasing quantum charge content.

$$\exp\left(\frac{\mu_p^{can}}{T}\right) = \frac{Z^{\vec{Q}-\vec{Q}_p}}{Z^{\vec{Q}}} \qquad \exp\left(\frac{\mu_{\pi^-}^{can}}{T}\right) = \frac{Z^{\vec{Q}-\vec{Q}_{\pi^+}}}{Z^{\vec{Q}}} \tag{3.22}$$

The same volume and strangeness suppression γ_S was used for all values of (B, S, Q), while all were constrained to $\frac{\langle E \rangle}{\langle N \rangle} = 1.0GeV$. The low temperature end point is at $(B, S, Q) = (14, 0, 7)$ and a step size of $\Delta\vec{Q} = (2, 0, 1)$ was used. The consequence of a higher B is a drop in temperature T. The normalized entropy density $\frac{\langle s \rangle}{T^3}$ changes only very modestly along that curve of constant $\frac{\langle E \rangle}{\langle N \rangle}$ and increasing baryon and charge content. Further one can remove the effect of (electrical) charge conservation on the proton by dividing its canonical correction factor by the one of the positive pion and thus define canonical chemical correction factors

$$\exp\left(\frac{\mu_B}{T}\right) \approx \frac{\mathcal{Z}^{\vec{Q}-\vec{Q}_p}}{\mathcal{Z}^{\vec{Q}-\vec{Q}_{\pi^+}}} \equiv \exp\left(\frac{\mu_B^{can}}{T}\right).$$

The equal sign would hold only in the thermodynamic limit. Or the effect of strangeness on μ_B by using the pair $\Lambda/\bar{K}^0$. Further pairs are for the strangeness chemical potential μ_S: Λ/n for B and K^-/π^- for Q and finally pairs for the charge chemical potential μ_Q: p/n for B and K^+/K^0 for S. In figure 3.9 these normalized canonical chemical correction factors agree well with the canonical chemical potentials for the charge (π^+) and strangeness $(\bar{K}^0)$ and baryon number (n), while showing similar behavior to $\sqrt{s}(\mu_B)$ of the freeze-out curve and most importantly suggesting that constant $\frac{\langle E \rangle}{\langle N \rangle}$ and $\frac{\langle s \rangle}{T^3}$ are good freeze-out conditions for (at least) low (quantum) charge densities. In a micro canonical ensemble the chemical factors would probably separate according to their mass, while in a canonical ensemble the curve $\sqrt{s}(B)$ would only be volume dependent (not density dependent as the size of colliding nuclei matters as well). Additionally is μ_Q always close to zero despite the fact that we have a net-charge of $Q = B/2$ while the strangeness chemical potential μ_S is low and negative despite the fact that the fireball doesn't contain any net strangeness $(S = 0)$. This is a consequence of the fact that a positive μ_B produces charged and strange baryons as well, what requires negative and anti-strange mesons to be produced in excess of their positive and strange counterparts. Again strong interplay between charges in the canonical partition function is observed.

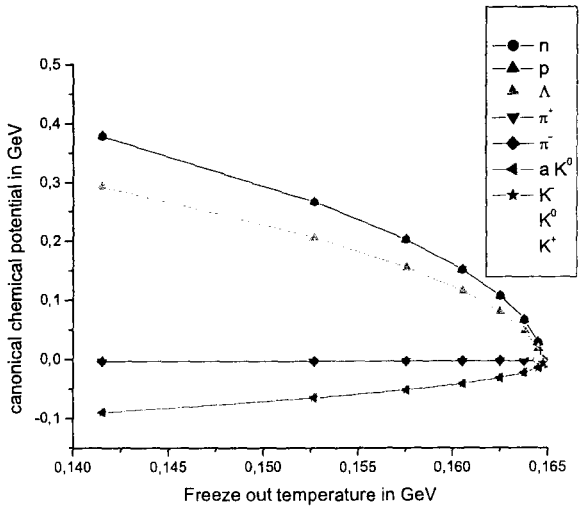

Figure 3.8: Temperature evolution of canonical chemical potentials for different particles

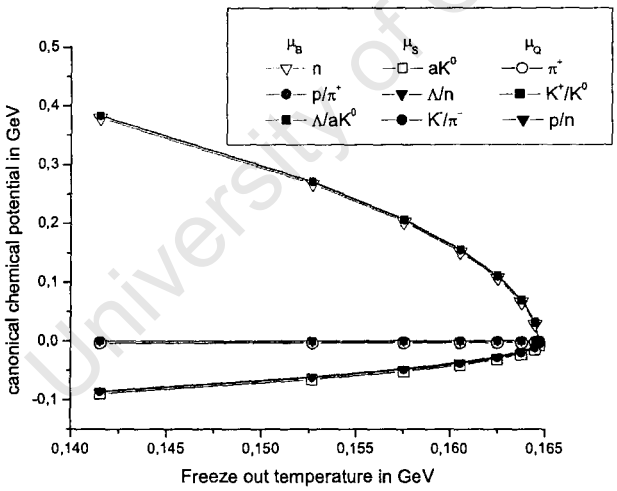

Figure 3.9: Temperature evolution of normalized canonical chemical potentials μ_B, μ_S, μ_Q

3.7 Freeze-Out Conditions

The thermal model itself does not provide any reasonable values for its parameters. It is a phenomenological model and thus depends on input from either theory or experiment. The partition thermodynamics of reference [5], QCD [21], a linear dependence of primary charged particle on the number of participating nucleons [44], thermal model fits to data [15], and probably most strikingly Hagedorn's considerations [3, 4], suggest all the existence of a highest hadronic temperature as well as a constant value for the average energy per particle

$$\frac{\langle E\rangle}{\langle N\rangle} \approx 1GeV. \tag{3.23}$$

Generally provide thermodynamic quantities like the normalized entropy density $\frac{\langle s\rangle}{T^3}$, pressure P or net baryon density $n_{b+\bar{b}}$ some insight into the conditions at breakup. Phenomenological parameterizations, like the connection of beam energy to baryon chemical potential $\sqrt{s}(\mu_B)$ [20], and the phase boundary $T(\mu_B)$ [19] derived for GC and SC give the thermal model even predictive power. In a canonical ensemble are from the previously six free parameters of the model, T, V, B, S, Q, γ_S, three immediately fixed through quantum content of the fireball $\vec{Q} = (B, S, Q)$, while the strong dependence of $\langle E\rangle/\langle N\rangle$ on T and system radius r allows for instance to constrain the pair volume and temperature to a particular average energy per particle, leaving us with only two, system size and phase space suppression to account for a strange sector out of equilibrium. The plots 3.10 and 3.11 show the freeze-out temperature for different values of $\frac{\langle E\rangle}{\langle N\rangle}$ in a charge system with $(B, S, Q) = (8, 0, 4)$ and a neutral system with $(B, S, Q) = (0, 0, 0)$ respectively. While for large radii, at fixed quantum content, e.g approaching neutrality, both cases produce a rather flat dependence of the freeze-out temperature on the system radius, this situation changes for small systems, where the T drops fast for decreasing r for charged systems, while a overall neutral system exhibits a constant T for vanishing volumes close to that of Karsch [21] and Fortunato *et al.* [5]. The second freeze-out condition discussed here is the normalized entropy density $\frac{\langle s\rangle}{T^3}$. Both lattice gauge results [45] as well as thermal model fits to data suggest a fixed value

$$\frac{\langle s\rangle}{T^3} \approx 7. \tag{3.24}$$

From a thermal model point of view this is rather surprising as along the freeze-out curve $\frac{\langle E\rangle}{\langle N\rangle}$ baryon chemical potential and temperature vary strongly from the lowest SPS to the highest RHIC energies, and thus the hadronic composition of the fireball changes accordingly and one would naively expect a change in $\frac{\langle s\rangle}{T^3}$. In reference [17] common features of charged particle

production in AA and e^+e^- collisions are discussed and similar values of the number of degrees of freedom were found for both cases. The entropy suppression at lower energies for nucleon nucleon collision is explained with a strong interplay of baryon chemical potential and freeze-out temperature. Figures 3.12 and 3.13 show the same quantum configurations as before with the pair r,T being constrained to a constant value of $\frac{\langle s \rangle}{T^3}$. Small and neutral systems have diverging values of T for constant $\frac{\langle s \rangle}{T^3}$. In the charged case T drops for small radii, while again for growing radius, hence approaching neutrality, approaches the values for T of the neutral case from below. Generally seems the conditions of a constant average energy per particle of about $1GeV$ to favor a lower freeze-out temperature than the condition of the normalized entropy density of about 7. Further should the entropy be rather sensitive to phase space suppression factors, in particular strangeness. As $\frac{\langle s \rangle}{T^3}$ is a density and we have still two free parameters, the volume and γ_S, it looks promising to correlate strangeness suppression to the normalized entropy density leaving us with only one free parameter, the system size or power of the thermal source. This should allow to describe a canonical ensemble only by its conserved quantities (B,S,Q), the fireball volume, the average energy per particle and the entropy density.

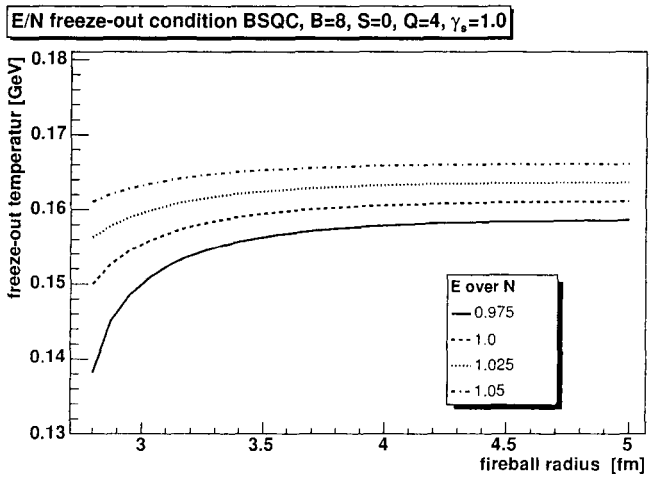

Figure 3.10: Freeze-out condition $\langle E \rangle / \langle N \rangle$, fixing a freeze-out temperature to a system of given radius, baryon number, strangeness, electrical charge and strangeness suppression factor

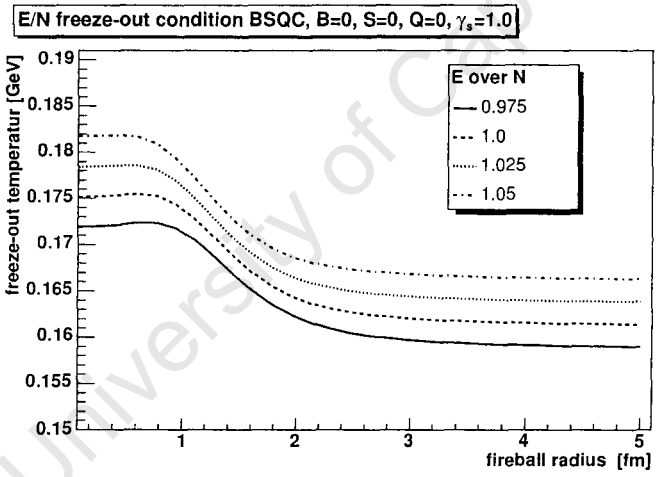

Figure 3.11: Freeze-out condition $\langle E \rangle / \langle N \rangle$, fixing a freeze-out temperature to a system of given radius, baryon number, strangeness, electrical charge and strangeness suppression factor

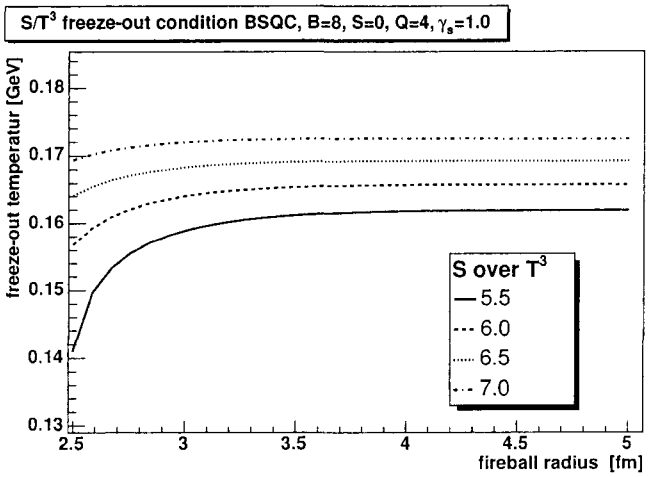

Figure 3.12: Freeze-out condition $\langle s \rangle / T^3$, fixing a freeze-out temperature to a system of given radius, baryon number, strangeness, electrical charge and strangeness suppression factor

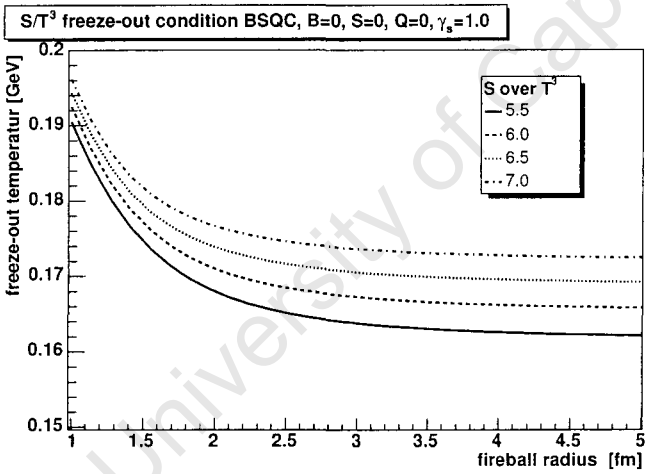

Figure 3.13: Freeze-out condition $\langle s \rangle / T^3$, fixing a freeze-out temperature to a system of given radius, baryon number, strangeness, electrical charge and strangeness suppression factor

3.8 Conclusion

Despite the fact that canonical models without quantum statistics and chemical potentials predict too low fluctuations, should the provided code, a description of the software package is in the appendix G, at least allow for a systematic discussion. In particular the effect of freeze-out conditions average energy per particle and normalized entropy density can be investigated and will be very useful to constrain parameter set and to classify events by its thermal conditions at hadronization. The statistical behavior and the mathematical aspects of a simple pion gas and a proper hadronic gas are not too different, although additional conserved charges, the hadronic resonance spectrum and a strong dependence of the hadronic composition on freeze-out conditions make the latter case far more complex. Additionally was feed down well handled with cumulants and moments which allows for a more economical calculation of final state distribution than the method of convolution of single particle distributions. Nevertheless one still has to preform a numerical integration of the approximated partition functions which puts considerable constraints on the range of applications. The results of chapter 5 and will show how to circumvent this problem and provide a analytical approximation method free of numerical integrations. A discussion and application of this model to the NA49 CC data at 158AGeV is in the following chapter.

Chapter 4

Pre-Analysis

To test the applicability of the canonical formalism to statistical multiplicity fluctuations found in high energy collision, we take the NA49 Carbon on Carbon data at $158AGeV$ taken at the SPS collider at CERN. The idea is to discuss fluctuations of observables, in particular particle number, and their dependence on thermal parameters and freeze-out conditions in the presence of exact conservation laws. Such fluctuations will carry signatures of the conditions at break up and the hadronization process itself. Even within one (narrow) centrality bin, like the one discussed here, one will find slightly different initial conditions for each event. Subsequent hydrodynamic evolution of the system can result in different system sizes, baryon content, freeze-out temperatures, average energy per particle, and phase space occupancy. A variation of parameters preserves, despite being similar in spirit to a application of the GC to a mid rapidity slice, the canonical character of fluctuations as well as multiplicities.

4.1 Model Assumptions

The assumption made closely reflect the limitations of code. The use of Boltzmann statistics, while quantum statistics would lead to stronger fluctuations, is the first and most important shortcoming. The correct Fermi and Bose statistics might become especially important at the transition from a fermion to a boson dominated hadron gas expected to be realized around the lowest SPS energies of about $\sqrt{s} = 8.2GeV$ [46], yet still well below the center of mass energy at $158AGeV$ ($\sqrt{s} = 17.3GeV$), of this data. A prominent feature of this transition is the 'horn', a pronounced peak in the K^+ to π^+ ratio [47, 48, 49]. Further are 4π integrated yields assumed, one static thermal source or fireball, described by one canonical parameter set, is as-

sumed to be in thermal contact with the unobserved regions of the collision. Yet the basic properties are allowed to vary from collision to collision about some mean values constrained by global properties like the average energy per particle or the normalized entropy density. At some point of the evolution the charge content of the fireball should be fixed and be followed by a single (thermal and chemical) freeze-out. No phase transitions description is contained in a standard thermal model, in particular would a 1st or 2nd order phase transition from a deconfined QGP phase to a hadron gas, expected at lower temperature and higher baryon chemical potential, have enhance fluctuations when compared to a crossover [21]. No excluded volume corrections are taken into account, which can have considerable effect on thermal parameters and would additionally allow for description of phase transitions [22]. The strangeness suppression factor γ_S is chosen over a canonical volume to describe an out of equilibrium strangeness sector. Lastly was a Breit-Wigner width for particle masses omitted which would increase sub thresh hold particle production and would affect heavier resonances more strongly. Strange particles are assumed to be stable in the sense of the model as their live time is generally larger than the time of flight to the detector. The canonical ensemble can phenomenologically account for a variation in quantum content of the fireball or its volume, temperature or degree of equilibration, $(B, S, Q, R, T, \gamma_S)$, or its freeze-out properties $(\frac{\langle E \rangle}{\langle N \rangle}, \frac{\langle s \rangle}{T^3}, n_{b+\bar{b}})$ due to impact parameter variation, evolution, stopping and correct for particle decay. The CC system was chosen as already for the next data point $(SiSi)$ at $158AGeV$ has a too large multiplicity to allow for a similar discussion, while proton proton collision produce only a few particles which makes approximations more difficult.

4.2 NA49 Carbon on Carbon Data

The starting or mean values of this discussion come from a combination of experimental data and previous thermal model analysis. In reference [34] the charged particle fluctuations for pp, CC, $SiSi$, $PbPb$ collisions are presented for the data of $158AGeV$ CERN SPS heavy ion program, providing experimental values for the scaled variance for the multiplicity distributions of charged, positively and negatively charged particles (CC: $\omega_{ch} \approx 2.1$, $\omega_{pos} \approx 1.4$, and $\omega_{neg} \approx 1.4$). A very narrow centrality bin was chosen according to the energy deposited by spectator nucleons in the forward calorimeter ($E_{veto} = 0.5TeV$). Yet even though the number of participating projectile nucleons N_{part}^{proj} is fixed, the number of participating target nucleons N_{part}^{targ} can still vary on a purely statistical basis and a significant mixing of both

domains is observed what leads to charged particle fluctuations on top of those expected from a really fixed system size [50]. In reference [51] the event centrality was estimated using the information of energy deposited in the forward calorimeter or the average event multiplicity. A energy deposition of $E_{veto} \approx 0.5TeV$ was found to describe the same centrality bin as an average charged particle multiplicity of $\langle N_{ch} \rangle \approx 52$. On the theoretical side was this system, CC at $158AGeV$, analyzed with thermal model fits [52]. Although the model implementations are slightly different they will nevertheless be good starting values for this discussion. The parameter set $T = 0.16377GeV$, $r = 3.225fm$, $\gamma_S = 0.6$, and $(B, S, Q) = (4, 0, 2)$ is in agreement with the above reference, the freeze-out condition $\frac{\langle E \rangle}{\langle N \rangle} = 1.0$ and the experimental value for the charged particle multiplicity $\langle N_{ch} \rangle \approx 52$. In addition to the results summarized in table 4.1 are the normalized entropy density $\frac{\langle s \rangle}{T^3} \approx 4.67$ and baryon anti-baryon density $n_{b+\bar{b}} \approx 0.069fm^{-3}$. In

	$\langle N \rangle$	ω
N_{pos}	27.3697	0.652497
N_{neg}	25.4223	0.737072
N_{ch}	52.1413	1.02239
	$\langle R \rangle$	RMS_R
$\frac{K^+}{\pi^+}$	0.13617	0.0808674

Table 4.1: Summary table for a final state hadronic resonance gas in a BSQC , $\vec{Q} = (4, 0, 2)$, $T = 0.16377GeV$, $r = 3.225fm$, $\gamma_S = 0.6$, and $\frac{\langle E \rangle}{\langle N \rangle} = 1.0GeV$

the light of the above discussion we obviously fail to reproduce the high values of ω. Additionally are both values for the normalized entropy density and total baryon density well below the proposed ones $\frac{\langle s \rangle}{T^3} \approx 7$ [17] and $n_b + n_{\bar{b}} \approx 0.12fm^{-3}$ [18]. For the former strangeness suppression γ_S and modest T are to blame, while for the latter a low baryon content, radius and temperature. For a detailed recent discussion of freeze-out conditions see reference [19]. Unfortunately exists no event-by-event measurements of the $\frac{K^+}{\pi^+}$ ratio for this particular system and is only available for Pb Pb collisions at this energy [53]. But its mean ratio is consistent with expectations. Nevertheless are these values included into the discussion, as particle ratios should be less sensitive to dynamical effects and variations of parameters making them a better probe than yields. The $\frac{K^+}{\pi^+}$ ratio was chosen as kaons and pions are the most dominant strange and light mesons in the system.

4.3 Discussion

4.3.1 Temperature Dependence

The temperature dependence of statistical multiplicity fluctuations is shown for net-charges of $(B, S, Q) = (0, 0, 0)$ in figure 4.1, $(B, S, Q) = (4, 0, 2)$ in figure 4.2, and $(B, S, Q) = (8, 0, 4)$ in figure 4.3 respectively. A larger radius of $r = 3.65fm$ and complete strangeness equilibration ($\gamma_S = 1.0$) was chosen to allow for high enough multiplicities to extent the graphs to low temperatures. The first finding is that, like in a simple particle anti-particle gas, the fluctuations of the preferred particle are suppressed with respect to ones disfavored by the net-charge. The similar masses of proton and neutron make them nearly degenerate particles, hence they are produced in similar numbers, as long as the temperature is high enough to allow for π^- production to balance the charge taken up by protons. Therefore are multiplicities of positive particles enhanced while their fluctuations are suppressed with respect to negative particles even for electrically neutral systems with low baryon content. The gap between ω^{pos} and ω^{neg} widens in charged systems with decreasing temperature, since fewer and fewer negative particles are produced, suppressing relative fluctuations of positive particles.
We next attend to the temperature dependence of various proposed freeze-out conditions. In figures 4.4, 4.5, and 4.6 the average energy per particle, normalized entropy density, and baryon plus anti-baryon density are shown for net-baryon numbers $B = 0, 2, 4, 6, 8, 10$ and a net-charge of always half the baryon number. In order to allow for a systematic discussion of phenomenological freeze-out conditions should their values be rather stable against the assumed variations of the thermal parameters around the mean. Despite a strong dependence at low temperatures on the baryon content reach all three cases for $T \approx 165MeV$ similar values, reflecting that the system approaches charge neutrality, e.g. the number of produced particles is much larger than the number of conserved charges. Additionally is the pressure nearly independent of B, while $\frac{\langle E \rangle}{\langle N \rangle}$ exhibits the strongest dependence. The normalized entropy density and the average energy per particle show a minimum as a function of T with its location depending on the baryon density. The baryon plus anti-baryon density is rather flat for low temperatures as additional (anti)baryon density production is only slowly picking up. Nevertheless suggest these graphs that for temperatures $T \approx 0.165 - 0.17GeV$ the proposed freeze-out conditions [15, 17, 18] are well reached.

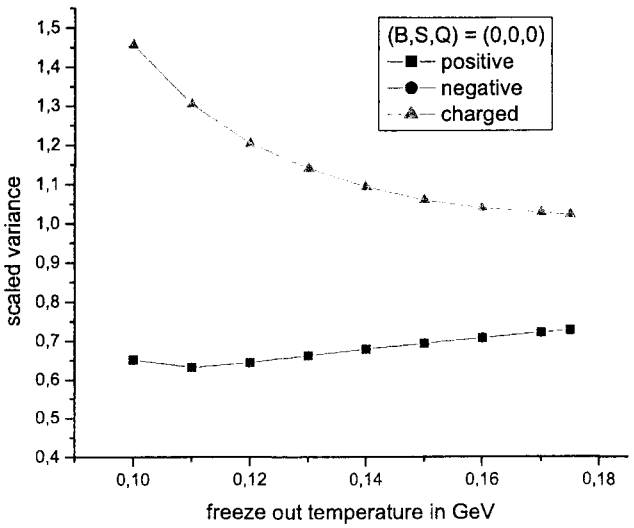

Figure 4.1: Temperature dependence of multiplicity fluctuation for positive, negative, and charged particles for $(B, S, Q) = (0, 0, 0)$

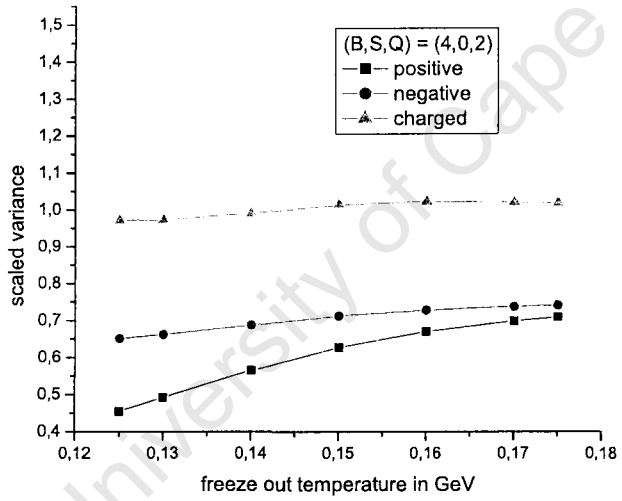

Figure 4.2: Temperature dependence of multiplicity fluctuation for positive, negative, and charged particles for $(B, S, Q) = (4, 0, 2)$

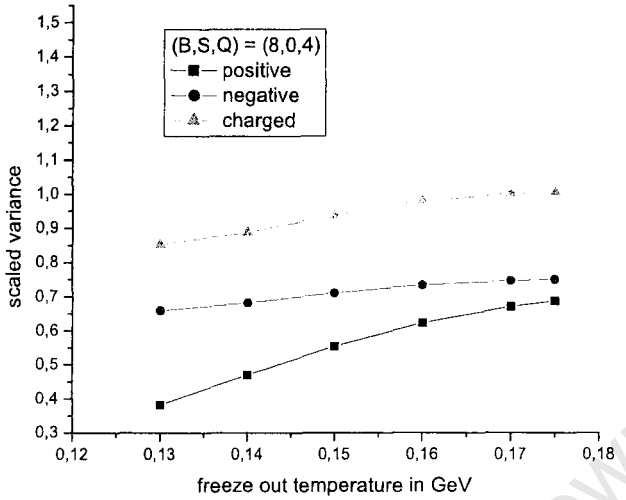

Figure 4.3: Temperature dependence of multiplicity fluctuation for positive, negative, and charged particles for $(B, S, Q) = (8, 0, 4)$

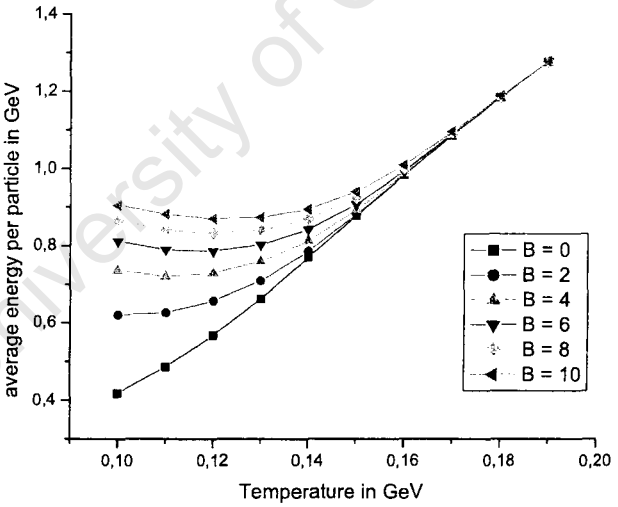

Figure 4.4: Temperature dependence of average energy per particle

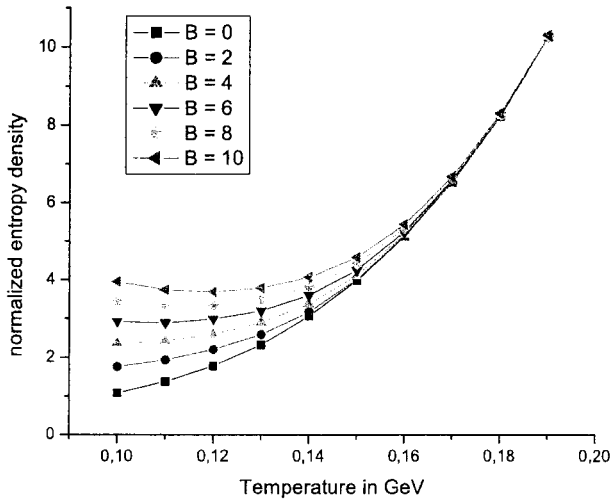

Figure 4.5: Temperature dependence of the normalized entropy density

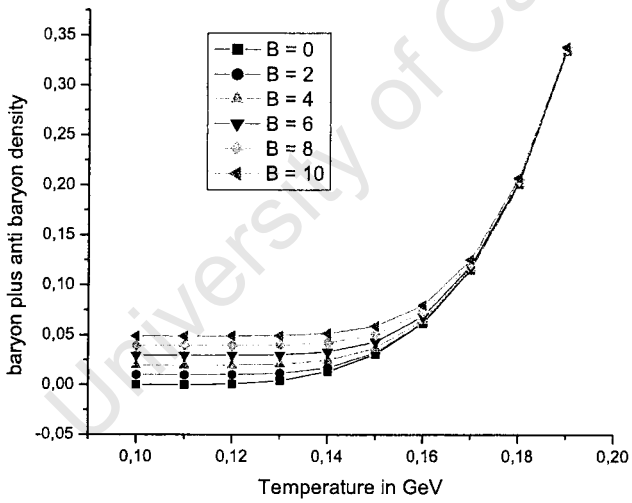

Figure 4.6: Temperature dependence of baryon plus anti-baryon density

4.3.2 Baryon and Charge Content

A variation of conserved quantum numbers could arise on either a purely statistical(thermal) basis by assuming the analyzed part of the system is in, not necessarily ideal, thermal and chemical contact with the remainder and subject to hydrodynamic evolution. Or originate form different initial condition, like impact parameter or different collision dynamics, so depends the amount of energy and baryons deposited in the central region in a simple picture on both the number of participating nucleons N_{part} and the number of binary collisions N_{coll} they suffer. The thermal model cannot distinguish these two sources, but we assume that the initial conditions are well fixed by the narrow centrality bin and ascribe the variation to thermal and hydrodynamical effects and assume further that the collision dynamics therefore lead to similar quantum charge content and thermal properties before hadronization in all selected events. In table 4.2 the results obtained from parameter mix in the table below. The values are only slightly above the ones for fixed (B, S, Q)

weight	(B, S, Q)	$T[GeV]$
10%	$(0, 0, 0)$	0.1647
20%	$(2, 0, 1)$	0.1645
40%	$(4, 0, 2)$	0.1638
20%	$(6, 0, 3)$	0.1625
10%	$(8, 0, 4)$	0.1605

$= (4, 0, 2)$ at same γ_S, radius and $\frac{\langle E \rangle}{\langle N \rangle}$. A overall only weakly charged system, with the freeze-out temperature only changing slowly with the baryon number is responsible for this. Due to the relatively high mass of the baryons are

	$\langle N \rangle$	ω
N_{pos}	27.1594	0.651337
N_{neg}	25.2107	0.798381
N_{ch}	51.7172	1.06169
	$\langle R \rangle$	RMS_R
$\frac{K^+}{\pi^+}$	0.136487	0.0797212

Table 4.2: Summary table for a final state hadronic resonance gas in a BSQC, with variations in $\vec{Q}$ around $\vec{Q} = (4, 0, 2)$, $T = 0.16377GeV$, $r = 3.225fm$, $\gamma_S = 0.6$, and $\frac{\langle E \rangle}{\langle N \rangle} = 1.0GeV$

relative canonical chemical potentials $\frac{\mu}{m}$ low (μ_B is raising form $0.066GeV$

at $(B, S, Q) = (4, 0, 2)$ to $0.151 GeV$ for $(B, S, Q) = (8, 0, 4)$), while the ratio $\frac{m}{T}$ holds baryons at a low relative temperature, hence should the Boltzmann approximation do well for baryons (see chapter 5).

4.3.3 Average Energy per Particle

Apart from the evidence presented in the previous chapter which suggest a highest temperature for hadronic matter as well as a constant energy per particle, we assume it is a thermal parameter. The origin of such variation of the average energy per particle could be the hadronization process itself, e.g. not a single freeze-out model, or due to conditions in the early stages of the collision, leading to a different energy density of the fireball. In general should the assumption of a constant value not be required. Further is a variation in the average energy per particle mimicking volume fluctuations for high temperatures and low chemical potentials. Due to the strong interplay between temperature and fireball radius for weakly charged systems would volume fluctuations at constant $\frac{\langle E \rangle}{\langle N \rangle}$ have a weaker temperature dependence. See figures 3.10 and 3.11 and discussion in chapter 3. The following superposition was taken and the results are summarizes in table 4.3. While a

weight	$\frac{\langle E \rangle}{\langle N \rangle} [GeV]$	$T [GeV]$
10%	0.950	0.1584
20%	0.975	0.1611
40%	1.000	0.1638
20%	1.025	0.1664
10%	1.050	0.1689

temperature difference of about $10 MeV$ is rather large, the bulk of the assumed events comes from a narrow region $T = 163 \pm 3 MeV$. This is so far the best candidate to explain the high values for the charge fluctuations of the CC system at $158 AGeV$. A quantum statistical treatment of in particular light mesons and additional (trivial) volume fluctuations should thus allow to close the remaining gap to the NA49 measurements.

	$\langle N \rangle$	ω
N_{pos}	27.5248	1.02341
N_{neg}	25.5769	1.1367
N_{ch}	52.4535	1.79993
	$\langle R \rangle$	RMS_R
$\frac{K^+}{\pi^+}$	0.136759	0.0794136

Table 4.3: Summary table for a final state hadronic resonance gas in a BSQC, with small variations in $\frac{\langle E \rangle}{\langle N \rangle}$ around $\vec{Q} = (4, 0, 2)$, $T = 0.16377 GeV$, $r = 3.225 fm$, $\gamma_S = 0.6$, and $\frac{\langle E \rangle}{\langle N \rangle} = 1.0 GeV$

4.3.4 Strangeness Suppression γ_S

The influence of strangeness suppression γ_S on freeze-out temperature for constant $\frac{\langle E \rangle}{\langle N \rangle} = 1.0$ along the 'phase boundary', e.g. growing B, is shown in figure 4.7. With an increase in equilibration of the strange sector comes a cooling of the system. While the normalized entropy density does not vary too much along the 'phase boundary' for fixed γ_S, it changes almost linearly with γ_S, rising from about 3.5 (no strange particles produced) to over 5 for a completely equilibrated strange sector (figure 4.8) with the temperature dropping from about $168 MeV$ to $162 MeV$ for a neutral system. Due to the strong and simple correlation between $\frac{\langle s \rangle}{T^3}$ and γ_S along $\frac{\langle E \rangle}{\langle N \rangle} = const$ line acts γ_S as something like an 'entropy thermometer ' for weakly charged systems. Quite surprisingly neither $\langle R \rangle$ nor RMS_R are affected by this γ_S variations. Despite the fact that individual distributions have different mean values, a superposition of distributions leads hardly to a widening of the curve (figure 4.9).

weight	γ_S	$T[GeV]$
33,3%	0.5	0.1645
33,3%	0.6	0.1638
33,3%	0.7	0.1630

	$\langle N \rangle$	ω
N_{pos}	27.3715	0.652896
N_{neg}	25.4241	0.737497
N_{ch}	52.1447	1.02327
	$\langle R \rangle$	RMS_R
$\frac{K^+}{\pi^+}$	0.136448	0.0808882

Table 4.4: Summary table for a final state hadronic resonance gas in a BSQC, with variations in γ_S around $\vec{Q} = (4, 0, 2)$, $T = 0.16377GeV$, $r = 3.225fm$, $\gamma_S = 0.6$, and $\frac{\langle E \rangle}{\langle N \rangle} = 1.0GeV$

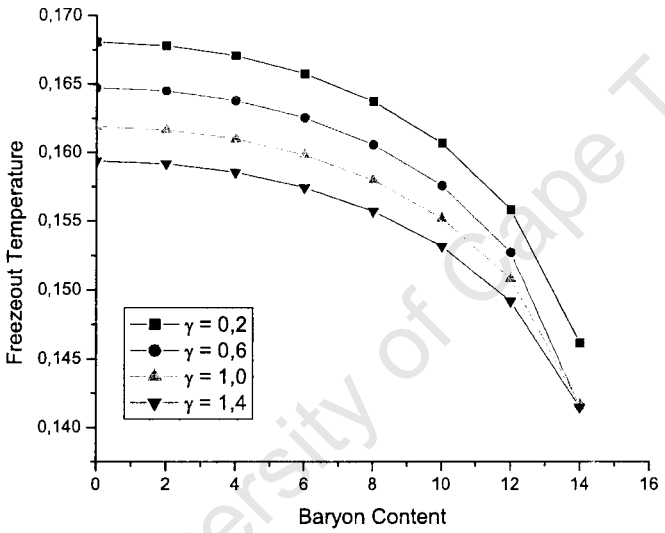

Figure 4.7: Phase boundary as described by the line of constant energy per particle for different values of γ_S

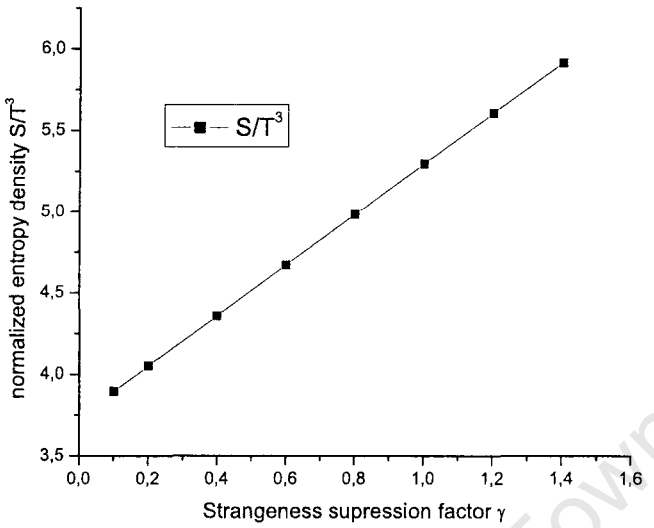

Figure 4.8: Normalized entropy density as a function of γ_S

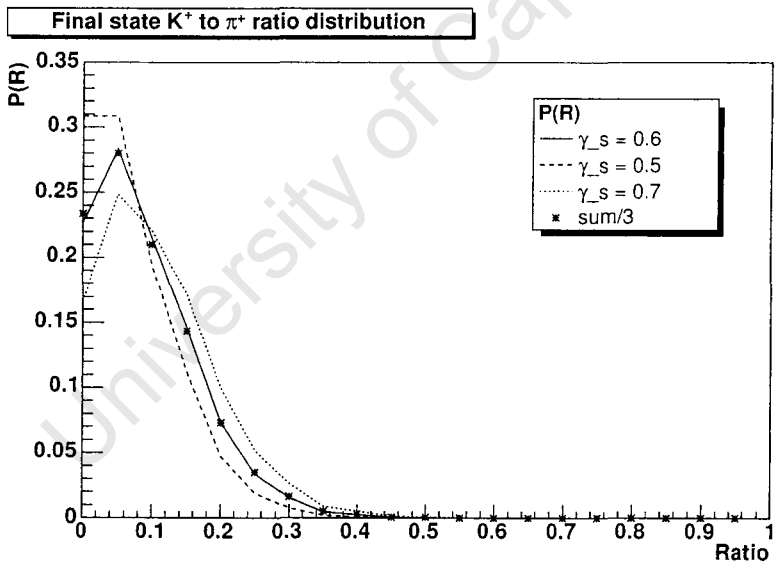

Figure 4.9: Final state K^+ to π^+ ratio for different values of γ_S

4.4 Conclusion

A combination of a variation in (either) average energy per particle and/or volume and quantum statistics will certainly be able to reproduce a wide range of values of statistical fluctuations. A strong correlation of the parameter pair fireball volume and temperature via the condition of a constant energy per particle leads to a weak temperature dependence for volume fluctuations while somewhat stronger for $\frac{\langle E\rangle}{\langle N\rangle}$ variations. For this discussion of the narrow centrality bin of the NA49 CC data at 158 AGeV volume fluctuations were omitted in favor of the latter. The normalized entropy density is nearly constant along the freeze-out curve in figure 4.7, hence baryon and charge content seem have not too much of an effect on neither fluctuations nor the freeze-out condition $\frac{\langle s\rangle}{T^3}$, as long as the number of produced particles is sufficiently larger than the number of conserved charges, while the gap between ω^{pos} and ω^{neg} slowly widens with growing baryon number. The total baryon density $n_{b+\bar{b}} = 0.0695 fm^{-3}$ is rather stable against similar variation. Strangeness suppression again wont affect to strongly the fluctuations of charged particles, not even the K^+/π^+ ratio, due a almost linear dependence of $\frac{\langle s\rangle}{T^3}$ (the number of states) along the $\frac{\langle E\rangle}{\langle N\rangle} = const$ freeze-out line for all assumed baryon and charge contents. As a consequence one can constrain the pair (T, r) to the average energy per particle and γ_S with the normalized entropy density. The first indication is that one can understand the CC charge particle fluctuation measurement of the NA49 collaboration in a canonical ensemble with quantum statistics. Yet better assumptions on reasonable values for the parameter mix than the ad hoc choice made for this pre-analysis are needed. Chapter 5 will show how to use the central limit theorem to make reasonable approximations to distributions for finite systems, allowing for the use of Fermi and Bose statistics this and further analysis.

Chapter 5

Probability And Characteristic Function

5.1 Motivation

The success of the statistical hadronization model in describing data obtained from high energy collisions and a partly puzzling statistical behavior of thermal systems make a further investigation of statistical-thermal distributions and their mathematical properties a worthwhile exercise. As commonly employed experimental observables are average yields, e.g. the first moment, and the use of the GC is often sufficient, comprehensive software has been developed for those cases. The THERMUS [11] package for instance allows for calculation of average multiplicities in the BSQC, but only in Boltzmann approximation, while SHARE [12] and THERMINATOR [13] allow additionally for calculation of fluctuations and spectra and the use of quantum statistics, yet only for the GC. But multiplicity distributions have been found to differ from simple Poissonians even under the thermodynamic limit as soon as one does not assume GC and Boltzmann approximation. So show canonical [24], and even stronger micro canonical ensembles (MC) [25, 26], for particle anti-particle gases as well as canonical hadronic gases [42] suppressed fluctuations. For finite volumes are only for a simple Boltzmann particle anti-particle gas [23] analytical solutions possible, while a canonical Boltzmann hadron gas even with a reduced number of integrals (see chapter 3), still requires considerable computation time. For quantum statistics an analytical approach might well be out of reach, and one has to use Monte Carlo techniques [54]. In this chapter a different approach is presented. It is known that if one has good knowledge of the moments of a probability distribution function one can obtain an approximation of this distribution

through those moments, or rather through its, ultimately better suited, cumulants. For multi variable distributions moments and cumulants will be tensors who's off-diagonal components are a measure for the anisotropy, or the degree of correlation of their variables, and ultimately the distribution's shape. In this chapter the central limit theorem and its associated expansions are employed to calculate the scaled variance under the thermodynamic limit and in a further step its is shown how one can approximate distributions for finite system size.

5.2 Characteristic Function

Let us consider a probability distribution of some observable χ which can take values $f_\chi(x)$ on the real x axis and who's normalization requires that

$$\int_{-\infty}^{\infty} f_\chi(x) = 1. \tag{5.1}$$

And hence $f_\chi(x)$ defines the probability of finding a value x for the observable χ. One can now further define the characteristic function $\Phi_\chi(i\omega)$ to be the Fourier back transformation of the probability distribution $f_\chi(x)$

$$\Phi_\chi(i\omega) \equiv \hat{f}_\chi(x) = \int_{-\infty}^{\infty} e^{i\omega x} f_\chi(x)\, dx. \tag{5.2}$$

The moments $\mathcal{E}^n(\chi)$ can directly be calculated from the characteristic function from the respective derivatives at the origin.

$$\begin{aligned} \frac{d^n\Phi_\chi(i\omega)}{d\omega^n} &= \int_{-\infty}^{\infty} e^{i\omega x} f_\chi(x)(ix)^n dx \\ \frac{d^n\Phi_\chi(i\omega)}{d\omega^n}\Big|_{\omega=0} &= i^n \int_{-\infty}^{\infty} f_\chi(x)x^n dx \equiv i^n\mathcal{E}^n(\chi) \end{aligned} \tag{5.3}$$

With the probability distribution $f_\chi(x)$ therefore being the Fourier transform of the characteristic function $\Phi_\chi(i\omega)$

$$f_\chi(x) = \int_{-\pi}^{\pi} \frac{d\omega}{2\pi} e^{-ix\omega}\Phi_\chi(i\omega)\, d\omega. \tag{5.4}$$

On the other hand one can, in a thermal model approach, calculate the moments $\langle N_j^n\rangle$ of an observable (multiplicty of particle j) form the derivatives

of the partition function $\mathcal{Z}$.

$$\langle N_j^n \rangle = \frac{1}{\mathcal{Z}} \left(T \frac{\partial}{\partial \nu_j} \right)^n \mathcal{Z}(\nu_j)\Big|_{\nu_j=0} = \frac{1}{\mathcal{Z}} \left(-i \frac{\partial}{\partial \phi_j} \right)^n \mathcal{Z}(\phi_j)\Big|_{\phi_j=0}$$

where the substitution $\frac{\nu_j}{T} = i\phi_j$ was made to allow for easier notation and simple integration, and hence

$$i^n \langle N_j^n \rangle = \frac{1}{\mathcal{Z}} \frac{d^n \mathcal{Z}(\phi_j)}{d\phi_j^n}\Big|_{\phi_j=0} = \frac{d^n \mathcal{Z}'(\phi_j)}{d\phi_j^n}\Big|_{\phi_j=0}. \tag{5.5}$$

The normalized partition function $\mathcal{Z}' = \frac{\mathcal{Z}(\phi_j)}{\mathcal{Z}}$ is the characteristic function and its probability distribution $P(N_j)$ can be found by Fourier transformation

$$P(N_j) = \frac{1}{\mathcal{Z}} \int_{-\pi}^{\pi} \frac{d\phi_j}{2\pi} e^{-iN_j\phi_j} \mathcal{Z}(\phi_j) = \int_{-\pi}^{\pi} \frac{d\phi_j}{2\pi} e^{-iN_j\phi_j} \mathcal{Z}'(\phi_j). \tag{5.6}$$

Basically the whole problem comes down to the calculation of Fourier integrals of various forms of the partition function $\mathcal{Z}$. As mentioned earlier, this is unfortunately not always possible. Analytical solutions, or a analytical reduction of the number of integrals, only work in Boltzmann approximation, while even with a reduced number of integrals numerical calculations become increasingly expensive when a large number of conserved charges is considered, or simply the product VT^3 is large. As mentioned in the introduction to this chapter, it is rather difficult and impractical to construct an approximated characteristic function from the knowledge of the moments of a distribution and one should rather use cumulants, which are linear combinations of moments. Tables for cumulant and moment relations can be found in appendices I and J.

5.3 Cumulant Tensor

To introduce the cumulant tensor let us consider a probability distribution function of d variables which can be obtained from the Fourier transform of its characteristic, or moment generating, function $\Phi\left(\vec{k}\right)$

$$P(\vec{x}) = \int \frac{d^d\vec{k}}{(2\pi)^d} e^{-i\vec{k}\cdot\vec{x}} \Phi\left(\vec{k}\right) = \int \frac{d^d\vec{k}}{(2\pi)^d} e^{-i\vec{k}\cdot\vec{x}+\Psi(\vec{k})}. \tag{5.7}$$

where $\Psi\left(\vec{k}\right) = \ln \Phi\left(\vec{k}\right)$ is the cumulant generating function. The cumulant of order n is given through the Taylor coefficients at the origin. And as these

are d dimensional tensors

$$\kappa_n^{q_1,q_2,\ldots,q_n} = (-i)^n \frac{\partial^n \Psi}{\partial k_{q_1} \partial k_{q_2} \ldots \partial k_{q_n}}\Big|_{\vec{k}=\vec{0}}. \tag{5.8}$$

The indexes $q_1, q_2, \ldots, q_n$ could be baryon number, strangeness, charge and particle multiplicities, or even denote to energy and momentum. The cumulant generation function reads in terms of the Taylor expansion

$$\Psi(\vec{k}) = \ln \Phi(\vec{k}) = \sum_{n=1}^{\infty} \frac{i^n}{n!} \kappa_n^{q_1,q_2,\ldots,q_n} k_{q_1} k_{q_2} \ldots k_{q_n}, \tag{5.9}$$

and the probability in terms of the expanded partition function

$$P(\vec{x}) = \int \frac{d^d\vec{k}}{(2\pi)^d} e^{-i\vec{k}\cdot\vec{x}} e^{\sum_{n=1}^{\infty} \frac{i^n}{n!} \kappa_n^{q_1,q_2,\ldots,q_n} k_{q_1} k_{q_2} \ldots k_{q_n}}. \tag{5.10}$$

The $n = 0$ term in the Taylor expansion, the 0-th derivative, is the partition function $\mathcal{Z}$ itself and is the normalization. In the one-dimensional case $d = 1$ the first four cumulants are in terms of the central moments, which are the ones used in the thermal model,

$$\begin{aligned}
\kappa_1 &= \langle N \rangle \\
\kappa_2 &= \langle N^2 \rangle - \langle N \rangle^2 \\
\kappa_3 &= \langle N^3 \rangle - 3\langle N \rangle \langle N^2 \rangle + 2\langle N \rangle^3 \\
\kappa_4 &= \langle N^4 \rangle - 3\langle N^2 \rangle^2 - 4\langle N \rangle \langle N^3 \rangle + 12\langle N \rangle^2 \langle N^2 \rangle - 6\langle N \rangle^4
\end{aligned}$$

and are called the mean, variance, skewness and kurtosis or excess and describe the shape of the distribution. As mentioned earlier, the condition for a Poisson distribution is $\kappa_n = \langle N \rangle$ for all orders n of cumulants. Generally can the l-th cumulant κ_l be expressed in terms of the first l moments in closed form via the determinant of an almost lower triangular matrix, with $m_l = \langle N^l \rangle$.

$$\kappa_l = (-1)^{l+1} \begin{vmatrix}
m_1 & 1 & 0 & 0 & 0 & 0 & \ldots & 0 \\
m_2 & m_1 & 1 & 0 & 0 & 0 & \ldots & 0 \\
m_3 & m_2 & \binom{2}{1} m_1 & 1 & 0 & 0 & \ldots & 0 \\
m_4 & m_3 & \binom{3}{1} m_2 & \binom{3}{2} m_1 & 1 & 0 & \ldots & 0 \\
m_5 & m_4 & \binom{4}{1} m_3 & \binom{4}{2} m_2 & \binom{4}{3} m_1 & 1 & \ldots & 0 \\
\vdots & \vdots & \vdots & \vdots & \vdots & \ddots & \ddots & \vdots \\
m_{l-1} & m_{l-2} & \ldots & \ldots & \ldots & \ldots & \ddots & 1 \\
m_l & m_{l-1} & \ldots & \ldots & \ldots & \ldots & \ldots & \binom{l-1}{l-2} m_1
\end{vmatrix}$$

In thermodynamics cumulants are extensive quantities, so they scale linearly with the volume

$$\Psi_V\left(\vec{\phi}\right) = \ln \mathcal{Z}_V\left(\vec{\phi}\right) - \ln \mathcal{Z}_V\left(\vec{0}\right) = V \sum_{j=1}^{P} z_j^0\left(\vec{\phi}\right) - V \sum_{j=1}^{P} z_j^0\left(\vec{0}\right). \qquad (5.11)$$

where $V z_j^0$ is the usual single particle partition function 2.2 or 2.70, and the last term is the normalization or the $0\text{-}th$ expansion term, and hence

$$\Psi_{V_1+V_2}\left(\vec{\phi}\right) = \ln \mathcal{Z}'_{V_1+V_2}\left(\vec{\phi}\right) = (V_1+V_2) \sum_{j=1}^{P} z_j^0\left(\vec{\phi}\right) - (V_1+V_2) \sum_{j=1}^{P} z_j^0\left(\vec{0}\right), \qquad (5.12)$$

if temperature T, chemical potentials $\vec{\mu}$, and the respective phase space suppression factors γ are the same for all considered domains. In case this condition is not met, one can define local values for parameters and still take the same derivatives with respect to the angles (see appendix B).

5.4 Central Limit Theorem

In previous calculations (chapter 2 and 3) we expanded the generating function in terms of the Taylor coefficients, which had two advantages over the exact version. Firstly the integrand was simpler and allowed for approximation of Bose and Fermi distributions, and secondly it allowed to handle resonance decays and compute final state distributions. Here we want to exploit a further trick, the central limit theorem. Previously the cumulants had explicitly a volume dependence, or rather the employed moments carried powers of it. In the central limit theorem we are first going to separate off the volume dependence, and in a second step calculate corrections which contain decreasing powers of the same. This is a promising approach as the scaled variance converges fast as a function of the volume for both a Boltzmann pion gas [23] as well as for a Boltzmann BSQC with a full hadronic resonance table [42].

5.4.1 One Dimensional

To start off we want to consider a simple gas containing only the positive and the negative pion. Both cases, Boltzmann approximation and quantum statistics, are identical in this formulation. Only one type of charge is conserved, so one has either a probability distribution $P(Q)$ or $P(N)$ with no further conserved charges. The canonical partition function for such a system

divided by the grand canonical one gives the distribution $P_V(Q)$

$$P_V(Q) = \frac{1}{e^{z_+(0)+z_-(0)}} \int_{-\pi}^{\pi} \frac{d\phi_Q}{2\pi} e^{-iQ\phi_Q} e^{z_+(\phi_Q)+z_-(\phi_Q)}$$

$$P_V(Q) = \frac{1}{e^{z_+(0)+z_-(0)}} \int_{-\pi}^{\pi} \frac{d\phi_Q}{2\pi} e^{-iQ\phi_Q+V\left(z_+^0(\phi_Q)+z_-^0(\phi_Q)\right)}. \quad (5.13)$$

The main contribution to the integral comes form the region around the origin, so it is a good idea to expand around $\phi = 0$. The 0-th term in the Taylor expansion is again the normalization $\mathcal{Z} = e^{z_+(0)+z_-(0)}$. This yields

$$P_V(Q) = \int_{-\pi}^{\pi} \frac{d\phi_Q}{2\pi} e^{-iQ\phi_Q+V\left(\frac{\kappa_1}{1!}i\phi_Q+\frac{\kappa_2}{2!}\left(i\phi_Q\right)^2+\frac{\kappa_3}{3!}\left(i\phi_Q\right)^3+\frac{\kappa_4}{4!}\left(i\phi_Q\right)^4+\ldots\right)}. \quad (5.14)$$

Now we substitute $\omega = \sqrt{V}\sigma\ \phi_Q$, where $\sigma = \sqrt{\kappa_2}$ is the variance and extended the limits of integration to $\pm\infty$. The error made is going to be small, as the main contribution comes from around the origin and the integrand is not 2π periodic anymore, but a superposition of a decaying and a oscillating part (chapter 2).

$$P_V(Q) \approx \int_{-\infty}^{\infty} \frac{d\omega}{2\pi\sigma\sqrt{V}} e^{-i\frac{Q\omega}{\sigma\sqrt{V}}+i\frac{V\kappa_1\omega}{\sigma\sqrt{V}}+\frac{(i\omega)^2}{2!}+V\left[\frac{\kappa_3}{3!}\frac{(i\omega)^3}{(\sigma\sqrt{V})^3}+\frac{\kappa_4}{4!}\frac{(i\omega)^4}{(\sigma\sqrt{V})^4}+\ldots\right]} \quad (5.15)$$

Introducing the normalized cumulants $\lambda_n = \frac{\kappa_n}{\sigma^n}$ and a new variable $z = \frac{Q-V\kappa_1}{\sigma\sqrt{V}}$ allows to express the probability as

$$P_V(z) \approx \int_{-\infty}^{\infty} \frac{d\omega}{2\pi\sigma\sqrt{V}} e^{-i\omega z-\frac{\omega^2}{2!}} e^{\left[\frac{\lambda_3}{3!}\frac{(i\omega)^3}{V^{1/2}}+\frac{\lambda_4}{4!}\frac{(i\omega)^4}{V}+\frac{\lambda_5}{5!}\frac{(i\omega)^5}{V^{3/2}}+\mathcal{O}\left(V^{-2}\right)\right]}. \quad (5.16)$$

One can now again expand the second exponential and take terms up to some power of the volume into account

$$P_V(z) \approx \int_{-\infty}^{\infty} \frac{d\omega}{2\pi\sigma\sqrt{V}} e^{-i\omega z-\frac{\omega^2}{2!}} \quad (5.17)$$

$$\times \left[1+\frac{\lambda_3}{3!}\frac{(i\omega)^3}{V^{1/2}}+\frac{\lambda_4}{4!}\frac{(i\omega)^4}{V}+\frac{1}{2!}\left(\frac{\lambda_3}{3!}\right)^2\frac{(i\omega)^6}{V}+\mathcal{O}\left(V^{-3/2}\right)\right],$$

which is now a sum of almost identical integrals. Noting the definition of the Hermite polynomials these integrals can be solved.

$$H_n(z) = (-1)^n e^{\frac{z^2}{2}} \frac{d^n}{dz^n} e^{-\frac{z^2}{2}} \quad (5.18)$$

$$P_V(z) \approx \frac{e^{\frac{-z^2}{2}}}{\sigma\sqrt{2\pi V}}\left[1+\frac{\lambda_3}{3!}\frac{H_3(z)}{\sqrt{V}}+\frac{\lambda_4}{4!}\frac{H_4(z)}{V}+\frac{1}{2!}\left(\frac{\lambda_3}{3!}\right)^2\frac{H_6(z)}{V}+\mathcal{O}\left(V^{-3/2}\right)\right] \tag{5.19}$$

The first six Hermite polynomials are:

$$\begin{aligned} H_1 &= z \\ H_2 &= z^2-1 \\ H_3 &= z^3-3z \\ H_4 &= z^4-6z^2+3 \\ H_5 &= z^5-10z^3+15z \\ H_6 &= z^6-15z^4+45z^2-15 \end{aligned}$$

And introducing a further shorthand notation:

$$\begin{aligned} h_3(z) &= \frac{\lambda_3}{3!}H_3(z) \\ h_4(z) &= \frac{\lambda_4}{4!}H_4(z)+\frac{1}{2!}\left(\frac{\lambda_3}{3!}\right)^2 H_6(z) \\ h_5(z) &= \frac{\lambda_5}{5!}H_5(z)+\frac{\lambda_3}{3!}\frac{\lambda_4}{4!}H_7(z)+\frac{1}{3!}\left(\frac{\lambda_3}{3!}\right)^3 H_9(z) \end{aligned}$$

One finds for the final line of the calculation a Gaussian distribution with the first correction term being of order $\mathcal{O}\left(V^{-\frac{1}{2}}\right)$. As the volume of the system is increased the volume corrections will become less important.

$$P_V(z) \approx \frac{e^{\frac{-z^2}{2}}}{\sigma\sqrt{2\pi V}}\left[1+\frac{h_3(z)}{\sqrt{V}}+\frac{h_4(z)}{V}+\frac{h_5(z)}{V^{3/2}}+\mathcal{O}\left(V^{-2}\right)\right] \tag{5.20}$$

The 1-dimensional expansion related to the central limit theorem is commonly referred to as the Edgeworth expansion. This expansion is, in Boltzmann approximation, compared to the analytical solution 2.23 for the charge distribution in figures 5.1 to 5.4 for a small and a large volume. But already for rather small volumes one finds good agreement. The behavior under the thermodynamic limit of 2.23 is compared to this approximation in appendix F

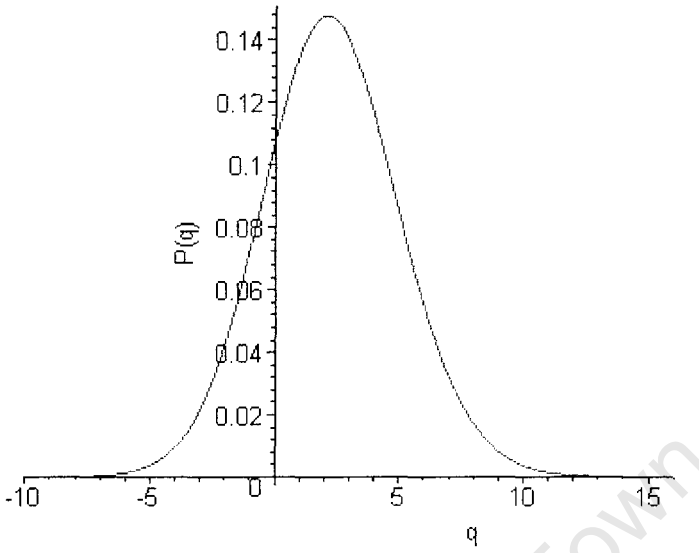

Figure 5.1: Charge distribution in a Boltzmann $\pi^{\pm}$ gas, approximation including terms of order V^{-2}, parameters $T = 0.16GeV$, $r = 2.1fm$, $\mu_Q = 0.05GeV$

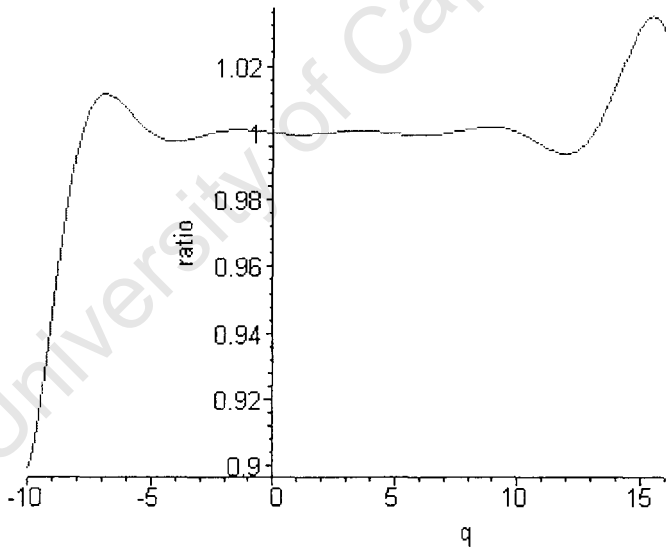

Figure 5.2: Ratio of approximation to analytical solution for the charge distribution in a Boltzmann $\pi^{\pm}$ gas, approximation including terms of order V^{-2}, parameters $T = 0.16GeV$, $r = 2.1fm$, $\mu_Q = 0.05GeV$

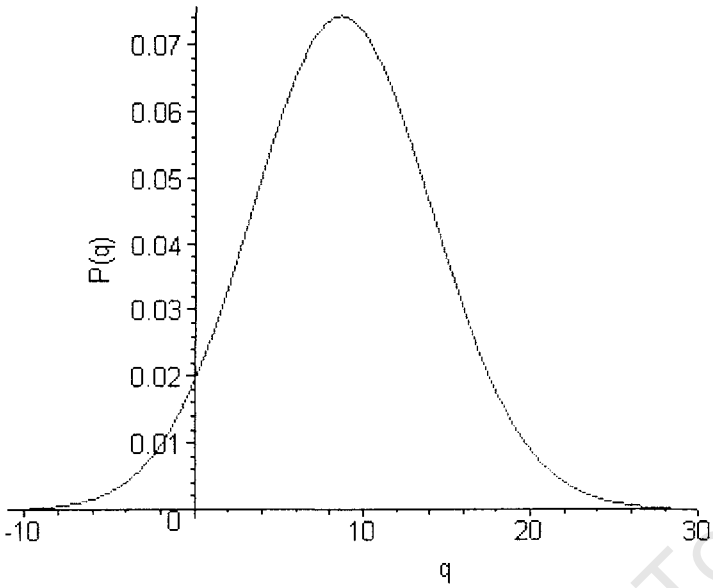

Figure 5.3: Charge distribution in a Boltzmann $\pi^{\pm}$ gas, approximation including terms of order V^{-2}, parameters $T = 0.16GeV$, $r = 3.3fm$, $\mu_Q = 0.05GeV$

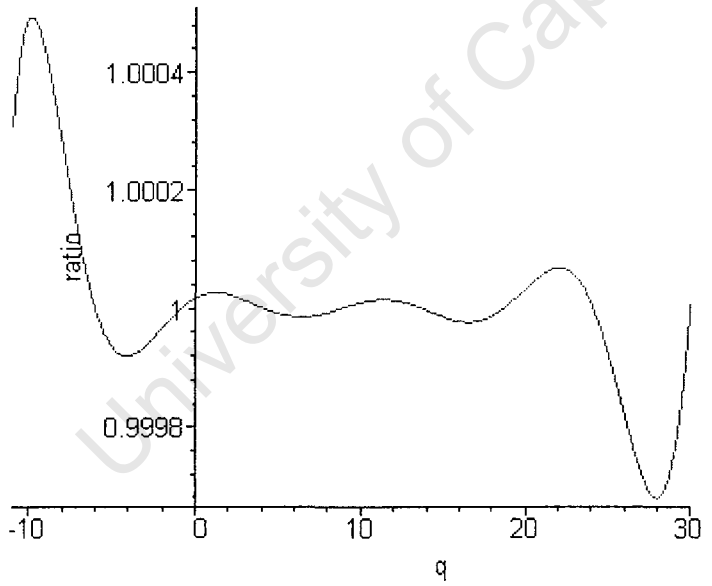

Figure 5.4: Ratio of approximation to analytical solution for the charge distribution in a Boltzmann $\pi^{\pm}$ gas, approximation including terms of order V^{-2}, parameters $T = 0.16GeV$, $r = 3.3fm$, $\mu_Q = 0.05GeV$

5.4.2 Width of Central Region

Cumulants which grow with their order will result in pronounced tails in the probability distribution which are commonly named 'fat tails'. The existence and finiteness of the cumulants will be of practical importance. In the thermal model cumulants would diverge, the volume dependence was split off, in Bose-Einstein statistics near condensation or degenerate Fermi-Dirac gases for low $\frac{m}{T}$ and high $\frac{\mu}{m}$. Nevertheless we will need some estimate for a region in which the approximation is reliable. The central limit theorem begins to break down when the first expansion term in 5.19 becomes $\sim \mathcal{O}(1)$.

$$\frac{h_3(z_{max})}{\sqrt{V}} \sim \mathcal{O}(1) \tag{5.21}$$

Approximating the Hermite polynomial $H_3 \sim z^3$, one can get an estimate for z_{max}.

$$z_{max} \simeq \left(\frac{3!}{\lambda_3}\right)^{1/3} V^{1/6} \tag{5.22}$$

While, when switching back to the definition of $z = \frac{Q - V\kappa_1}{\sigma\sqrt{V}}$, the width of the central region can be estimated

$$\frac{|Q - V\kappa_1|_{max}}{\sigma} \simeq \left(\frac{3!}{\lambda_3}\right)^{1/3} V^{2/3} \tag{5.23}$$

Hence the width of the central region scales as $V^{2/3}$, while the width of the curve should scale as $V^{1/2}$ and the central limit theorem approximation should be quite good. Even though larger volumes work better, they will still be sufficiently small enough to allow for calculation of distributions relevant for heavy ion collisions. In case a better approximation is needed, one will have to go back to equation 5.16 and employ Laplace's method of asymptotic expansion. The figures 5.5 and 5.6 show equation 5.21 as a function of the charge q. The plots are on the same scales as the figures 5.1, 5.2, 5.3, and 5.4 to allow for comparison with the distributions.

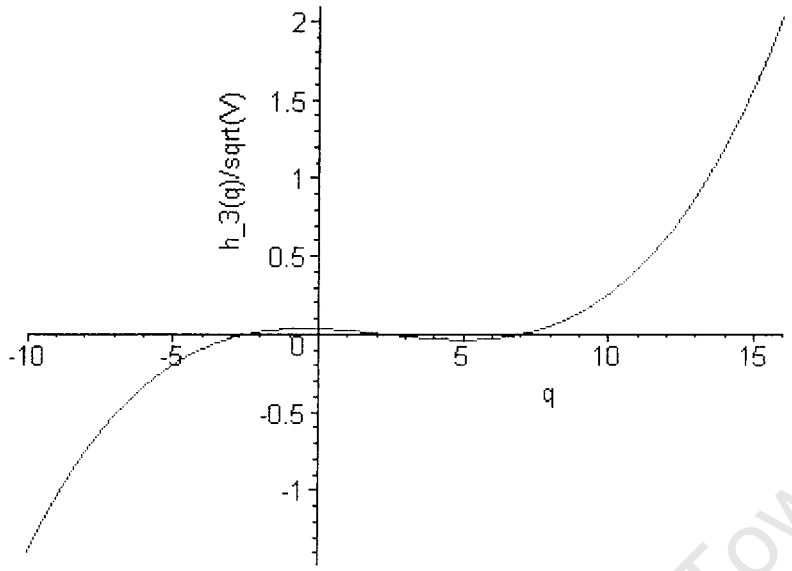

Figure 5.5: $h_3(z)V^{-1/2}$ for a Boltzmann $\pi^{\pm}$ gas, parameters $T = 0.16GeV$, $r = 2.1fm$, $\mu_Q = 0.05GeV$

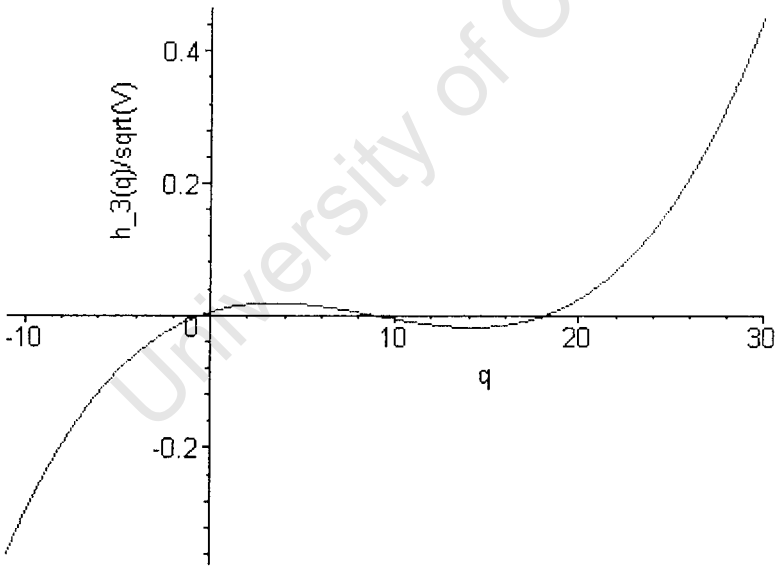

Figure 5.6: $h_3(z)V^{-1/2}$ for a Boltzmann $\pi^{\pm}$ gas, parameters $T = 0.16GeV$, $r = 3.3fm$, $\mu_Q = 0.05GeV$

5.4.3 Multi Dimensional

In principle one can treat any number of conserved quantities this way, with each conserved quantum number resulting in an additional integral, in general a number d. In a BSQC this would be 3 dimensions to approximate the partition function $\mathcal{Z}$, plus another 2 for particle correlations. Although the latter might not be necessary at all, since one can again get the moments of the distribution from the partition function and these will give by themselves information about the degree of correlation. The canonical pion gas ($P(Q,N)$), which is a two dimensional integral will be used for the examples.

$$P_V\left(Q^j\right) = \int_{-\pi}^{\pi} \frac{d^d\phi^j}{(2\pi)^d} e^{-iQ^j\phi_j + Vz(\phi_j)} \tag{5.24}$$

The function $z\left(\phi_j\right) = \sum_{n=1}^{P} z_n^0\left(\phi_j\right)$ is a sum of single particle partition functions of the type 2.2 or 2.70 with the volume being split off. Expanding equation 5.24 in term of its cumulants yields:

$$P_V\left(Q^j\right) = \int_{-\pi}^{\pi} \frac{d^d\phi^j}{(2\pi)^d} e^{-iQ^j\phi_j + iV\kappa_1^j\phi_j - V\frac{\kappa_2^{j_1,j_2}}{2!}\phi_{j_1}\phi_{j_2} + V\sum_{n=3}^{\infty} i^n \frac{\kappa_n^{j_1,j_2,\ldots,j_n}}{n!}\phi_{j_1}\phi_{j_2}\ldots\phi_{j_n}} \tag{5.25}$$

The variance σ will be a tensor of rank 2, while the variable ω will be its contraction with ϕ times $\sqrt{V}$

$$\omega_{j_1} = \sqrt{V}\,\sigma_{j_1}{}^{j_2}\,\phi_{j_2}, \tag{5.26}$$

where $\sigma_{j_1}{}^{j_2} = \left(\kappa_2^{1/2}\right)_{j_1}^{j_2}$. To take the square root of a matrix one needs first to diagonalize κ_2 with the orthogonal transformation matrix Q which can be found from the eigenvectors of κ_2. Hence $\kappa_2^{1/2} = Q\tilde{\kappa}^{1/2}Q^T$, where $\left(\tilde{\kappa}^{1/2}\right)_{d,b} = k_d^{1/2}\delta_{d,b}$ is a diagonal matrix with k_d being the d eigenvalues of κ_2. For every considered charge one will pick up an additional dimension and hence an additional factor of $\sqrt{V}$ from the determinant of σ.

$$d^d\omega_j = \det\left|\sqrt{V}\sigma\right| d^d\phi_j = V^{d/2}\det|\sigma|\; d^d\phi_j \tag{5.27}$$

Defining the normalized cumulant tensors:

$$\lambda_n^{j_1,j_2,\ldots,j_n} = \kappa_n^{k_1,k_2,\ldots,k_n}\left(\sigma^{-1}\right)_{k_1}^{j_1}\left(\sigma^{-1}\right)_{k_2}^{j_2}\ldots\left(\sigma^{-1}\right)_{k_n}^{j_n} \tag{5.28}$$

And the new variable:

$$z^j = \left(Q^k - V\kappa_1^k\right)\left(\sigma^{-1}\right)_k{}^j\, V^{-1/2} \tag{5.29}$$

$$P_V\left(z^j\right) \approx \int_{-\infty}^{\infty} \frac{d^d\omega^j}{\left(2\pi\sqrt{V}\right)^d \det|\sigma|} e^{-z_j\omega^j - \frac{\omega_j\omega^j}{2!} + \sum_{n=3}^{\infty} i^n V^{-\frac{n}{2}+1} \frac{\lambda_n^{j_1,j_2,\ldots,j_n}}{n!}\omega_{j_1}\omega_{j_2}\ldots\omega_{j_n}} \tag{5.30}$$

Again expanding the sum in the exponential and making use of the Hermite polynomials finally gives a result similar to that for the one dimensional case.

$$\left(H_n\left(z\right)\right)_{j_1,j_2,\ldots,j_n} = (-1)^n e^{\frac{z^j z_j}{2}} \frac{d^n}{dz_{j_1}\, dz_{j_2}\ldots dz_{j_n}} e^{-\frac{z^j z_j}{2}} \tag{5.31}$$

$$P_V\left(z^j\right) = \frac{e^{-\frac{z_j z^j}{2}}}{(2\pi V)^{d/2}\det|\sigma|}\left[1 + \frac{h_3\left(z\right)}{\sqrt{V}} + \frac{h_4\left(z\right)}{V} + \frac{h_5\left(z\right)}{V^{3/2}} + \mathcal{O}\left(V^{-2}\right)\right] \tag{5.32}$$

With the adjusted shorthand notation previously employed:

$$\begin{aligned}
h_3\left(z\right) &= \frac{\lambda_3^{j_1,j_2,j_3}}{3!}\left(H_3\left(z\right)\right)_{j_1,j_2,j_3} \\
h_4\left(z\right) &= \frac{\lambda_4^{j_1,j_2,j_3,j_4}}{4!}\left(H_4\left(z\right)\right)_{j_1,j_2,j_3,j_4} + \frac{1}{2!}\frac{\lambda_3^{j_1,j_2,j_3}}{3!}\frac{\lambda_3^{j_4,j_5,j_6}}{3!}\left(H_6\left(z\right)\right)_{j_1,\ldots,j_6} \\
h_5\left(z\right) &= \frac{\lambda_5^{j_1,\ldots,j_5}}{5!}\left(H_5\left(z\right)\right)_{j_1,\ldots,j_5} + \frac{\lambda_3^{j_1,j_2,j_3}}{3!}\frac{\lambda_4^{j_1,j_2,j_3,j_4}}{4!}\left(H_7\left(z\right)\right)_{j_1,\ldots,j_7} \\
&\quad + \frac{1}{3!}\frac{\lambda_3^{j_1,j_2,j_3}}{3!}\frac{\lambda_3^{j_4,j_5,j_6}}{3!}\frac{\lambda_3^{j_7,j_8,j_9}}{3!}\left(H_9\left(z\right)\right)_{j1,\ldots,j_9}
\end{aligned}$$

The same arguments for the width of the central region hold as in the one dimensional case. Figures 5.7 and 5.8 show the approximated conditional distribution $P(Q,N)$ and the ratio of approximation to the analytical solution 2.42 respectively. The approximation converges on an elliptic region under the body of the distribution, which features in the plots. The expansion only includes terms up to order V^{-1}. The best agreement is achieved for the canonical distribution with $Q = \langle Q\rangle$ as defined by the chemical potential. The plots 5.9 and 5.10 show the canonical distributions for $Q = 20$ at $\mu_Q = 0.05$. The values for the scaled variance are $\omega^{exact} = 0.350$ and $\omega^{approx} = 0.352$ respectively.

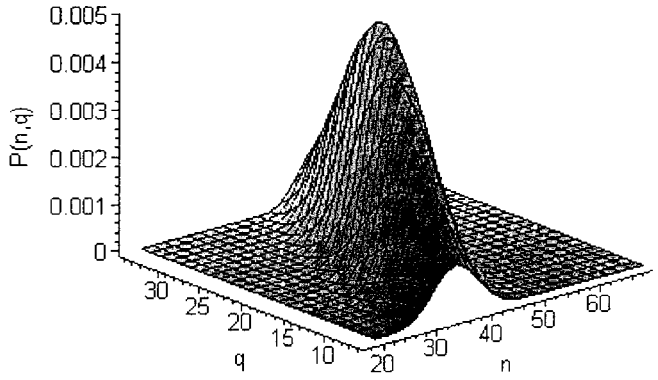

Figure 5.7: Approximation for the conditional probability distribution $P(N,Q)$ for a Boltzmann $\pi^{\pm}$ gas, approximation including terms of order V^{-1}, parameters $T = 0.16GeV$, $r = 4.33fm$, $\mu_Q = 0.05GeV$, $\langle Q \rangle = 20$

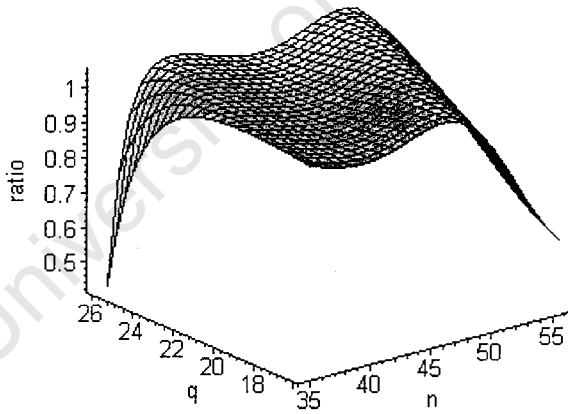

Figure 5.8: Ratio of approximation to analytical solution for the conditional probability distribution $P(N,Q)$ for a Boltzmann $\pi^{\pm}$ gas, approximation including terms of order V^{-1}, parameters $T = 0.16GeV$, $r = 4.33fm$, $\mu_Q = 0.05GeV$, $\langle Q \rangle = 20$

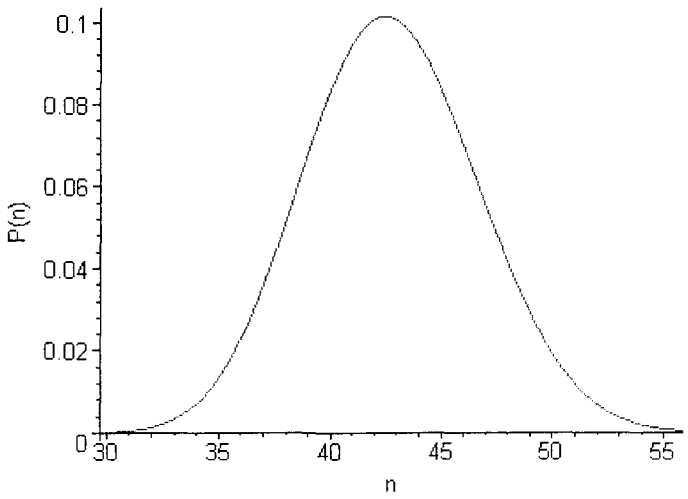

Figure 5.9: Approximation for the canonical probability distribution $P_Q(N)$ for a Boltzmann $\pi^{\pm}$ gas, approximation including terms of order V^{-1}, parameters $T = 0.16GeV$, $r = 4.33fm$, $\mu_Q = 0.05GeV$, $Q = 20$

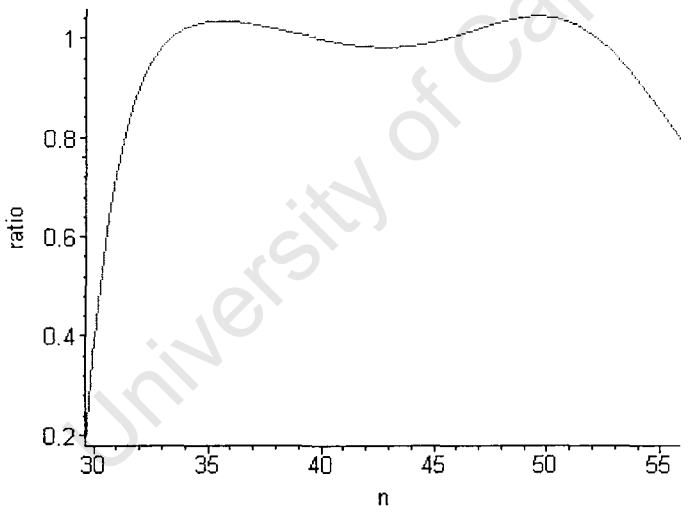

Figure 5.10: Ratio of approximation to analytical solution for the canonical probability distribution $P_Q(N)$ for a Boltzmann $\pi^{\pm}$ gas, approximation including terms V^{-1}, parameters $T = 0.16GeV$, $r = 4.33fm$, $\mu_Q = 0.05GeV$, $Q = 20$

5.5 Micro Canonical Ensemble

5.5.1 Massless Gas

To present an applictation of the central limit theorem we want to calculate distributions for a MC. The simplest choice is a neutral ultra relativistic gas made up of one kind of massless particles. The only conserved quantities then are the total energy E and the three momentum $\vec{p}$. Particles have energy $E = \mid p \mid = \sqrt{p_x^2 + p_y^2 + p_z^2}$. The thermodynamic partition function can be written as

$$\mathcal{Z} = \exp\left(V \frac{g}{(2\pi)^3} \int d^3p f(\vec{p})\right), \tag{5.33}$$

where $f(\vec{p})$ is the probability of having a particular state occupied, $f(\vec{p}) = \exp(-\beta E)$ in the Boltzmann approximation, or in the correct quantum statistics treatment $f(\vec{p}) = \ln(1 \pm \exp(-\beta E))^{\pm 1}$, where the upper sign denotes fermions, while the lower sign stands for the bosons. The probability for one of the micro canonical states is

$$P(N, \beta E, \beta\vec{p}) = \int_{-\pi}^{\pi} \frac{d\phi_N}{2\pi} \int_{-\infty}^{\infty} \frac{d\phi_E}{2\pi} \int_{-\infty}^{\infty} \frac{d\vec{\phi}_p}{(2\pi)^3} e^{-iN\phi_N} e^{-i\beta E\phi_E} e^{-i\beta\vec{p}\vec{\phi}_p} \Phi\left(\phi_N, \phi_E, \vec{\phi}_p\right), \tag{5.34}$$

where we use βE rather than E for the Fourier integrals, since the exponential requires a dimensionless argument. The different integration domain for discrete variables (particle number) and continous variables (energy and momentum) stems from the fact that for the former a Kronecker delta is used, while for the latter Dirac's delta function has to be employed. For the following consideration this distinction is not important. Using shorthand $Q_j = (N, \beta E, \beta p_x, \beta p_y, \beta p_z)$ and $\phi_j = \left(\phi_N, \phi_E, \phi_{p_x}, \phi_{p_y}, \phi_{p_z}\right)$ one can simplify the notation.

$$\begin{aligned} P(Q_j) &\approx \int_{-\infty}^{\infty} \frac{d\phi_j}{(2\pi)^5} e^{-iQ^j\phi_j} \exp\left(V \sum_{n=1}^{\infty} \frac{i^n}{n!} \kappa_n^{j_1 \ldots j_n} \phi_{j_1 \ldots j_n}\right) \\ &\approx \frac{1}{(2\pi V)^{5/2}} \frac{\exp\left(-\frac{z^j z_j}{2}\right)}{\det \mid \sigma \mid} \end{aligned} \tag{5.35}$$

And only use the asymptotic solution for large volumes derived earlier in this section, where $z^j = \left(Q^k - V\kappa_1^k\right)(\sigma^{-1})_k^j V^{-1/2}$ and the inverse of the sigma tensor $(\sigma)_k^j = \left(\kappa_2^{1/2}\right)_k^j$. The cumulant generating function can be expressed

with a suitable choice for the complex Lagrange multipliers ϕ_E and $\vec{\phi}_p$

$$\ln \mathcal{Z} = V \frac{g}{(2\pi)^3} \int d^3p \, e^{-\beta\sqrt{p_x^2+p_y^2+p_z^2}} \, e^{i\phi_N} \, e^{i\beta E \phi_E} \, e^{i\beta \vec{p}\vec{\phi}_p}. \tag{5.36}$$

The cumulants needed are now given by the respective derivatives at the origin. The expectation values for the Boltzmann approximation are:

$$\begin{aligned}
\kappa_1^N &= \frac{1}{V}\left(-i\frac{\partial}{\partial\phi_N}\right) \ln \mathcal{Z} \mid_{\phi_N=0} = \frac{g}{2\pi} \int d^3p e^{-\beta E} \\
\kappa_1^E &= \frac{1}{V}\left(-i\frac{\partial}{\partial\phi_E}\right) \ln \mathcal{Z} \mid_{\phi_E=0} = \frac{g}{2\pi} \int d^3p e^{-\beta E} E \\
\kappa_1^{p_x} &= \frac{1}{V}\left(-i\frac{\partial}{\partial\phi_{p_x}}\right) \ln \mathcal{Z} \mid_{\phi_{p_x}=0} = \frac{g}{2\pi} \int d^3p e^{-\beta E} p_x = 0
\end{aligned}$$

In case Fermi-Dirac or Bose-Einstein statistics are used one will employ the same set of derivative operators, which result in the usual, yet slightly more difficult, integrals due to the logarithm. Some selected elements from the sigma tensor:

$$\begin{aligned}
\kappa_2^N &= \frac{1}{V}\left(-i\frac{\partial}{\partial\phi_N}\right)^2 \ln \mathcal{Z} \mid_{\phi_N=0} = \frac{g}{2\pi} \int d^3p e^{-\beta E} \\
\kappa_2^E &= \frac{1}{V}\left(-i\frac{\partial}{\partial\phi_E}\right)^2 \ln \mathcal{Z} \mid_{\phi_E=0} = \frac{g}{2\pi} \int d^3p e^{-\beta E} E^2 \\
\kappa_2^{p_x} &= \frac{1}{V}\left(-i\frac{\partial}{\partial\phi_{p_x}}\right)^2 \ln \mathcal{Z} \mid_{\phi_{p_x}=0} = \frac{g}{2\pi} \int d^3p e^{-\beta E} p_x^2 = \frac{1}{3}\kappa_2^E \\
\kappa_2^{E,N} &= \frac{1}{V}\left(-i\frac{\partial}{\partial\phi_E}\right)\left(-i\frac{\partial}{\partial\phi_N}\right) \ln \mathcal{Z} \mid_{\phi_E=\phi_N=0} = \frac{g}{2\pi} \int d^3p e^{-\beta E} E = \kappa_1^E
\end{aligned}$$

Generally give the diagonal terms of the second cumulant tensor the fluctuations in a GC, i.e. with no further conserved charge, while most of the off-diagonal elements are zero due to the antisymmetric nature of the first momentum integral.

$$\kappa_2^{N,p_x} = \kappa_2^{E,p_x} = \kappa_2^{p_x,p_y} = 0$$

Thus the first and second cumulants are in Boltzmann approximation:

$$\kappa_1 = \frac{g}{(2\pi)^3} \begin{pmatrix} 8\pi T^3 & 24\pi T^4 & 0 & 0 & 0 \end{pmatrix}$$

and

$$\kappa_2 = \frac{g}{(2\pi)^3} \begin{pmatrix} 8\pi T^3 & 24\pi T^4 & 0 & 0 & 0 \\ 24\pi T^3 & 96\pi T^5 & 0 & 0 & 0 \\ 0 & 0 & 32\pi T^5 & 0 & 0 \\ 0 & 0 & 0 & 32\pi T^5 & 0 \\ 0 & 0 & 0 & 0 & 32\pi T^5 \end{pmatrix}$$

	Boltzmann	Fermi	Bose
κ_1^N	$8\pi T^3$	$6\pi\zeta(3)T^3$	$8\pi\zeta(3)T^3$
κ_1^E	$24\pi T^4$	$\frac{7}{30}\pi^5 T^4$	$\frac{4}{15}\pi^5 T^4$
κ_2^N	$8\pi T^3$	$\frac{2}{3}\pi^3 T^3$	$\frac{4}{3}\pi^3 T^3$
$\kappa_2^{E,N}$	$24\pi T^4$	$18\pi\zeta(3)T^4$	$24\pi\zeta(3)T^4$
κ_2^E	$96\pi T^5$	$\frac{14}{15}\pi^5 T^5$	$\frac{16}{15}\pi^5 T^5$

$$\kappa_2^{p_x} = \frac{1}{3}\kappa_2^E$$

Table 5.1: Selected elements of the cumulant tensor for a massless gas in Fermi-Dirac, Bose-Einstein statistics and Boltzmann approximation

The remaining relevant integrals for Fermi and Bose statistics are summarized in table 5.1. The Riemann Zeta function is $\zeta(3) \approx 1.202$. After having found the eigenvectors and eigenvalues of κ_2 one can calculate $P(z_j)$. The distribution $P\left(N, V\kappa_1^E, 0, 0, 0\right) = P_{\beta E,\vec{0}}(N)$ is the micro canonical equilibrium particle number distribution for fixed total energy E for a gas at rest with $\vec{p} = \vec{0}$. Independent of the temperature one finds for the large volume limit, or more precisely for large VT^3, the following asymptotic values for the scaled variance ω which are in agreements with [26] in table 5.2:

	Boltzmann	Fermi	Bose
ω_{micro}	0.25	0.198313	0.535462

Table 5.2: Asymptotics of the scaled variance in a MC for a neutral massless gas

For volume corrections one will need to go back a few pages and calculate the higher order cumulants and contract them with the sigma tensor to get the correction terms.

5.5.2 Neutral Gas of Massive Neutral Particles

For a more general system, a gas of massive neutral particles, which carry no charge and hence have no anti-particles, the width of the distributions depends on the ratio of the particle mass to the temperature $\frac{m}{T}$. Again we reproduce the results of reference [26] with having found the third order correction to the distribution converging to 0 for large volumes. The energy of a relativistic, rather than ultra relativistic, particle is $E = \sqrt{p^2 + m^2}$, which requires the integrals to be solved numerically and leads to $\kappa_{p_x} \neq \frac{1}{3}\kappa_E$. We further find low temperature agreements in all three statistics, while the high temperature domain, e.g. low $\frac{m}{T}$, the different particle species (fermions, bosons and the Boltzmann approximation) show a distinctly different behavior.

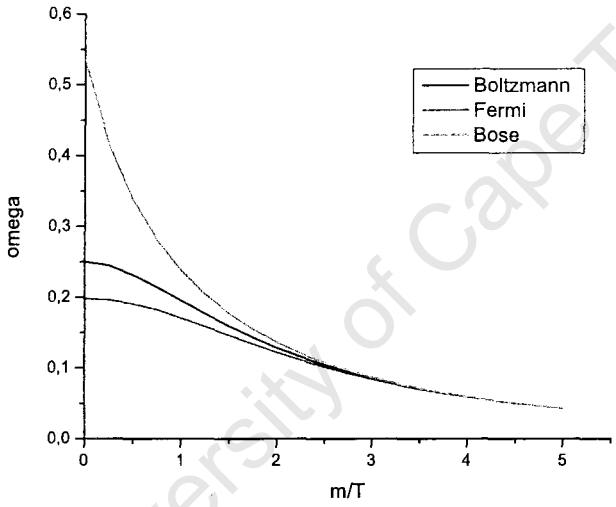

Figure 5.11: Asymptotic scaled variance ω as a function of $\frac{m}{T}$ for a gas of neutral particles, for different statistics

5.5.3 Neutral Gas of Massive Charged Particles

In a next step we want to include anti-particles which now requires particles to carry Abelian charges, e.g. electrical charge, angular momentum or a spin. Hence one further conserved charge in the partition function $\mathcal{Z}$. The restriction of a conserved quantity links particle to anti-particle production and leads to, in combination with energy and momentum conservation to further reduction of ω by a factor of one half. Due to the overall neutrality of the system the same number of particles and anti-particles are produced, in which case low as well as high temperature behavior for both, the particles and its anti-particle, is the same.

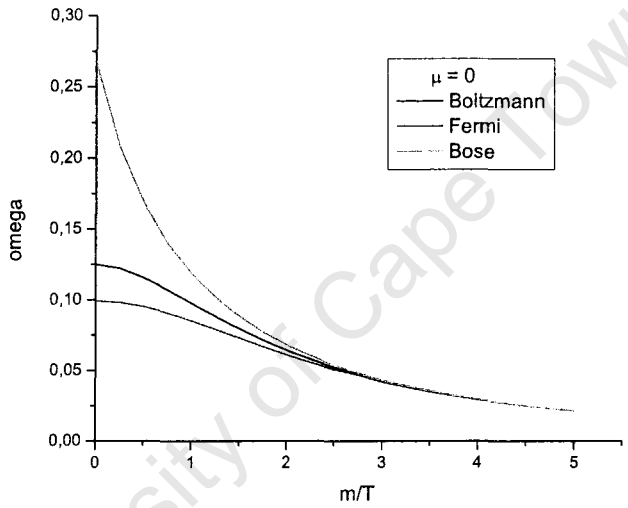

Figure 5.12: Asymptotic scaled variance ω as a function of $\frac{m}{T}$ for a neutral gas of charged particles, for different statistics

5.5.4 Charged Gas of Massive Charged Particles

Lastly we want to give the gas a finite and conserved net-charge density, and hence we need a chemical potential. In a first step we take a small chemical potential of $\mu = \frac{m}{5}$ and for comparison include $\mu = 0$ into the calculation. The particle carrying a charge with a likewise sign as the chemical potential has a suppressed multiplicity, while its scaled variance is enhanced. The particle with opposite charge sign has its multiplicity enhanced, while its scaled variance is suppressed. In a simple canonical Boltzmann ensemble for a particle anti-particle system this effect is less strong and the sum of ω^+ and ω^-, the scaled variances of the positve and the negative charge carrier, is always very close and above 1, while small systems with particle numbers $\mathcal{O}(1)$, hence $\lim_{z\to 0}(\omega^+ + \omega^-) = 2$, are the exception. (In the Boltzmann canonical ensemble the chemical potentials μ dropped out and the distributions are given by equation 2.37). Due to a restricted total energy one cannot produce an ever larger number of particles like in the canonical ensemble. The high multiplicity of one of the particles takes up most of the energy while charge conservation requires some amount of the energy being spent on its anti-particles. As there are only two multiplicity distributions with a conserved charge linking them, one will have to be narrow with high multiplicity and one will have to be wide with low multiplicity. An additional feature is a turning point at low temperature for the low multiplicity particle. In general is the scaled variance, once chemical potentials are around, not a monotonic function anymore. But we still have the low temperature agreements of the different statistics. The figures 5.13 and 5.14 show the scaled variance as a function of $\frac{m}{T}$ with either a positive or a negative chemical potential of $\mu = \pm\frac{1}{5}m$. Figures 5.15, 5.16 and 5.17 compare essentially the particle and anti-particle distributions at fixed chemical potential for the three statistics. Generally one finds $\omega^{BE} > \omega^{Boltz} > \omega^{FD}$ (no condensation for Bose and non degenerate Fermi gases). The central limit theorem does not do that well for low temperature systems due to the fact that a small product of VT^3 leads to a less sharply peaked integrand. At the same time pose strong chemical potential a problem of the same kind as they affect higher order cumulant more than the first three, which are the ones employed here.

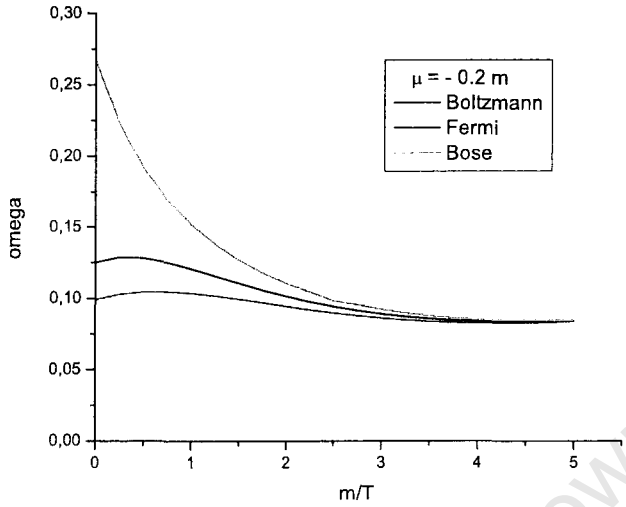

Figure 5.13: Asymptotic scaled variance ω as a function of $\frac{m}{T}$ for a negatively charged gas of charged particles with $\mu = -\frac{m}{5}$, for different statistics

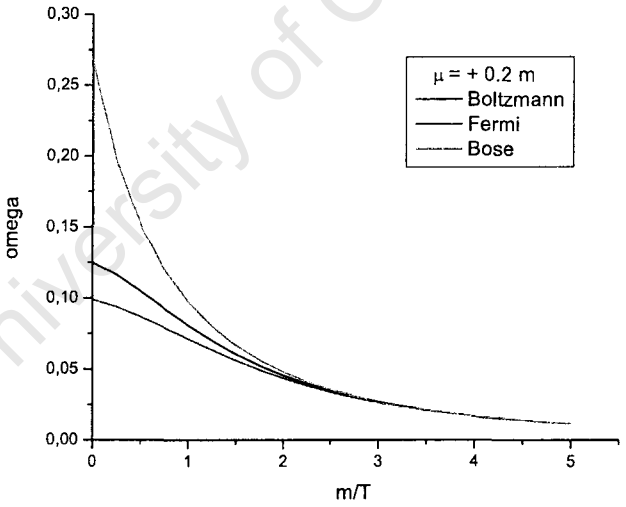

Figure 5.14: Asymptotic scaled variance ω as a function of $\frac{m}{T}$ for a positively charged gas of charged particles with $\mu = +\frac{m}{5}$, for different statistics

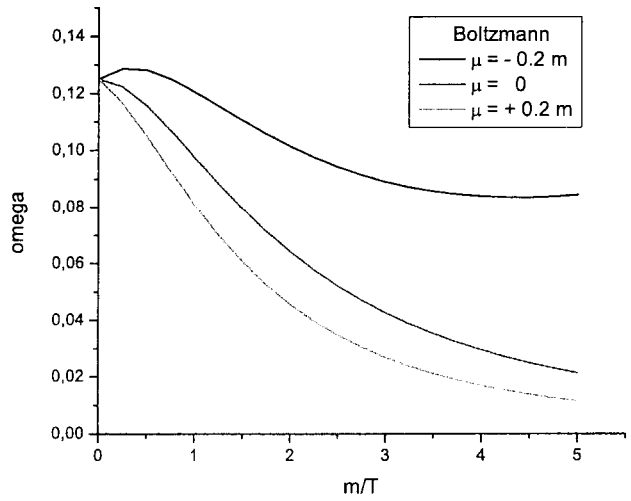

Figure 5.15: Asymptotic scaled variance ω as a function of $\frac{m}{T}$ for a gas of charged Boltzmann particles, $\mu = \pm\frac{m}{5}$,0

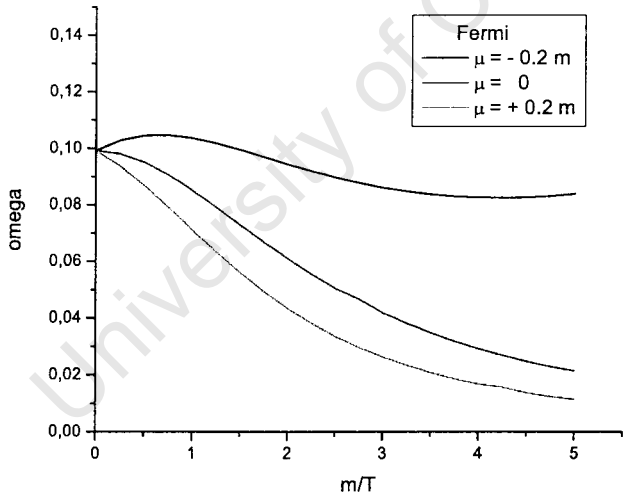

Figure 5.16: Asymptotic scaled variance ω as a function of $\frac{m}{T}$ for a gas of charged Fermi particles, $\mu = \pm\frac{m}{5}$,0

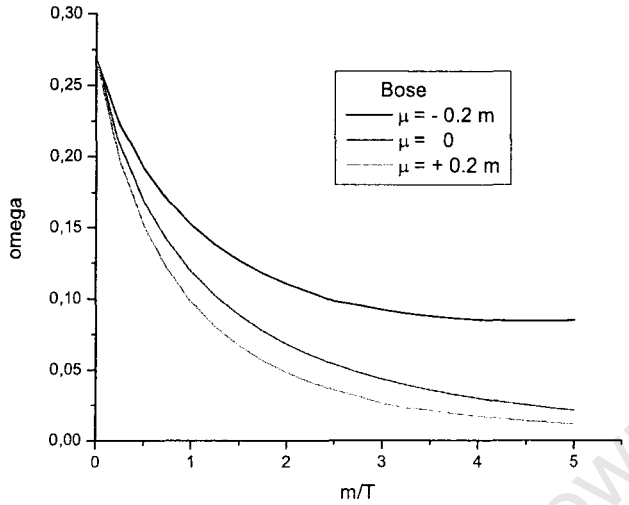

Figure 5.17: Asymptotic scaled variance ω as a function of $\frac{m}{T}$ for a gas of charged Bose particles, $\mu = \pm\frac{m}{5}$,0

5.5.5 Strong Chemical Potentials

For stronger chemical potentials we now observe a strong rise in the scaled variance for the suppressed particle. So should for instance in a MC for a hadron gas in the low temperature and high baryon chemical potential region anti-baryon fluctuations be strongly enhanced to baryon fluctuations. This is so far the only mechanism to enhance fluctuations that strongly even without giving up on thermal or chemical equilibrium. Non-equilibrium would in this picture be a actual energy, charge or momentum value which does not correspond to the expectation value derived form the cumulants. The trouble with that is that all distributions (energy, charge, momentum) are rather narrow functions of their variables and the approximation becomes quickly unreliable as soon as the central region is left. Nevertheless provide these considerations a reliable and flexible frame work to discuss statistical fluctuations in various statistical ensembles and can be applied to a range of physical systems.

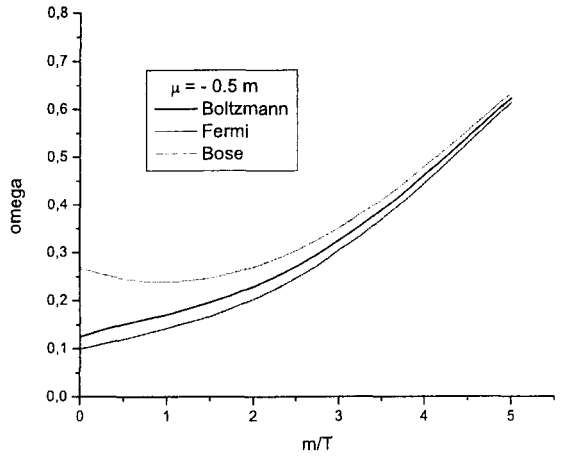

Figure 5.18: Asymptotic scaled variance ω as a function of $\frac{m}{T}$ for a negatively charged gas of charged particles with a strong chemical potential $\mu = -\frac{m}{2}$, for different statistics

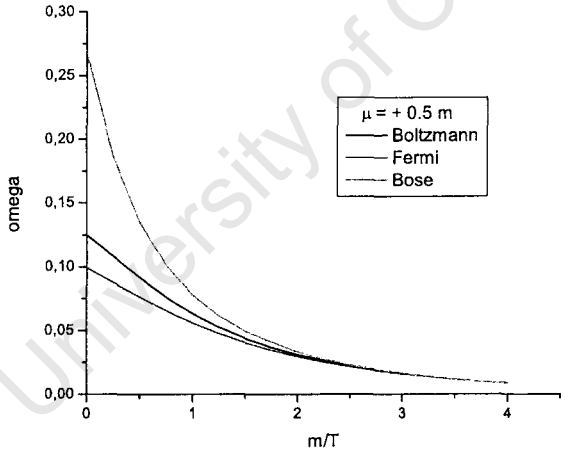

Figure 5.19: Asymptotic scaled variance ω as a function of $\frac{m}{T}$ for a positively charged gas of charged particles with a strong chemical potential $\mu = +\frac{m}{2}$, for different statistics

5.6 Thermodynamic Limit Formulation for Hadron Gas

In this last section a simplified form for calculation of the scaled variance of a distribution in the thermodynamic limit is presented in the example of a hadron gas with 3 conserved charges. The agruments in this section are general and can be extended to other ensmebles and scenarios. Having found the finite volume corrections to disappear for sufficiently large volume, gives justification to this approach. Under the thermodynamic limit all probability distributions become Gaussian. This is in particular true for distributions of charges or particle numbers for a hadronic gas in the thermal model. The system partition function of such a gas is no exception. The probability for any canonical state with a charge vector $Q^j = (B, S, Q)$ in a grand canonical formulation is therefore the number of states consistent with Q^j divided by all grand canonical states. The sum over all such canonical states in return is the grand canonical version.

$$\mathcal{Z}^{GC} = \sum_{B=-\infty}^{\infty} \sum_{S=-\infty}^{\infty} \sum_{Q=-\infty}^{\infty} \mathcal{Z}^{C}_{B,S,Q} \tag{5.37}$$

and

$$P(Q^j) = \frac{\mathcal{Z}^{C}_{B,S,Q}}{\mathcal{Z}^{GC}} \tag{5.38}$$

If one omits the the finite volume corrections the distributions reads (eq. 5.30):

$$P(Q^j) \approx \frac{1}{(2\pi V)^{3/2}\, det\sigma} \exp\left(-\frac{z^j\, z_j}{2}\right) \tag{5.39}$$

with

$$z^j = \left(Q^j - \kappa_1^j V\right) \sigma_j^{-1\,k}\, V^{-1/2} \tag{5.40}$$

The expansion terms κ are essentially from a Taylor expansion of $\ln \mathcal{Z}^{GC}$:

$$\kappa_1^{q_1} = \left(-i\frac{\partial}{\partial \phi_{q_1}}\right) \ln \mathcal{Z}^{GC} \tag{5.41}$$

and

$$\kappa_2^{q_1,q_2} = \left(-i\frac{\partial}{\partial \phi_{q_1}}\right)\left(-i\frac{\partial}{\partial \phi_{q_2}}\right) \ln \mathcal{Z}^{GC} \tag{5.42}$$

Hence

$$\kappa_1 = \left(\kappa^B, \kappa^S, \kappa^Q\right) \tag{5.43}$$

and

$$\kappa_2 = \begin{pmatrix} \kappa^{BB} & \kappa^{BS} & \kappa^{BQ} \\ \kappa^{SB} & \kappa^{SS} & \kappa^{SQ} \\ \kappa^{QB} & \kappa^{QS} & \kappa^{QQ} \end{pmatrix}$$

The further matrices σ and σ^{-1} are calculated from the eigenvectors and eigenvalues of κ_2.

$$\sigma = \kappa_2^{1/2} \quad \text{and} \quad \sigma^{-1} = \kappa_2^{-1/2} \tag{5.44}$$

The determinant of σ is therefore the product of the square roots of the eigenvalues λ_i of σ.

$$det\sigma = \sqrt{\lambda_1 \lambda_2 \lambda_3} \tag{5.45}$$

Assuming thermal equilibrium the system should be in the state $Q^j = \kappa^j V$. Thus $P(\kappa^j V)$ reads

$$P(\kappa^j V) \approx \frac{1}{(2\pi V)^{3/2} det\sigma} \tag{5.46}$$

The same arguments hold if one is interested in particle number distributions. So would the probability in a grand canonical ensemble of having the state $\tilde{Q}^j = (B, S, Q, N)$, where N denotes the particle number, realized be:

$$\tilde{P}(\tilde{Q}^j) = \frac{\mathcal{Z}^C_{B,S,Q,N}}{\mathcal{Z}^{GC}} \approx \frac{1}{(2\pi V)^{4/2} det\tilde{\sigma}} \exp\left(-\frac{\tilde{z}^j_q \ \tilde{z}_{q\,j}}{2}\right) \tag{5.47}$$

with

$$\tilde{z}^j_q = \left(\tilde{Q}^j - \tilde{\kappa}^j_q V\right) \tilde{\sigma}^{-1\,k}_j \, V^{-1/2} \tag{5.48}$$

For this distribution the second cumulant is:

$$\tilde{\kappa}_2 = \begin{pmatrix} \kappa^{BB} & \kappa^{BS} & \kappa^{BQ} & \kappa^{BN} \\ \kappa^{SB} & \kappa^{SS} & \kappa^{SQ} & \kappa^{SN} \\ \kappa^{QB} & \kappa^{QS} & \kappa^{QQ} & \kappa^{QN} \\ \kappa^{NB} & \kappa^{NS} & \kappa^{NQ} & \kappa^{NN} \end{pmatrix}$$

The canonical distribution $P^Q(N)$ is the probability of finding the state $\tilde{Q}^j = (B, S, Q, N)$ realized in a grand canonical ensemble divided by the probability of finding the system in the state $Q^j = (B, S, Q)$. The new variable of this distribution $\tilde{z}^j = 0$ for $j = B, S, Q$, due to the assumption of chemical equillibrium, and non zero only for $j = 4$. Hence P^Q is a one dimensional distribution.

$$P^Q(N) \approx \frac{\tilde{P}(\tilde{Q}^j)}{P(Q^j)} \tag{5.49}$$

$$\approx \frac{(2\pi V)^{3/2}\, det\sigma}{(2\pi V)^{4/2}\, det\tilde{\sigma}} \exp\left(-\frac{\tilde{z}_q^j\ \tilde{z}_{q\,j}}{2}\right) \tag{5.50}$$

$$\approx \frac{det\sigma}{(2\pi V)^{1/2}\, det\tilde{\sigma}} \exp\left(-\frac{\tilde{z}_q^j\ \tilde{z}_{q\,j}}{2}\right) \tag{5.51}$$

Further and finally assuming that this distribution is again a Gaussian under the thermodynamic limit, it should of the form:

$$P(x) = \frac{1}{(2\pi\xi^2)^{1/2}} \exp\left(-\frac{(x-\mu)^2}{2\xi}\right) \tag{5.52}$$

where ξ is used for the variance to avoid confusion with the previous variances, and μ for the mean of this Gaussian. For the scaled variance of a Gaussian one can write:

$$\xi^2 = \langle x^2\rangle - \langle x\rangle^2 = \omega\ \langle x\rangle \tag{5.53}$$

Therefore:

$$\omega = \frac{\xi^2}{\langle x\rangle} \tag{5.54}$$

When switching back to our distribution $P^Q(N)$:

$$\xi = \frac{V^{1/2}\, det\tilde{\sigma}}{det\sigma} \tag{5.55}$$

Together with $\langle N\rangle = V\kappa_N$ one gets for the scaled variance of the particle number distribution:

$$\omega = \frac{\xi^2}{\langle N\rangle} = \frac{V\ det\tilde{\sigma}^2}{V\ \kappa_N\ det\sigma^2} = \frac{det\tilde{\sigma}^2}{\kappa_N\ det\sigma^2} \tag{5.56}$$

In words, this is the ratio of the product of the eigenvalues of the 4 dimensional matrix $\tilde{\kappa}_2$ and the 3 dimensional matrix κ_2 divided by the particle density of the particle under investigation.

Comparison with reference [54]

The following plots will compare this equation to the results of Becattini et. al. The markers always denote the results in reference [54], the continuous lines are from formula (5.56). The minor deviations can probably be attributed due to the differences in hadronic tables used for the respective calculations.

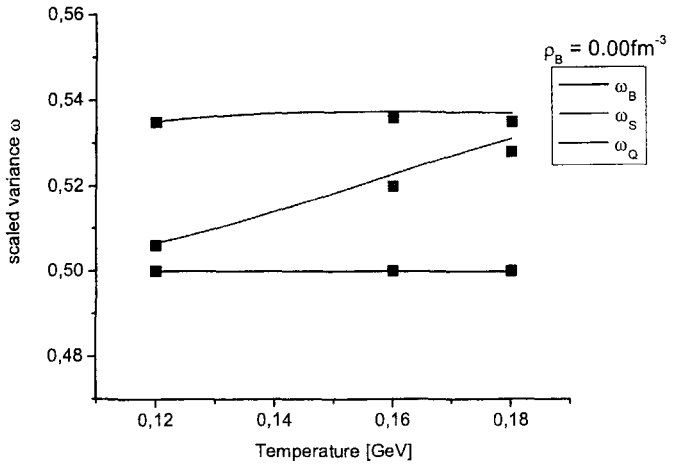

Figure 5.20: asymptotic scaled variance in a hadron gas, baryon density $\rho_B = 0.0fm^{-3}$

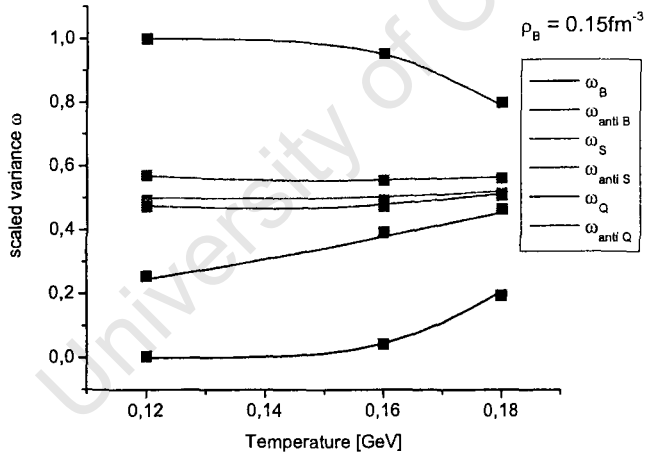

Figure 5.21: asymptotic scaled variance in a hadron gas, baryon density $\rho_B = 0.15fm^{-3}$

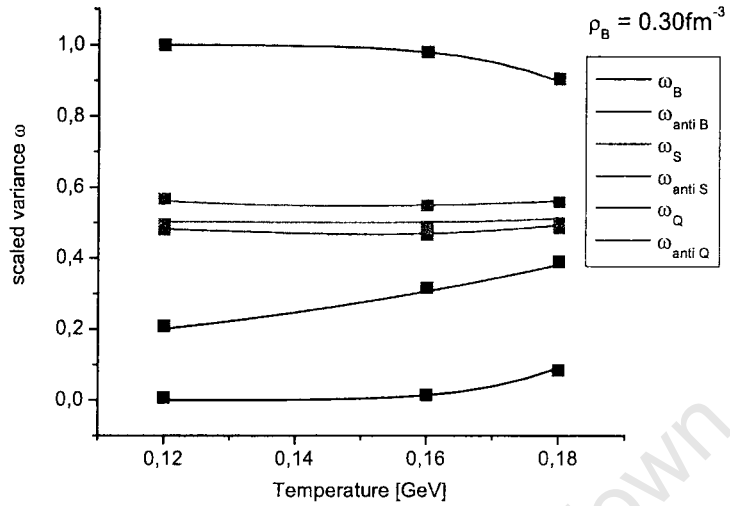

Figure 5.22: asymptotic scaled variance in a hadron gas, baryon density $\rho_B = 0.30 fm^{-3}$

5.7 Summary

The central limit theorem provides a mathematical formulation of the thermodynamic limit, while the expansion in terms of the cumulants allows for application to finite systems. Comparison to the analytic solutions of chapter 2 suggest that one can derive reliable approximations at the very least for Boltzmann gases and quantum gases with weak chemical potentials for system sizes relevant for heavy ion collisions. Even though multidimensional expansions work less well, it wont affect the derived canonical equilibrium multiplicity distributions that strongly. In particular would, due to the large number of degrees of freedom and their respective conserved charges, in a hadron gas charge correlations be 'washed out'. A important feature of MC is that energy is conserved and on short supply as far as fluctuations are concerned. Extreme or rare events will therefore naturally be suppressed. The situation gets even more interesting when chemical potentials break the particle anti-particle symmetry, where the requirement of charge conservation force the system to spend some of the available energy on anti-particle production. The influence of momentum conservation was thus far omitted. Assigning a fixed energy and a net-momentum, for instance p_T, to a fireball in a not comoving frame will require particles to have high momenta and will yet again affect the systems ability to produce (cold) anti-particles to balance the net-charge. In general is the scaled variance not a monotonic function anymore and exhibits turning points and extrema. As far as non-equilibrium distributions are concerned is the linear phase space suppression factor γ probably a unsatisfying choice, as the resulting distributions effectively will equilibrium distributions where the most likely state (the mean) is where the peak of the distributions is. In a different picture would the expectation value sit far of the center of body (bell) of the distribution, and should have a quite different canonical normalization. The phase space structure is thus distinctly altered and beyond the scope of these considerations.

Chapter 6

Conclusion and Outlook

The recent publications on the statistical properties of static thermal sources have shown a number of effects which could in principle provide a further deeper test of the thermal model idea. In this work the focus was put on an attempt to make careful enough approximations which would allow for a simplified mathematical way to derive final state probability distributions for particle production, their correlations, and the system partition function itself from which all physical (thermodynamic) quantities can be obtained through the Helmholtz potential and the corresponding Maxwell relations. The language of statistical mathematics was used in a very pragmatic way, more justified by its ability to reproduce known results than a strict mathematical treatment. In chapter 2 the method of Fourier analysis provided a consistent and flexible mathematical language to derive statistical distributions of various observables. This frame work has proven its worth in the pre-analysis in chapters 3 and 4 of the NA49 Carbon Carbon data, and suggests that it should be possible to understand multiplicity fluctuations within a statistical hadronization approach. Classifying events in terms of its conditions at freeze-out gives this approach even predictive qualities. The results of chapter 5 finally allow for an applictation of quantum statistical canonical or even micro canonical ensembles to high energy collision data, in particular the data set of the NA49 collaboration for charged particle fluctuations. A further exploration of the properties of the expansion will ultimately provide further insight and give more certainty to numerical results. One the other side will a micro canonical ensemble in quantum statistics be home to many effects which would be less pronounced in less rigid ensembles, even under large volume limits, which might be visible in data. Lastly there are striking similarities of this approach to 0+0 dimensional thermal field theory. After all the Hamiltonian assumed is the Klein Gordon equation with a uniform potential. That connection has been thus far not been exploited and might give

further clues on how to get better results for quantum statistical ensembles and insight into cumulant structure.

Appendix A

Kinematic Variables

Throughout this thesis a system of variables is employed known as kinematic variables, which has emerged from the need to use a suitable set to take advantage of symmetries characteristic to high energy collisions. In addition a simplifying set of units is used in which quantities appear in their natural units. Temperature, momentum and mass are given in electron Volts $[eV]$, length and time in femto meter $[fm]$. In such a system important physical constants are dimensionless.

$$\hbar = k_B = c = 1 \tag{A.1}$$

Physical quantities are easiest described with respect to a prefered direction defined by the beam axis. The azimuthal angel ϕ, the rapidity y and the transverse mass m_T form the kinematic variables. Their connection to the conventional variables three momentum $\vec{p}$, mass m and energy E is given by the following relations

$$E = m_T \cosh(y) \tag{A.2}$$

$$p_z = m_T \sinh(y). \tag{A.3}$$

With transverse mass m_T and rapidity y being

$$m_T^2 = p_T^2 + m^2 = p_x^2 + p_y^2 + m^2 \tag{A.4}$$

$$y = \frac{1}{2} \ln \left(\frac{E + p_z}{E - p_z} \right) = \tanh^{-1} \left(\frac{p_z}{E} \right). \tag{A.5}$$

Finally the volume element d^3p expressed in the kinematic variables.

$$d^3p = m_T^2 \cosh y \; dy \; dm_T \; d\phi \tag{A.6}$$

Appendix B

System Partition Function Equation 2.3

For a gas composed of different particles with labels i. the system will be described by a set of Hamilton operators $\hat{H}_i$ and their energy eigen values ϵ_i^j and particle number operators $\hat{N}_i$ with the corresponding chemical potentials $\mu_i = \vec{\mu}\cdot\vec{Q}_i$, defined by the particles charge vector $\vec{Q}_i$ and the effective potential $\vec{\mu}$. The index j denotes to a particular energy level which is occupied by a number n_i^j of particles of hadron species i. The partition function for particle species i is thus given by:

$$\begin{aligned}
\mathcal{Z}_i^{GC}(T,V,\mu_i) &= Tr\left(e^{-\beta\left(\hat{H}-\mu_i\hat{N}\right)}\right) \\
&= \sum_{\{n_i^j\}}\langle n_i^1, n_i^2, \ldots|e^{-\beta\left(\hat{H}-\mu_i\hat{N}\right)}|n_i^1, n_i^2, \ldots\rangle \\
&= \prod_j\sum_{n_i^j}\langle n_i^j|e^{-\beta\left(\hat{H}-\mu_i\hat{N}\right)}|n_i^j\rangle \\
&= \prod_j\sum_{n_i^j}e^{-\beta\left(\epsilon_i^j-\mu_i\right)n_i^j} \\
&= \prod_j\left(1\pm e^{-\beta\left(\epsilon_i^j-\mu_i\right)}\right)^{\pm 1} \qquad \text{(B.1)}
\end{aligned}$$

Where $\beta = \frac{1}{T}$. For the Fermions, due to the Pauli principle, one has occupation numbers zero and one, while for Bosons any number of particles can be in a particular energy state

$$\sum_{n=0}^{1}e^{-xn} = \left(1+e^{-x}\right) \qquad \sum_{n=0}^{\infty}e^{-xn} = \left(1-e^{-x}\right)^{-1} \qquad \text{(B.2)}$$

Taking the logarithm of the partition function then yields

$$\ln \mathcal{Z}_i^{GC}(T,V,\mu_i) = \sum_j \ln\left(1 \pm e^{-\beta(\epsilon_i^j - \mu_i)}\right)^{\pm 1}. \tag{B.3}$$

For a large and homogeneous system, the sum over the number of states can be turned into a integral over the spacial and momentum parts $\sum_j \rightarrow \frac{g_i V}{(2\pi)^3}\int d^3p$ and using, now continuous, energy values $E_i = \sqrt{p^2 + m_i^2}$:

$$\ln \mathcal{Z}_i^{GC}(T,V,\mu_i) = g_i V \int \frac{d^3p}{(2\pi)^3} \ln\left(1 \pm e^{-\beta(E_i - \mu_i)}\right)^{\pm 1}, \tag{B.4}$$

where g_i is the particles degeneracy. For a gas composed of different particles the sum over all hadronic species has to be taken

$$\ln \mathcal{Z}^{GC}(T,V,\vec{\mu}) = \sum_{\text{species } i} g_i V \int \frac{d^3p}{(2\pi)^3} \ln\left(1 \pm e^{-\beta(E_i - \vec{Q}_i\vec{\mu})}\right)^{\pm 1}, \tag{B.5}$$

which is the cumulant generating function used in this thesis. In Boltzmann approximation this expression simplifies to:

$$\ln \mathcal{Z}^{GC}(T,V,\vec{\mu}) = \sum_{\text{species } i} g_i V \int \frac{d^3p}{(2\pi)^3} e^{-\beta(E_i - \vec{Q}_i\vec{\mu})}. \tag{B.6}$$

Appendix C

Single Particle Partition Function Equation 2.2

Starting off from the Boltzmann factor the expectation value for the yield can be calculated by integration over the available phase space. Assuming spherical symmetry and Boltzmann statistics this reads

$$\frac{dN}{d^3p} = gVe^{-\frac{E}{T}}. \tag{C.1}$$

The factor g is the particle's degeneracy and V is the spacial volume, essentially equation B.4 in Boltzmann approximation,

$$z = gV \int \frac{d^3p}{(2\pi)^3}\, e^{-\frac{E}{T}}. \tag{C.2}$$

After integration over the angular part of the momentum space:

$$z = \frac{gV}{2\pi^2} \int_0^\infty p^2\, dp\, e^{-\frac{E}{T}}. \tag{C.3}$$

Using the trigonometric relation $\cosh(y)^2 - \sinh(y)^2 = 1$, where y is not the rapidity defined earlier

$$\begin{aligned} E^2 &= p^2 + m^2 \\ E &= m\cosh y \\ p &= m\sinh y. \end{aligned}$$

Hence the variable of integration changes to $dp = m\cosh y\, dy$.

$$z = \frac{gV}{2\pi^2} \int_0^\infty dy\, m^2 \sinh^2(y)\, m\cosh(y)\, e^{-\frac{m}{T}\cosh(y)} \tag{C.4}$$

After integration by parts:

$$z = \frac{gV}{2\pi^2}\, m^2 T \int_0^\infty dy \left(\sinh^2(y) + \cosh^2(y)\right) e^{-\frac{m}{T}\cosh(y)}. \tag{C.5}$$

Lastly using another trigonometric relation $\sinh^2(y) + \cosh^2(y) = \cosh(2y)$ and the definition of the modified Bessel Functions, the MacDonald Functions [55], yields

$$K_2(x) = \int_0^\infty dy \cosh(2y)\, e^{-x\cosh(y)}. \tag{C.6}$$

Thus the single particle partition function in Boltzmann approximation is

$$z = \frac{gV}{2\pi^2}\, m^2 T K_2\left(\frac{m}{T}\right). \tag{C.7}$$

Appendix D

Rapidity Distribution Equation 2.58

Using the result of appendix A, one can express

$$E\,\frac{d^3N}{dp^3} = \frac{d^3N}{m_T dm_T dy d\phi} = \frac{gV}{(2\pi)^3}\,E\,e^{-\frac{E}{T}+\frac{\mu}{T}}. \tag{D.1}$$

Thus the rapidity distribution of produced particles is

$$\frac{dN}{dy} = \frac{gV}{(2\pi)^3}\,e^{\frac{\mu}{T}}\int_0^{2\pi} d\phi \int_m^{\infty} m_T dm_T m_T \cosh(y)\,e^{-\frac{m_T\cosh(y)}{T}}. \tag{D.2}$$

Integrating over the angular yields

$$\frac{dN}{dy} = \frac{gV}{(2\pi)^2}\,e^{\frac{\mu}{T}}\int_m^{\infty} dm_T m_T^2 \cosh(y)\,e^{-\frac{m_T\cosh(y)}{T}}. \tag{D.3}$$

Substituting $\frac{m_T}{T} = \alpha$ will allow to integrate the transverse mass part

$$\frac{dN}{dy} = \frac{gVT^3}{(2\pi)^2}\,e^{\frac{\mu}{T}}\cosh(y)\int_{\frac{m}{T}}^{\infty} d\alpha\,\alpha^2 e^{-\alpha\cosh(y)}. \tag{D.4}$$

This integral can be integrated by parts or is simply of the type:

$$\int x^2 e^{ax} dx = e^{ax}\left(\frac{x^2}{a} - \frac{2x}{a^2} + \frac{2}{a^3}\right) \tag{D.5}$$

What gives the final line for the rapidity distribution

$$\frac{dN}{dy} = \frac{gVT^3}{(2\pi)^2}\,e^{\frac{\mu}{T}}\,e^{-\frac{m\cosh(y)}{T}}\left(\frac{m^2}{T^2} - \frac{2m}{T\cosh(y)} + \frac{2}{\cosh(y)^2}\right). \tag{D.6}$$

Appendix E

Radius of Convergence in a Bosonic Gas

The grand canonical partition function for a bosonic gas reads

$$\mathcal{Z} = \exp\left(\frac{gV}{2\pi^2}\left[\int_0^\infty p^2 dp \ln\left(1 - e^{-\frac{E}{T}+\frac{\mu_Q}{T}}\right)^{-1} + \int_0^\infty p^2 dp \ln\left(1 - e^{-\frac{E}{T}-\frac{\mu_Q}{T}}\right)^{-1}\right]\right). \tag{E.1}$$

The radius of convergence is:

$$\rho = \lim_{n\to\infty} \rho_n = \lim_{n\to\infty} \sqrt{|\frac{\kappa_n}{n!}\frac{(n+1)!}{\kappa_{n+1}}|}. \tag{E.2}$$

E.1 Radius of convergence for $P(N)$ and $P(Q)$ when $\mu_Q = 0$

The particle number distribution for a neutral system is determent through the cumulants κ_n

$$\kappa_n = \frac{gVTm^2}{2\pi^2}\left[\sum_{k=1}^{\infty} K_2\left(\frac{km}{T}\right)k^{n-2}\right] \tag{E.3}$$

For large order cumulants one can replace the summation with an integral and extend to $k = 0$:

$$\begin{aligned}\lim_{n\to\infty}\kappa_n &= \frac{gVTm^2}{2\pi^2}\left[\int_{k=0}^{\infty} K_2\left(\frac{km}{T}\right)k^{n-2}\right] \\ &= \frac{gVTm^2}{2\pi^2}\left[2^{n-3}\left(\frac{m}{T}\right)^{1-n}\Gamma\left(\frac{n}{2}-\frac{3}{2}\right)\Gamma\left(\frac{n}{2}+\frac{1}{2}\right)\right]\end{aligned} \tag{E.4}$$

Using some rules for Gamma functions one finds for the radius of convergence

$$\rho = \lim_{n\to\infty} \sqrt{\frac{m}{T} \frac{2\,(n-2)\,n\Gamma\left(\frac{n}{2}+\frac{3}{2}\right)^2}{(n-3)\,(n^2-1)\,\Gamma\left(\frac{n}{2}+1\right)^2}} = \sqrt{\frac{m}{T}}. \tag{E.5}$$

For the charge distribution of a neutral gas ($\mu_Q = 0$), one needs to consider only even order cumulants

$$\kappa_q = \frac{gVTm^2}{2\pi^2} 2 \left[\sum_{k=1}^{\infty} K_2\left(\frac{km}{T}\right) k^{q-2}\right] \quad q \text{ even}. \tag{E.6}$$

And hence one obtains the same radius of convergence as for the particle number distribution. Generally one finds the larger the product VT^3, e.g. system size, the more sharply peaked is integrand itself.

E.2 Radius of convergence for $P(N)$ and $P(Q)$ when $\mu_Q \neq 0$

The cumulants for $P(N)$ now have a μ_Q dependence and read

$$\kappa_n = \frac{gVTm^2}{2\pi^2} \left[\sum_{k=1}^{\infty} K_2\left(\frac{km}{T}\right) \exp\left(\frac{k\mu_Q}{T}\right) k^{n-2}\right]. \tag{E.7}$$

For large orders for cumulants one can again take the sum from $k = 0$ and convert into a integral

$$\begin{aligned} \lim_{n\to\infty} \kappa_n \;=\; & \frac{gVTm^2}{2\pi^2}\, 2^{n-3} \left(\frac{m}{T}\right)^{1-n} \\ & \Big[\; \Gamma\left(\frac{n}{2}+\frac{1}{2}\right)\Gamma\left(\frac{n}{2}-\frac{3}{2}\right) F\left(\frac{n}{2}-\frac{3}{2}, \frac{n}{2}+\frac{1}{2}; \frac{1}{2}; \frac{\mu_Q^2}{m^2}\right) \\ & + \;\frac{\mu_Q}{m}\,\Gamma\left(\frac{n}{2}+1\right)\Gamma\left(\frac{n}{2}-1\right) F\left(\frac{n}{2}+1, \frac{n}{2}-1; \frac{3}{2}; \frac{\mu_Q^2}{m^2}\right) \Big] \end{aligned} \tag{E.8}$$

The definition of the hypergeometric functions $F(a, b; c; z)$ [55] is

$$F(a, b; c; z) = \frac{\Gamma(c)}{\Gamma(a)\,\Gamma(b)} \sum_{n=0}^{\infty} \frac{\Gamma(a+n)\,\Gamma(b+n)}{\Gamma(c+n)} \frac{z^n}{n!}. \tag{E.9}$$

This yields for the radius of convergence for the particle number distribution

$$\rho = \lim_{n\to\infty} \rho_n = \sqrt{\frac{m}{T} - \frac{\mu_Q}{T}}. \tag{E.10}$$

For the charge distribution one has expansion terms

$$\kappa_q = \frac{gVTm^2}{2\pi^2}\left[2\sum_{k=1}^{\infty} K_2\left(\frac{km}{T}\right)\cosh\left(\frac{k\mu_Q}{T}\right)k^{q-2}\right] \quad q \text{ odd} \quad \text{(E.11)}$$

$$\kappa_q = \frac{gVTm^2}{2\pi^2}\left[2\sum_{k=1}^{\infty} K_2\left(\frac{km}{T}\right)\sinh\left(\frac{k\mu_Q}{T}\right)k^{q-2}\right] \quad q \text{ even} \quad \text{(E.12)}$$

Thus

$$\lim_{q\to\infty}\kappa_q = \frac{gVTm^2}{2\pi^2}\,2^{n-2}\left(\frac{m}{T}\right)^{1-n}\Gamma\left(\frac{n}{2}+\frac{1}{2}\right)\Gamma\left(\frac{n}{2}-\frac{3}{2}\right)F\left(\frac{n}{2}-\frac{3}{2},\frac{n}{2}+\frac{1}{2};\frac{1}{2};\frac{\mu_Q^2}{m^2}\right) \quad q \text{ even}$$

$$\lim_{q\to\infty}\kappa_q = \frac{gVTm^2}{2\pi^2}\,2^{n-1}\left(\frac{m}{T}\right)^{-n}\frac{\mu_Q}{T}\Gamma\left(\frac{n}{2}+1\right)\Gamma\left(\frac{n}{2}-1\right)F\left(\frac{n}{2}+1,\frac{n}{2}-1;\frac{3}{2};\frac{\mu_Q^2}{m^2}\right) \quad q \text{ odd}$$

But remarkably for both, even and odd, orders of q the radius of convergence is again

$$\rho = \lim_{n\to\infty}\rho_n = \sqrt{\frac{m}{T}-\frac{\mu_Q}{T}}.$$

Appendix F

Thermodynamic Limit

Now we have for the Boltzmann pion gas two descriptions for the charge distribution $P(Q)$. One analytic one in the form of equation 2.23 and the approximation 5.20. Under the thermodynamic limit both should agree. Let us start with the analytic solution from chapter 2.

$$P_{\langle Q\rangle}(Q) = I_Q(2z)\,\frac{e^{Q\frac{\mu_Q}{T}}}{\exp\{2z\cosh\left(\frac{\mu_Q}{T}\right)\}}$$

Using the identities 2.25 and 2.26 together with the chemical potential μ_Q in equation 2.21, one can re-express the probability in terms of the expectation value of the charge $\langle Q\rangle$ and the value of the single particle partition function z.

$$P_{\langle Q\rangle}(Q) = I_Q(2z)\,e^{Q\ln\left(\frac{\langle Q\rangle}{2z}+\sqrt{1+\left(\frac{\langle Q\rangle}{2z}\right)^2}\right)-2z\sqrt{1+\left(\frac{\langle Q\rangle}{2z}\right)^2}} \tag{F.1}$$

Separating now the volume dependence from the temperature dependence, $z = Vz_0(T)$ and $V = Q/\rho$ we define auxiliary variables

$$\begin{aligned} x(T) &= \frac{2z}{Q} = \frac{2z_0}{\rho} \\ y(T) &= \frac{2z}{\langle Q\rangle} = \frac{2z_0}{\langle\rho\rangle}. \end{aligned}$$

$$P_{\langle Q\rangle}(Q) = I_Q(2z)\,e^{Q\left[\ln\left(\frac{1+\sqrt{1+y^2}}{y}\right)-\frac{x}{y}\sqrt{1+y^2}\right]} \tag{F.2}$$

We next attend to the Bessel function. Under the thermodynamic limit both the expectation value of the charge $\langle Q\rangle$ and the single particle partition function tend to ∞, while $\langle\rho\rangle = \langle Q\rangle/V$ as well as $x(T)$ and $y(T)$ are kept at

fixed values. We use the expansion for large orders and large arguments [55]

$$I_Q(Qx) = \frac{1}{\sqrt{2\pi Q}} \frac{e^{Q\eta}}{(1+x^2)^{\frac{1}{4}}} \left(1 + \sum_{k=1}^{\infty} \frac{u_k(t)}{Q^t}\right). \tag{F.3}$$

where

$$t = \frac{1}{\sqrt{1+x^2}}$$

and

$$\eta = \sqrt{1+x^2} + \ln\left(\frac{x}{1+\sqrt{1+x^2}}\right)$$

Putting the pieces together yields

$$P_{\langle Q\rangle}(Q) = \frac{1}{\sqrt{2\pi Q}}\, e^{Q\left[\sqrt{1+x^2} - \frac{x}{y}\sqrt{1+y^2} + \ln\left(\frac{x\left(1+\sqrt{1+y^2}\right)}{y\left(1+\sqrt{1+x^2}\right)}\right)\right]} \frac{\left(1 + \sum_{k=1}^{\infty} \frac{u_k(t)}{Q^k}\right)}{(1+x^2)^{\frac{1}{4}}}. \tag{F.4}$$

The exponential will tend to 0 for similar but different values of x and y and large values of the absolute charge Q, that is when $\rho \approx \langle\rho\rangle$ and $V \to \infty$ and will be 1 for $\rho = \langle\rho\rangle$. The $u_k(t)$ are polynomials in t of order $3k$. The charge density in a pion gas can never be larger than the particle density,

$$t = \left(\sqrt{1+x^2}\right)^{-1} = \frac{1}{\sqrt{1+\left(\frac{2z}{Q}\right)^2}} < \frac{1}{\sqrt{5}} < 1 \tag{F.5}$$

which ensures that the summation over the u_k converges. Further will the value of the bracket be $\mathcal{O}(1)$ for large values of Q. The first three polynomials are [55]:

$$u_1(t) = (3t + 5t^3)/24$$

$$u_2(t) = (81t^2 - 462t^4 + 385t^6)/1152$$

$$u_3(t) = (30375t^3 - 369603t^5 + 765765t^7 - 425425t^9)/414720$$

Hence for large volumes the central region of the distribution, or rather its peak, can be approximated by

$$P_{\langle Q\rangle}(Q) = \frac{1}{\sqrt{2\pi Q}} \frac{1}{\left(1+\left(\frac{2z}{Q}\right)^2\right)^{\frac{1}{4}}}$$

$$
\begin{aligned}
&= \frac{1}{\sqrt{2\pi V}} \frac{1}{\left(\rho^2 + (2z_0)^2\right)^{\frac{1}{4}}} \\
&= \frac{1}{\sqrt{2\pi V}} \frac{1}{\sqrt{2z_0}\left(\sinh\left(\frac{\mu_Q}{T}\right)^2 + 1\right)^{\frac{1}{4}}} \\
&= \frac{1}{\sqrt{2\pi V}} \frac{1}{\sqrt{2z_0 \cosh\left(\frac{\mu_Q}{T}\right)}} \\
&= \frac{1}{\sqrt{2\pi V}} \frac{1}{\sigma},
\end{aligned} \tag{F.6}
$$

where we have made use of the fact that $\rho \approx \langle\rho\rangle = 2z_0 \sinh\left(\frac{\mu}{T}\right)$ and used $\langle\rho^2\rangle = 2z_0 \cosh\left(\frac{\mu}{T}\right)$. This is the same asymptotic behavior as 5.20. The probability distribution for the density will be, $dQ = V d\rho$

$$
P_{\langle\rho\rangle}(\rho) = \frac{\sqrt{V}}{\sqrt{2\pi\sigma}}, \tag{F.7}
$$

and will under the limit $V \to \infty$ and $\rho = const$ tend to a δ function [24]. The central limit theorem thus provides a useful mathematical basis to calculate quantities even for finite systems and can be used as a mathematical formulation of the thermodynamic limit.

Appendix G

Software

This is a description of the software which was written for incorporation into the THERMUS package. The code uses core THERMUS classes as a basis and requires some degree of familiarity with it. A user guide can be found online under http://hep.phy.uct.ac.za/THERMUS/.
The provided classes basically fall into a few groups. Thermal model partition functions (`TTMPartitionFunctionX`), who's purpose is to calculate values $\ln \mathcal{Z}$ for one of the three available ensembles. Both the classes for calculation of thermal distributions (`TTMThermalDistributionX`) and cumulants (`TTMCumulantX`) are derived classes from the partition function classes and are for calculation of particle multiplicity distributions or their expansion terms respectively. Cumulants are stored in container classes (`TTMCumulantObj`) and allow to approximate distributions (`TTMApproximatedDistribution`) for both primordial and final state distributions. Event-by-event particle ratio distributions (`TTMRatioInfoObj`) can be obtain from the 2 dimensional conditional probability distributions calculated from the above classes. Finally is a set of constraining functions included into the basic THERMUS class `TTMThermalModelCanBSQ` which allows for fixing the parameter pair temperature and system radius to a particular value of the average energy per particle $\frac{\langle E \rangle}{\langle N \rangle}$ or the normalized entropy density $\frac{\langle s \rangle}{T^3}$.

G.1 Partition Functions

Two partition function classes, `TTMPartitionFunctionCanS` for the SC and `TTMPartitionFunctionCanBSQ` for the BSQC, provide the basis for the integration of canonical thermal model partition functions. Values for the GC partition function can be obtained from either class which use them for normalization. Like in THERMUS, particles which carry one of the charges

conserved in the partition function, will have to be in the Boltzmann approximation, unconstrained charges can be done in quantum statistics. The input is always a pointer to a `TTMThermalModelBSQ`, which contains all the information about the `TTMParameterSetBSQ` and the `TTMParticleSet`. While the `TTMPartitionFunctionCanS` can handle non zero chemical potentials (μ_B, μ_S, μ_Q), one has to, due to the structure of the integration routine, use zero chemical potentials for the `TTMPartitionFunctionCanBSQ`. Both classes can nevertheless handle a Breit-Wigner type width, which will have to be specified in the `TTMThermalModelBSQ`. A set of conserved quantum numbers can be specified and a value $\ln(\mathcal{Z})$ is returned. For the BSQC the integration is done with the Gauss-Laguerre method, while the SC can be done by summation [35]. For both ensembles plotting functions are provided which return histograms showing the integrand of the respective partition function. One dimensional in case only strangeness is conserved, while in the BSQC, baryon angle was solved analytically [39], a two dimensional histogram is returned. Further can one specify the order of the polynomial and the number of intervals as well as restrict the integration to the relevant region around the origin to save run time. For the following macro, the temperature was constrained to fit $r = 3.225fm$, $(B, S, Q) = (4, 0, 2)$, $\gamma_S = 0.6$, and $\frac{\langle E \rangle}{\langle N \rangle} = 1GeV$.

```
root [0] TTMParticleSet set("~/THERMUS/particles/PartList_PPB2002.txt")
root [1] set.InputDecays("~/THERMUS/particles");
root [2] TTMParameterSetBSQ par;
root [3] par.SetT(0.16377);
root [4] par.SetMuB(0.0);
root [5] par.SetMuQ(0.0);
root [6] par.SetMuS(0.0);
root [7] par.SetGammas(0.6);
root [8] par.SetRadius(3.225);
root [9] TTMThermalModelBSQ mod(&set,&par);
root [10] mod.SetWidth(0);
root [11] mod.SetQStats(0);
root [12] mod.GenerateParticleDens();
```

The partition function classes take a pointer to a `TTMThermalModelBSQ`, and return the value of $\ln \mathcal{Z}$ for a chosen (B, S, Q), or (S) respectively.

```
root [13] TTMPartitionFunctionCanBSQ pf(&mod);
root [14] cout<<pf.CalcLnZ(4,0,2)<<endl;
4.68573164805239841e+01
```

G.2 Thermal Distributions

The provided classes are for the GC `TTMThermalDistributionGCan`, for the SC `TTMThermalDistributionCanS`, and `TTMThermalDistributionCanBSQ` for the BSQC respectively. Only Boltzmann approximation is considered, while the main purpose the GC, which will always produce Poisson distributions, is to have something to compare the other two ensembles to. Due to the structure of the integration routine of the BSQC, where particle and anti-particle appear together and cannot be separated, a sum over the anti-particle distribution will have be taken.

$$P(N_j) = \frac{z_j^{N_j}}{N_j!} \sum_{n=0}^{\infty} \frac{z_j^n}{n!} \frac{Z^{\vec{Q}-(N_j-n)\vec{Q}_j}_{\text{particles } j \text{ and } \bar{j} \text{ excl}}}{Z^{\vec{Q}}_{\text{all particles}}} \tag{G.1}$$

For two particle distributions a double summation is necessary.

$$P(N_j, N_l) = \frac{z_j^{N_j}}{N_j!} \frac{z_l^{N_l}}{N_l!} \sum_{n=0}^{\infty} \sum_{m=0}^{\infty} \frac{z_j^n}{n!} \frac{z_l^m}{m!} \frac{Z^{\vec{Q}-(N_j-n)\vec{Q}_j-(N_l-m)\vec{Q}_l}_{\text{particles } j,\, \bar{j},\, l, \text{ and } \bar{l} \text{ excl}}}{Z^{B,S,Q}_{\text{all particles}}} \tag{G.2}$$

A three dimensional histogram is used for storage of only the required values of the partition function to avoid multiple calculation of the same quantum numbers. In the SC case a one dimensional histogram takes the same job. A short example macro shows how to generate a histogram for primordial distributions. The line number `root [13]` indicates were to continue form former.

```
root [13] TTMThermalDistributionCanBSQ dist(4,0,2,&mod);
root [14] dist.GenerateDistribution(211)->Draw();
```

The output is in figure 3.1, without the red curve, while the next one is the primordial π^+ versus K^+ distribution in figure 3.2.

```
root [13] TTMThermalDistributionCanBSQ dist(4,0,2,&mod);
root [14] dist.GenerateCondDistribution(211,321)->Draw("COLZ");
```

G.3 Cumulants

Three classes calculate cumulants for the various ensembles, implemented by `TTMCumulantGCan`, `TTMCumulantCanS`, and `TTMCumulantCanBSQ` for the GC, SC and the BSQC and take pointers to `TTMThermalModelBSQ` as info container for parameters and particle set as input and return, based on the

function used, a pointer to either of the two cumulant container. Two types of distributions, hence a `TTMCumulantObj` and a `TTMCumulantObjTwo` for the one and two dimensional distributions respectively. The container itself is given a list of central moments which then are used together with the relations in Appendix J to populate a list of cumulants. For the primordial distributions the results can be compared to the calculations done above. The main advantage of this method is the final state distribution can be estimated this way as well. Particles are selected either via particle id, as stated in the THERMUS user-guide, while a particular set of particles can be specified via a `TString`. Available at the moment are $p1$, $p2$, $m1$, $m2$ and *zero*, for charged particles with $Q = \pm 1, \pm 2$ and neutral ones carrying no electrical charge. A set of functions is provided to calculate the cumulants for primordial (`GenerateCumulants(xxx)`) and final state (`GenerateFinalCumulants(xxx)`) distributions. Up to order 6 in the expansion is taken into account for one dimensional primordial distributions, up to order 5 for the two dimensional primordial distributions, up to order 4 for the final one dimensional, and finally up to order 3 for final two dimensional. When the selection went via a TString the first 4 cumulants are used for both primordial and final distributions. For instance the primordial positively charged particle distribution in figure 3.6:

```
root [13] TTMCumulantCanBSQ cum(4,0,2,&mod);
root [14] TTMCumulantObj *co = new TTMCumulantObj;
root [15] co = cum.GenerateCumulants("p1");
```

This was used for final state K^+ to π^+ distribution in figure 3.4.

```
root [13] TTMCumulantCanBSQ cum(4,0,2,&mod);
root [14] TTMCumulantObjTwo *cot = new TTMCumulantObj;
root [15] cot = cum.GenerateFinalCumulants(211,321);
```

G.4 Approximated Distributions

The `TTMApproximatedDistribution` then takes pointers to either of the cumulant container classes. Based on the type of the container received, the class will integrate either the one dimensional or the two dimensional characteristic function, where again the Gauss-Laguerre method is used. The larger the difference between the expectation value and the actual value for the particle number, the more oscillations will the integrand show. So is for instance in the region around to expectation value $\langle N \rangle$ the integrand smoothest. Functions allow for choosing suitable values for the order of the

polynomial and the number of intervals on the area of integration. In both cases a histogram is returned. The type of distribution is specified in the `TTMCumulantX` classes, both the container and the integration classes merely hold the data and do the integration. From the pointers to `TTMCumulantObj` (`*co`) and `TTMCumulantObjTwo` (`*cot`) objects created earlier one can get the approximated distributions.

```
root [16] TTMApproximatedDistribution ad(0);
root [17] TH1D *h = GenerateDistHisto(co);
```

For the 1-dim case, while for conditional distributions a TH2D pointer is returned.

```
root [16] TTMApproximatedDistribution ad(0);
root [17] TH2D *h2 = GenerateDistCondHisto(cot);
```

G.5 Particle Ratios

`TTMRatioInfoObj` class serves to extract ratios from TH2D histograms. The expectation values are calculated from the histogram and not the moments or the cumulants of the distribution. In the following lines a histogram containing the distribution of primordial π^+ (211) and K^+ (321) is passed to a `TTMRatioInfoObj` class and an overview is put on the screen.

```
root [14] TH2D *hdist = dist.GenerateCondDistribution(211,321);
root [15] TTMRatioInfoObj rio(hdist);
root [16] rio.GenerateRatioHisto();
root [17] rio.List();
 **** Info sheet for particle ratios ****
 ******  0000000211 vs 0000000321  ******
 <N_1>   =      6.87516
 <N_2>   =      1.41188
 <R>     =      0.236102
 RMS     =      0.219625
 <N_2>/<N_1> =  0.20536
```

The output of

```
root [18] TH1D *hratio = rio.GetRatioHisto();
```

for the BSQC ratio distribution is in figure 3.3.

G.6 Constraining Functions

For the BSQC one can get constrained parameters form an updated version of the `TTMThermalModelCanBSQ`. The new constraining functions are `ConstrainREoverN`, `ConstrainTEoverN`, `ConstrainRSoverT3`, and lastly `ConstrainTSoverT3`. To give a particular value of $\frac{\langle E \rangle}{\langle N \rangle}$, or $\frac{\langle s \rangle}{T^3}$, a parameter set $(B, S, Q, V, T, \gamma_S)$ is specified, while either T or r are constrained.

```
root [0] TTMParticleSet set("~/THERMUS/particles/PartList_PPB2002.txt")
root [1] TTMParameterSetCanBSQ par;
root [2] par.SetT(0.16);
root [3] par.SetB(4);
root [4] par.SetS(0);
root [5] par.SetQ(2);
root [6] par.SetGammas(.6);
root [7] par.SetRadius(3.225);
root [8] TTMThermalModelCanBSQ mod(&set,&par);
root [9] mod.SetWidth(0);
root [10] mod.ConstrainTEoverN(1.0);
root [11] par.List();
**************************** Thermal Parameters ********************

      T         =       0.16377                        (*CONSTRAINED*)

      B         =             4                        (FIXED)

      S         =             0                        (FIXED)

      Q         =             2                        (FIXED)

 gammas         =           0.6                        (FIXED)

 radius         =         3.225                        (FIXED)

                        E/N Successfully Constrained

*********************************************************************
```

Appendix H

Higher Order Moments

As an example for higher order final state moments the third moment is discussed. Only effective branching ratios are considered. In general one can write:

$$\begin{aligned}\langle N_k \cdot N_l \cdot N_m \rangle &= \langle \sum_{a=1}^{P} \tilde{N}_{a,k} \cdot \sum_{b=1}^{P} \tilde{N}_{b,l} \cdot \sum_{c=1}^{P} \tilde{N}_{c,m} \rangle \\ &= \sum_{a=1}^{P} \sum_{b=1}^{P} \sum_{c=1}^{P} \langle \tilde{N}_{a,k} \cdot \tilde{N}_{b,l} \cdot \tilde{N}_{c,m} \rangle \end{aligned} \tag{H.1}$$

Where k, l, and m denote to the respective final state particle species, while a, b, and c stand for the parent particles. As we only have either one or two particle distributions we have to consider only a few combinations.
In the case where $k = l = m$, or effectively a one particle moment, one has to distinguish three further cases. The first one is $a = b = c$, in words, only one parent particle type and one product particle type is considered.

$$\langle \tilde{N}_{a,k}^3 \rangle = (z_a \Gamma_{a \to k})^3 \, \tilde{\mathcal{Z}}^{\vec{Q} - 3\vec{Q}_a} + 3 \, (z_a \Gamma_{a \to k})^2 \, \tilde{\mathcal{Z}}^{\vec{Q} - 2\vec{Q}_a} + (z_a \Gamma_{a \to k}) \, \tilde{\mathcal{Z}}^{\vec{Q} - \vec{Q}_a} \tag{H.2}$$

When again only one kind of daughter particle is considered, which is $k = l = m$, but now we have correlations between two different production channels, $a = b \neq c$,

$$\langle \tilde{N}_{a,k}^2 \cdot \tilde{N}_{c,k} \rangle = (z_a \Gamma_{a \to k})^2 \, (z_c \Gamma_{c \to k}) \, \tilde{\mathcal{Z}}^{\vec{Q} - 2\vec{Q}_a - \vec{Q}_c} + (z_a \Gamma_{a \to k}) \, (z_c \Gamma_{c \to k}) \, \tilde{\mathcal{Z}}^{\vec{Q} - \vec{Q}_a - \vec{Q}_c}. \tag{H.3}$$

And the case with three different production channels, $a \neq b \neq c$, reads

$$\langle \tilde{N}_{a,k} \cdot \tilde{N}_{b,k} \cdot \tilde{N}_{c,k} \rangle = (z_a \Gamma_{a \to k}) \, (z_b \Gamma_{b \to k}) \, (z_c \Gamma_{c \to k}) \, \tilde{\mathcal{Z}}^{\vec{Q} - \vec{Q}_a - \vec{Q}_b - \vec{Q}_c}, \tag{H.4}$$

which requires the full triple summation. As we are omitting correlations due to production channels of the type $X \to K^+ + \pi^+$, there are only two

more cases. Firstly on the daughter particle side, two particles of the same type and one different to the former, $k = l \neq m$. One only has to distinguish $a = b \neq c$, which is

$$\langle \tilde{N}_{a,k}^2 \cdot \tilde{N}_{c,m} \rangle = (z_a \Gamma_{a \to k})^2 \, (z_c \Gamma_{c \to m}) \, \tilde{\mathcal{Z}}^{\vec{Q} - 2\vec{Q}_a - \vec{Q}_c} + (z_a \Gamma_{a \to k}) \, (z_c \Gamma_{c \to m}) \, \tilde{\mathcal{Z}}^{\vec{Q} - \vec{Q}_a - \vec{Q}_c}, \tag{H.5}$$

and $k = l \neq m$, while $a \neq b \neq c$, thus

$$\langle \tilde{N}_{a,k} \cdot \tilde{N}_{b,k} \cdot \tilde{N}_{c,m} \rangle = (z_a \Gamma_{a \to k}) \, (z_b \Gamma_{b \to k}) \, (z_c \Gamma_{c \to m}) \, \tilde{\mathcal{Z}}^{\vec{Q} - \vec{Q}_a - \vec{Q}_b - \vec{Q}_c}. \tag{H.6}$$

The canonical correction factors $\tilde{\mathcal{Z}}^{\vec{Q} - \vec{Q}_a - \vec{Q}_b - \vec{Q}_c}$, which would be equal to 1 in the GC, are shorthand for $\frac{\mathcal{Z}^{\vec{Q} - \vec{Q}_a - \vec{Q}_b - \vec{Q}_c}}{\mathcal{Z}^{\vec{Q}}}$.

Appendix I

Table of Moments

The moment of order n for particle species i is defined through

$$\langle N_i^n \rangle = \frac{1}{\mathcal{Z}^{\vec{Q}}} \left(T \frac{\partial}{\partial \mu_i} \right)^n \mathcal{Z}^{\vec{Q}}. \tag{I.1}$$

Using some shorthand notation, where $\vec{Q} = (B, S, Q)$

$$\tilde{\mathcal{Z}}^{\vec{Q}-\vec{Q}_i} = \frac{\mathcal{Z}^{\vec{Q}-\vec{Q}_i}}{\mathcal{Z}^{\vec{Q}}} \tag{I.2}$$

The single particle partition functions z_i are of type 2.2, hence in Boltzmann approximation.

$$\langle N_i \rangle = \tilde{\mathcal{Z}}^{\vec{Q}-\vec{Q}_i} z_i \tag{I.3}$$

$$\langle N_i^2 \rangle = \tilde{\mathcal{Z}}^{\vec{Q}-2\vec{Q}_i} z_i^2 + \tilde{\mathcal{Z}}^{\vec{Q}-\vec{Q}_i} z_i \tag{I.4}$$

$$\langle N_i^3 \rangle = \tilde{\mathcal{Z}}^{\vec{Q}-3\vec{Q}_i} z_i^3 + 3\tilde{\mathcal{Z}}^{\vec{Q}-2\vec{Q}_i} z_i^2 + \tilde{\mathcal{Z}}^{\vec{Q}-\vec{Q}_i} z_i \tag{I.5}$$

$$\langle N_i^4 \rangle = \tilde{\mathcal{Z}}^{\vec{Q}-4\vec{Q}_i} z_i^4 + 6\tilde{\mathcal{Z}}^{\vec{Q}-3\vec{Q}_i} z_i^3 + 7\tilde{\mathcal{Z}}^{\vec{Q}-2\vec{Q}_i} z_i^2 + \tilde{\mathcal{Z}}^{\vec{Q}-\vec{Q}_i} z_i \tag{I.6}$$

$$\begin{aligned} \langle N_i^5 \rangle = {} & \tilde{\mathcal{Z}}^{\vec{Q}-5\vec{Q}_i} z_i^5 + 10\tilde{\mathcal{Z}}^{\vec{Q}-4\vec{Q}_i} z_i^4 + 25\tilde{\mathcal{Z}}^{\vec{Q}-3\vec{Q}_i} z_i^3 \\ & + 15\tilde{\mathcal{Z}}^{\vec{Q}-2\vec{Q}_i} z_i^2 + \tilde{\mathcal{Z}}^{\vec{Q}-\vec{Q}_i} z_i \end{aligned} \tag{I.7}$$

$$\begin{aligned} \langle N_i^6 \rangle = {} & \tilde{\mathcal{Z}}^{\vec{Q}-6\vec{Q}_i} z_i^6 + 15\tilde{\mathcal{Z}}^{\vec{Q}-5\vec{Q}_i} z_i^5 + 65\tilde{\mathcal{Z}}^{\vec{Q}-4\vec{Q}_i} z_i^4 \\ & + 90\tilde{\mathcal{Z}}^{\vec{Q}-3\vec{Q}_i} z_i^3 + 31\tilde{\mathcal{Z}}^{\vec{Q}-2\vec{Q}_i} z_i^2 + \tilde{\mathcal{Z}}^{\vec{Q}-\vec{Q}_i} z_i \end{aligned} \tag{I.8}$$

Correlations between two particles are given by:

$$\langle N_i^n \cdot N_j^k \rangle = \frac{1}{\mathcal{Z}^{\vec{Q}}} \left(T \frac{\partial}{\partial \mu_i} \right)^n \left(T \frac{\partial}{\partial \mu_j} \right)^k \mathcal{Z}^{\vec{Q}} \tag{I.9}$$

Employing the same shorthand notation

$$\langle N_i \cdot N_j \rangle = \tilde{\mathcal{Z}}^{\vec{Q}-\vec{Q}_i-\vec{Q}_j} z_i z_j \tag{I.10}$$

$$\langle N_i^2 \cdot N_j \rangle = \tilde{\mathcal{Z}}^{\vec{Q}-2\vec{Q}_i-\vec{Q}_j} z_i^2 z_j + \tilde{\mathcal{Z}}^{\vec{Q}-\vec{Q}_i-\vec{Q}_j} z_i z_j \tag{I.11}$$

$$\begin{aligned} \langle N_i^3 \cdot N_j \rangle &= \tilde{\mathcal{Z}}^{\vec{Q}-3\vec{Q}_i-\vec{Q}_j} z_i^3 z_j + 3\tilde{\mathcal{Z}}^{\vec{Q}-2\vec{Q}_i-\vec{Q}_j} z_i^2 z_j \\ &\quad + \tilde{\mathcal{Z}}^{\vec{Q}-\vec{Q}_i-\vec{Q}_j} z_i z_j \end{aligned} \tag{I.12}$$

$$\begin{aligned} \langle N_i^2 \cdot N_j^2 \rangle &= \tilde{\mathcal{Z}}^{\vec{Q}-2\vec{Q}_i-2\vec{Q}_j} z_i^2 z_j^2 + \tilde{\mathcal{Z}}^{\vec{Q}-2\vec{Q}_i-\vec{Q}_j} z_i^2 z_j \\ &\quad + \tilde{\mathcal{Z}}^{\vec{Q}-\vec{Q}_i-2\vec{Q}_j} z_i z_j^2 + \tilde{\mathcal{Z}}^{\vec{Q}-\vec{Q}_i-\vec{Q}_j} z_i z_j \end{aligned} \tag{I.13}$$

$$\begin{aligned} \langle N_i^4 \cdot N_j \rangle &= \tilde{\mathcal{Z}}^{\vec{Q}-4\vec{Q}_i-\vec{Q}_j} z_i^4 z_j + 6\tilde{\mathcal{Z}}^{\vec{Q}-3\vec{Q}_i-\vec{Q}_j} z_i^3 z_j \\ &\quad + 7\tilde{\mathcal{Z}}^{\vec{Q}-2\vec{Q}_i-\vec{Q}_j} z_i^2 z_j + \tilde{\mathcal{Z}}^{\vec{Q}-\vec{Q}_i-\vec{Q}_j} z_i z_j \end{aligned} \tag{I.14}$$

$$\begin{aligned} \langle N_i^3 \cdot N_j^2 \rangle &= \tilde{\mathcal{Z}}^{\vec{Q}-3\vec{Q}_i-2\vec{Q}_j} z_i^3 z_j^2 + \tilde{\mathcal{Z}}^{\vec{Q}-3\vec{Q}_i-\vec{Q}_j} z_i^3 z_j \\ &\quad + 3\tilde{\mathcal{Z}}^{\vec{Q}-2\vec{Q}_i-2\vec{Q}_j} z_i^2 z_j^2 + 3\tilde{\mathcal{Z}}^{\vec{Q}-2\vec{Q}_i-\vec{Q}_j} z_i^2 z_j \\ &\quad + \tilde{\mathcal{Z}}^{\vec{Q}-\vec{Q}_i-2\vec{Q}_j} z_i z_j^2 + \tilde{\mathcal{Z}}^{\vec{Q}-\vec{Q}_i-\vec{Q}_j} z_i z_j \end{aligned} \tag{I.15}$$

Appendix J

Table of Cumulants

The cumulants can be calculated from the determinant in section 5.3 from the central moments

$$\langle N^k \rangle = \sum_{n=0}^{\infty} P(n)\, n^k. \tag{J.1}$$

For random distribution with one random variable N_i the cumulants are

$$\kappa^1 = \langle N_i \rangle \tag{J.2}$$

$$\kappa^2 = \langle N_i^2 \rangle - \langle N_i \rangle^2 \tag{J.3}$$

$$\kappa^3 = \langle N_i^3 \rangle - 3\langle N_i^2 \rangle \langle N_i \rangle + \langle N_i \rangle^3 \tag{J.4}$$

$$\kappa^4 = \langle N_i^4 \rangle - 4\langle N_i^3 \rangle \langle N_i \rangle - 3\langle N_i^2 \rangle^2 + 12\langle N_i^2 \rangle \langle N_i \rangle^2 - 6\langle N_i \rangle^4 \tag{J.5}$$

$$\begin{aligned} \kappa^5 = {} & \langle N_i^5 \rangle - 5\langle N_i^4 \rangle \langle N_i \rangle - 10\langle N_i^3 \rangle \langle N_i^2 \rangle + 20\langle N_i^3 \rangle \langle N_i \rangle^2 \\ & + 30\langle N_i^2 \rangle^2 \langle N_i \rangle - 60\langle N_i \rangle^3 \langle N_i^2 \rangle + 24\langle N_i \rangle^5 \end{aligned} \tag{J.6}$$

$$\begin{aligned} \kappa^6 = {} & \langle N_i^6 \rangle - 6\langle N_i^5 \rangle \langle N_i \rangle - 10\langle N_i^3 \rangle^2 - 15\langle N_i^4 \rangle \langle N_i^2 \rangle + 30\langle N_i^2 \rangle^3 \\ & + 120\langle N_i^3 \rangle \langle N_i^2 \rangle \langle N_i \rangle + 30\langle N_i^4 \rangle \langle N_i \rangle^2 - 270\langle N_i^2 \rangle^2 \langle N_i \rangle^2 \\ & - 120\langle N_i^3 \rangle \langle N_i \rangle^3 + 360\langle N_i^2 \rangle \langle N_i \rangle^4 - 120\langle N_i \rangle^6 \end{aligned} \tag{J.7}$$

For a random distribution with two random variables N_i and N_j the central moments are defined as

$$\langle N_i^k \cdot N_j^l \rangle = \sum_{n=0}^{\infty} \sum_{m=0}^{\infty} P(n,m)\, n^k m^l \tag{J.8}$$

From the same determinant one finds for the cumulants

$$\kappa^{1,1} = \langle N_i \cdot N_j \rangle - \langle N_i \rangle \langle N_j \rangle \tag{J.9}$$

$$\kappa^{2,1} = \langle N_i^2 \cdot N_j \rangle - 2\langle N_i \cdot N_j \rangle \langle N_i \rangle - \langle N_i^2 \rangle \langle N_j \rangle + 2\langle N_i \rangle^2 \langle N_j \rangle \tag{J.10}$$

$$\begin{aligned} \kappa^{3,1} = {} & \langle N_i^3 \cdot N_j \rangle - 3\langle N_i^2 \rangle \langle N_i \cdot N_j \rangle - 3\langle N_i^2 \cdot N_j \rangle \langle N_i \rangle \\ & - \langle N_i^3 \rangle \langle N_j \rangle + 6\langle N_i \cdot N_j \rangle \langle N_i^2 \rangle + 6\langle N_i^2 \rangle \langle N_i \rangle \langle N_j \rangle \\ & - 6\langle N_i \rangle^3 \langle N_j \rangle \end{aligned} \tag{J.11}$$

$$\begin{aligned} \kappa^{2,2} = {} & \langle N_i^2 \cdot N_j^2 \rangle - 2\langle N_i \cdot N_j \rangle^2 - \langle N_i^2 \rangle \langle N_j^2 \rangle - 2\langle N_i \cdot N_j^2 \rangle \langle N_i \rangle \\ & - 2\langle N_i^2 \cdot N_j \rangle \langle N_j \rangle + 2\langle N_i \rangle^2 \langle N_j^2 \rangle + 2\langle N_i^2 \rangle \langle N_j \rangle^2 \\ & + 8\langle N_i \cdot N_j \rangle \langle N_i \rangle \langle N_j \rangle - 6\langle N_i \rangle^2 \langle N_j \rangle^2 \end{aligned} \tag{J.12}$$

$$\begin{aligned} \kappa^{4,1} = {} & \langle N_i^4 \cdot N_j \rangle - 4\langle N_i \cdot N_j \rangle \langle N_i^3 \rangle - 6\langle N_i^2 \rangle \langle N_i^2 \cdot N_j \rangle \\ & - 4\langle N_i^3 \cdot N_j \rangle \langle N_i \rangle - \langle N_i^4 \rangle \langle N_j \rangle + 6\langle N_j \rangle \langle N_i^2 \rangle^2 \\ & + 24\langle N_i \rangle \langle N_i^2 \rangle \langle N_i \cdot N_j \rangle + 12\langle N_i^2 \cdot N_j \rangle \langle N_i \rangle^2 \\ & + 8\langle N_i^3 \rangle \langle N_i \rangle \langle N_j \rangle - 24\langle N_i \cdot N_j \rangle \langle N_i \rangle^3 \\ & - 36\langle N_i^2 \rangle \langle N_i \rangle^2 \langle N_j \rangle + 24\langle N_i \rangle^4 \langle N_j \rangle \end{aligned} \tag{J.13}$$

$$\begin{aligned} \kappa^{3,2} = {} & \langle N_i^3 \cdot N_j^2 \rangle - \langle N_i^3 \rangle \langle N_j^2 \rangle - 6\langle N_i^2 \cdot N_j \rangle \langle N_i \cdot N_j \rangle \\ & - 3\langle N_i^2 \rangle \langle N_i \cdot N_j^2 \rangle - 3\langle N_i^2 \cdot N_j^2 \rangle \langle N_i \rangle - 2\langle N_i^3 \cdot N_j \rangle \langle N_j \rangle \\ & + 12\langle N_i \cdot N_j \rangle \langle N_i^2 \rangle \langle N_j \rangle + 12\langle N_i \cdot N_j \rangle^2 \langle N_i \rangle + 6\langle N_i^2 \rangle \langle N_i \rangle \langle N_j^2 \rangle \\ & + 6\langle N_i \cdot N_j^2 \rangle \langle N_i \rangle^2 + 12\langle N_i^2 \cdot N_j \rangle \langle N_i \rangle \langle N_j \rangle + 2\langle N_i^3 \rangle \langle N_j \rangle^2 \\ & - 6\langle N_i \rangle^3 \langle N_j^2 \rangle - 36\langle N_i \cdot N_j \rangle \langle N_i \rangle^2 \langle N_j \rangle - 18\langle N_i^2 \rangle \langle N_i \rangle \langle N_j \rangle^2 \\ & + 24\langle N_i \rangle^3 \langle N_j \rangle^2 \end{aligned} \tag{J.14}$$

Bibliography

[1] H.Koppe, PR **76** (1949) 688

[2] E.Fermi, Progr.Theor. Phys. **5** (1950) 570

[3] R.Hagedorn, Nuovo Cim. Suppl. **3** (1965) 147

[4] R.Hagedorn, Nuovo Cim. **56A** (1968) 1027

[5] Ph.Blanchard, S.Fortunato, and H.Satz, Eur.Phys.J. C **34** (2004) 361-366

[6] W.Broniowski, W.Florkowski, and L.Y.Glozmann, Phys.Rev. D **70** (2004) 117503

[7] F.Cooper, and G.Frye, Phys.Rev. D **10** (1974) 186

[8] J.D.Bjorken, Phys.Rev. D **27** (1983) 140

[9] G.Torrieri, S.Jeon, and J.Rafelski, preprint nucl-th/0503026

[10] F.Becattini, J.Phys.Conf.Ser. **5** (2005) 175-188

[11] S.Wheaton, and J.Cleymans, preprint hep-ph/0407174

[12] G.Torrieri *et al.*, Comput.Phys.Commun. **167** (2005) 229-251

[13] A.Kisiel, T.Taluć, W.Broniowski, and W.Florkowski, preprint nucl-th/0504047

[14] W.Broniowski, and W.Florkowski, Phys.Rev.Lett. **87** (2001) 272302

[15] J.Cleymans, and K.Redlich, Phys.Rev.Lett. **81** (1998) 5284-5286

[16] J.Cleymans, and K.Redlich, Phys.Rev. C **60**, (1999) 054908

[17] J.Cleymans, M.Stankiewicz, P.Steinberg, and S.Wheaton, preprint nucl-th/0506027

[18] P.Braun-Munzinger, and J.Stachel, J.Phys. G **28** 1971 (2002)

[19] J.Cleymans, H.Oeschler, K.Redlich, and S.Wheaton, preprint hep-ph/0511094

[20] P.Braun-Munzinger, J.Cleymans, H.Oeschler, and K.Redlich, Nucl.Phys. A **697** (2002) 902-912

[21] F.Karsch, J.Phys. G **31** (2005) 633

[22] M.I.Gorenstein, M.Gaździcki, and W.Greiner, Phys.Rev. C **72** (2005) 024909

[23] V.V.Begun, M.Gaździcki, M.I.Gorenstein, and O.S.Zoulya, Phys.Rev. C **70** (2004) 034901

[24] J.Cleymans, K.Redlich, and L.Turko, Phys.Rev. C **71** (2005) 047902

[25] V.V.Begun, M.I.Gorenstein, A.P.Kostyuk, and O.S.Zoulya, Phys.Rev. C **71** (2005) 054904

[26] V.V.Begun, M.I.Gorenstein, A.P.Kostyuk, and O.S.Zoulya, preprint nucl-th/0505069

[27] J.Rafelski, and J.Letessier, Phys.Rev. C **22** (2000) 4695

[28] A.Dumitru, C.Spieles, and H.Stöcker, Phys.Rev. C **4** (1997) 2202

[29] S.Jeon, and V.Koch, Phys.Rev.Lett. **85** (2000) 2076-2079

[30] J.Cleymans, K.Redlich, and L.Turko, J.Phys. G **31** (2005) 1421-1435

[31] V.V.Begun, and M.I.Gorenstein, preprint nucl-th/0510022

[32] G.Torrieri, S.Jeon, and J.Rafelski, preprint nucl-th/0509077

[33] P.Braun-Munzinger, K.Redlich, and J.Stachel, preprint nucl-th/0304013

[34] M.Rybczyński *et al.* (for the NA49 Collaboration), J.Phys.Conf.Ser. **5** (2005) 74-85

[35] J.Cleymans, K.Redlich, and E.Suhonen, Z.Phys. C **51** (1991), 137

[36] A.Tounsi, and K.Redlich, preprint hep-ph/0111159

[37] G.Torrieri, S.Jeon, and J.Rafelski, preprint nucl-th/0503026

[38] Particle Data Group, Phys.Rev. D **66** (2002)

[39] A.Keränen, and F.Becattini, Phys.Rev. C **65** (2002) 044901

[40] F.Becattini, and U.Heinz, Z.Phys. C **76**, 269-286 (1997)

[41] J.Manninen, F.Becattini, A.Keränen, M.Gaździcki, and R.Stock, Acta Phys.Hung. A **24** (2005) 23-29

[42] A.Keränen, F.Becattini, V.V.Begun, M.I.Gorenstein, and O.S.Zozulya, J.Phys. G **31** (2005) S1095-S1100

[43] K.Wozniak (for the PHOBOS Collaboration), J.Phys. G **30** (2004) 1377

[44] P.Steinberg (for the PHOBOS collaboration), Nucl.Phys. A **715** (2003) 490-493

[45] A.Tawfik, preprint hep-ph/0508273

[46] J.Cleymans, H.Oeschler, K.Redlich, and S.Wheaton, Phys.Lett. B **615** (2005) 50-54

[47] J.Cleymans, H.Oeschler, K.Redlich, and S.Wheaton, preprint hep-ph/0504065

[48] The NA49 Collaboration (S.V. Afanasiev et al.), Phys.Rev. C **66** (2002) 054902

[49] The NA49 Collaboration (M. Gazdzicki et al.), J.Phys. G **30** (2004) 701-708

[50] M.Gaździcki, and M.I.Gorenstein, preprint hep-ph/0511058

[51] B.Boimska, (for the NA49 Collaboration) unpublished

[52] Jaako Manninen, J.Phys. G **31** (2005) 1101-1104

[53] C.Roland (for the NA49 Collaboration), J.Phys. G **31** (2005) 1075

[54] F. Becattini, A.Keränen, L.Ferroni, and T.Gabbriellini, Phys.Rev. C **72** (2005) 064904

[55] M. Abramowitz and I.A. Stegun, *Handbook of Mathematical Functions with Formulas, Graphs, and Mathematical Tables*, New York: Dover (1965).